Section 1 Elastic Material Properties

Elastic materials return to their original state after the external load is removed without any permanent deformation. FEA NX includes various linear elastic and nonlinear elastic material models. The properties of each material model are explained in this chapter. Table 4.1.1 lists the available elastic materials for each element.

Table 4.1.1 Available elastic materials for each element type

Failure condition	Element type								
	Truss/Elastic Link	Beam	Interface	Geogrid	Plane Stress	Shell	Plane strain	Axisymmetric Solid	Solid
Linear Elastic Isotropic	v	v		v	v	v	v	v	v
Linear Elastic 2D Orthotropic				v	v	v			
Linear Elastic Transversely Isotropic					v	v	v	v	v
Interface Elastic			v						
Nonlinear Elastic (1D)	v								
Jardine							v	v	v
D-Min							v	v	v
Hyperbolic (Duncan-Chang)							v	v	v

1.1 Isotropic Materials

Isotropic materials have the same properties in any arbitrary direction. Linear elastic isotropic materials based on Hooke's law can be used on all elements, excluding some special elements. Using the modulus of elasticity E, Poisson's ratio ν and coefficient of thermal expansion α, the stress-strain relationship for 3D isotropic materials can be expressed as follows:

$$\begin{Bmatrix}\sigma_{xx}\\ \sigma_{yy}\\ \sigma_{zz}\\ \tau_{xy}\\ \tau_{yz}\\ \tau_{zx}\end{Bmatrix}=\begin{bmatrix}\frac{E(1-\nu)}{(1+\nu)(1-2\nu)} & \frac{\nu E(1-\nu)}{(1+\nu)(1-2\nu)} & \frac{\nu E(1-\nu)}{(1+\nu)(1-2\nu)} & 0 & 0 & 0\\ & \frac{E(1-\nu)}{(1+\nu)(1-2\nu)} & \frac{\nu E(1-\nu)}{(1+\nu)(1-2\nu)} & 0 & 0 & 0\\ & & \frac{E(1-\nu)}{(1+\nu)(1-2\nu)} & 0 & 0 & 0\\ & \textit{symmetric} & & \frac{E}{2(1+\nu)} & 0 & 0\\ & & & & \frac{E}{2(1+\nu)} & 0\\ & & & & & \frac{E}{2(1+\nu)}\end{bmatrix}\begin{Bmatrix}\varepsilon_{xx}-\alpha\Delta T\\ \varepsilon_{yy}-\alpha\Delta T\\ \varepsilon_{zz}-\alpha\Delta T\\ \gamma_{xy}\\ \gamma_{yz}\\ \gamma_{zx}\end{Bmatrix} \quad (4.1.1)$$

For 2D analysis, $\tau_{yz}=\tau_{zx}=\gamma_{yz}=\gamma_{zx}=0$ and particularly for plane strain analysis, $\varepsilon_{zz}=0$.

$$\begin{Bmatrix}\sigma_{xx}\\ \sigma_{yy}\\ \tau_{xy}\end{Bmatrix}=\begin{bmatrix}\frac{E}{1-\nu^2} & \frac{\nu E}{1-\nu^2} & 0\\ \frac{\nu E}{1-\nu^2} & \frac{E}{1-\nu^2} & 0\\ 0 & 0 & \frac{E}{2(1+\nu)}\end{bmatrix}\begin{Bmatrix}\varepsilon_{xx}-\alpha\Delta T\\ \varepsilon_{yy}-\alpha\Delta T\\ \gamma_{xy}\end{Bmatrix} \quad (4.1.2)$$

As ν approaches 0.5, the $(1-2\nu)/2$ term approaches '0 (zero)', and this can cause numerical errors. Hence, the range of Poisson's ratio for isotropic materials is restricted as follows:

$$-1.0<\nu<0.5 \quad (4.1.3)$$

Increase in modulus of elasticity with height

The change in modulus of elasticity with height can be simulated. If the change is '0 (zero)', a constant modulus of elasticity is used, and if it is not '0 (zero)', the modulus of elasticity with reference to a certain height can be calculated as follows:

$$\begin{aligned} E &= E_{ref}+\left(y_{ref}-y\right)E_{inc} && \left(y\le y_{ref}\right)\\ E &= E_{ref} && \left(y>y_{ref}\right)\end{aligned} \quad (4.1.4)$$

E_{ref} : Input modulus of elasticity

E_{inc} : Incremental slope of modulus of elasticity

y_{ref} : Depth where E_{ref} is measured

Figure 4.1.1 Conceptual diagram for incremental modulus of elasticity

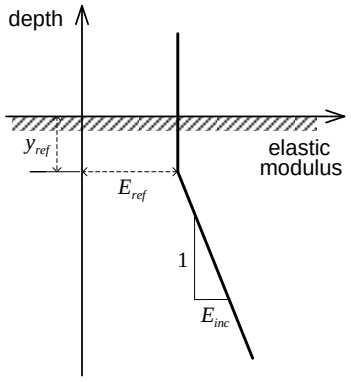

The y in equation (4.1.4) represents the position of the integral point where the element calculation occurs for the current finite element method. If the integral point y is positioned higher than y_{ref}, the modulus of elasticity can have a negative(-) value and so, the E_{ref} is used as the minimum value for modulus of elasticity E.

1.2 Orthotropic Materials

Orthotropic material is one that has different material properties or strengths in different orthogonal directions. The structure is geometrically orthotropic with significant different stiffness in horizontal and vertical direction. It is known that the axial stiffness in vertical direction is larger than the effective stiffness in horizontal direction. The stress-strain relationship for 3D orthotropic material can be expressed as follows:

$$\begin{Bmatrix} \sigma_{11} \\ \sigma_{22} \\ \sigma_{33} \\ \tau_{12} \\ \tau_{23} \\ \tau_{31} \end{Bmatrix} = \begin{bmatrix} \frac{1-\nu_{23}\nu_{32}}{E_2E_3\Delta} & \frac{\nu_{21}+\nu_{31}\nu_{23}}{E_2E_3\Delta} & \frac{\nu_{31}+\nu_{21}\nu_{32}}{E_2E_3\Delta} & 0 & 0 & 0 \\ & \frac{1-\nu_{13}\nu_{31}}{E_1E_3\Delta} & \frac{\nu_{32}+\nu_{12}\nu_{31}}{E_1E_3\Delta} & 0 & 0 & 0 \\ & & \frac{1-\nu_{12}\nu_{21}}{E_1E_2\Delta} & 0 & 0 & 0 \\ & \textit{symmetric} & & G_{12} & 0 & 0 \\ & & & & G_{23} & 0 \\ & & & & & G_{31} \end{bmatrix} \begin{Bmatrix} \varepsilon_{11}-\alpha_{11}\Delta T \\ \varepsilon_{22}-\alpha_{22}\Delta T \\ \varepsilon_{33}-\alpha_{33}\Delta T \\ \gamma_{12} \\ \gamma_{23} \\ \gamma_{31} \end{Bmatrix} \quad (4.1.5)$$

$$\Delta = \frac{1-\nu_{12}\nu_{21}-\nu_{23}\nu_{32}-\nu_{31}\nu_{13}-2\nu_{21}\nu_{32}\nu_{13}}{E_1E_2E_3}$$

The stress-strain relationship for 2D orthotropic material is as follows:

$$\begin{Bmatrix} \sigma_{11} \\ \sigma_{22} \\ \tau_{12} \end{Bmatrix} = \begin{bmatrix} \frac{E_1}{1-\nu_{12}\nu_{21}} & \frac{\nu_{21}E_1}{1-\nu_{12}\nu_{21}} & 0 \\ \frac{\nu_{12}E_2}{1-\nu_{12}\nu_{21}} & \frac{E_2}{1-\nu_{12}\nu_{21}} & 0 \\ 0 & 0 & G_{12} \end{bmatrix} \begin{Bmatrix} \varepsilon_{11}-\alpha_{11}\Delta T \\ \varepsilon_{22}-\alpha_{22}\Delta T \\ \gamma_{12} \end{Bmatrix} \tag{4.1.6}$$

The stress-strain relationship for shear in horizontal direction is as follows:

$$\begin{Bmatrix} \tau_{31} \\ \tau_{23} \end{Bmatrix} = \begin{bmatrix} G_{31} & 0 \\ 0 & G_{23} \end{bmatrix} \begin{Bmatrix} \gamma_{31} \\ \gamma_{23} \end{Bmatrix} \tag{4.1.7}$$

In case of orthotropic material, the following properties should be satisfied.

$$\nu_{21}^2 < \frac{E_2}{E_1},\ \nu_{12}^2 < \frac{E_1}{E_2},\ \nu_{32}^2 < \frac{E_3}{E_2},\ \nu_{23}^2 < \frac{E_2}{E_3},\ \nu_{13}^2 < \frac{E_1}{E_3},\ \nu_{31}^2 < \frac{E_3}{E_1} \tag{4.1.8}$$

$$1-\nu_{12}\nu_{21}-\nu_{23}\nu_{32}-\nu_{31}\nu_{13}-2\nu_{21}\nu_{32}\nu_{13} > 0 \tag{4.1.9}$$

1.3 Transversely Isotropic Materials

Transversely isotropic materials are material models defined by the isotropic cross-section and the axis perpendicular to it. The axis perpendicular to the cross-section displays symmetric physical behavior. Hence, the physical properties are the same within the cross-section and different in the perpendicular direction. Transversely isotropic materials display different physical properties (Modulus of elasticity, Poisson's ratio, Shear modulus) in each perpendicular direction.

▶ out-of-plane cross-sectional properties : E_1 , $\nu_{12}(=\nu_{13})$, $G_{12}(=G_{13})$

▶ in-plane cross-sectional properties : $E_2(=E_3)$, ν_{23} , G_{23}

Here, E_1 is the modulus of elasticity of the perpendicular axis to the cross-section, and ν_{12} , ν_{13} and G_{12} , G_{13} are the Poisson's ratio and shear modulus respectively in the plane created by the perpendicular axis and other axes of the cross-section. However, because the physical properties are axisymmetric about the perpendicular axis to the cross-section, $\nu_{12}=\nu_{13}$, $G_{12}=G_{13}$. E_2 and E_3 are the modulus of elasticity for each axis of the cross-section, ν_{23} is the Poisson's ratio and G_{23} is the shear modulus. Likewise, because the material is isotropic in the horizontal direction, $E_2=E_3$.

On the other hand, transversely isotropic materials and the out-of-plane Poisson's ratio have the following relationship: $\nu_{12} / E_1 = \nu_{21} / E_2$, $\nu_{13} / E_1 = \nu_{31} / E_2$. In other words, ν_{12} and ν_{21} need to be distinguished when defining the transversely isotropic material properties.

MCS / local coordinate system

FEA NX has a local coordinate system defined by the dip angle within the MCS to simulate the slope of the transversely isotropic material model. However, whilst the behavior of transversely isotropic material models is defined by the local coordinate system, the constitutive equation is expressed in the MCS. Hence, coordinate system conversion is needed for the constitutive equation between the local coordinate system and MCS using the dip angle (Detailed information on this is continued in the Constitutive equation and coordinate system conversion and Defining interface direction).

Figure 4.1.2 displays the 2D model where the $MCS - Z$ axis and the x' axis (tangent direction of the local coordinate system) have an angle α .

Figure 4.1.2 2D transversely isotropic material model

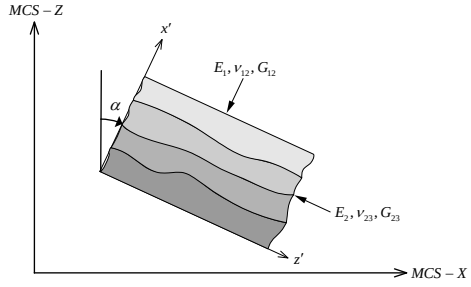

Constitutive equation and coordinate system conversion

The 3D elastic constitutive equation for the local coordinate axis $x'y'z'$ is equation (4.1.10).

$$\begin{Bmatrix} \varepsilon_{x'} \\ \varepsilon_{y'} \\ \varepsilon_{z'} \\ \gamma_{x'y'} \\ \gamma_{y'z'} \\ \gamma_{z'x'} \end{Bmatrix} = \begin{bmatrix} \frac{1}{E_1} & -\frac{\nu_{12}}{E_1} & -\frac{\nu_{12}}{E_1} & 0 & 0 & 0 \\ & \frac{1}{E_2} & -\frac{\nu_{23}}{E_2} & 0 & 0 & 0 \\ & & \frac{1}{E_2} & 0 & 0 & 0 \\ & \textit{symmetric} & & \frac{1}{G_{12}} & 0 & 0 \\ & & & & \frac{1}{G_{23}} & 0 \\ & & & & & \frac{1}{G_{12}} \end{bmatrix} \begin{Bmatrix} \sigma_{x'} \\ \sigma_{y'} \\ \sigma_{z'} \\ \tau_{x'y'} \\ \tau_{y'z'} \\ \tau_{z'x'} \end{Bmatrix} \tag{4.1.5}$$

Generally, the MCS XYZ and local coordinate system $x'y'z'$ are not the same. Because equation (4.1.10) is the constitutive equation corresponding to the local coordinate system, the stiffness matrix of the local coordinate system needs to be converted to the MCS stiffness matrix using the normalized direction vector of the local coordinate system in the MCS. The following equations (4.1.11) and (4.1.12) are the coordinate system conversion equations for stress and strain respectively:

$$\boldsymbol{\sigma}_{x'y'z'} = \mathbf{R}_{\sigma}\boldsymbol{\sigma}_{XYZ} \tag{4.1.11}$$

$$\boldsymbol{\varepsilon}_{x'y'z'} = \mathbf{R}_{\varepsilon}\boldsymbol{\varepsilon}_{XYZ} \tag{4.1.12}$$

$$\mathbf{R}_{\sigma} = \begin{bmatrix} n_X^2 & n_Y^2 & n_Z^2 & 2n_Xn_Y & 2n_Yn_Z & 2n_Zn_X \\ s_X^2 & s_Y^2 & s_Z^2 & 2s_Xs_Y & 2s_Ys_Z & 2s_Zs_X \\ t_X^2 & t_Y^2 & t_Z^2 & 2t_Xt_Y & 2t_Yt_Z & 2t_Zt_X \\ n_Xs_X & n_Ys_Y & n_Zs_Z & n_Xs_Y+n_Ys_X & n_Ys_Z+n_Zs_Y & n_Zs_X+n_Xs_Z \\ s_Xt_X & s_Yt_Y & s_Zt_Z & s_Xt_Y+s_Yt_X & s_Yt_Z+s_Zt_Y & s_Zt_X+s_Xt_Z \\ t_Xn_X & t_Yn_Y & t_Zn_Z & t_Xn_Y+t_Yn_X & t_Yn_Z+t_Zn_Y & t_Zn_X+t_Xn_Z \end{bmatrix} \tag{4.1.13}$$

$$\mathbf{R}_{\varepsilon} = \begin{bmatrix} n_X^2 & n_Y^2 & n_Z^2 & n_Xn_Y & n_Yn_Z & n_Zn_X \\ s_X^2 & s_Y^2 & s_Z^2 & s_Xs_Y & s_Ys_Z & s_Zs_X \\ t_X^2 & t_Y^2 & t_Z^2 & t_Xt_Y & t_Yt_Z & t_Zt_X \\ 2n_Xs_X & 2n_Ys_Y & 2n_Zs_Z & n_Xs_Y+n_Ys_X & n_Ys_Z+n_Zs_Y & n_Zs_X+n_Xs_Z \\ 2s_Xt_X & 2s_Yt_Y & 2s_Zt_Z & s_Xt_Y+s_Yt_X & s_Yt_Z+s_Zt_Y & s_Zt_X+s_Xt_Z \\ 2t_Xn_X & 2t_Yn_Y & 2t_Zn_Z & t_Xn_Y+t_Yn_X & t_Yn_Z+t_Zn_Y & t_Zn_X+t_Xn_Z \end{bmatrix} \tag{4.1.14}$$

$\mathbf{n}=(n_X,n_Y,n_Z)$, $\mathbf{s}=(s_X,s_Y,s_Z)$, $\mathbf{t}=(t_X,t_Y,t_Z)$ are the normalized direction vectors of the x', y', z' axis respectively in the MCS XYZ. For 2D problems, $n_Z=s_Z=t_X=t_Y=0$, $t_Z=-1$.

On the other hand, the following equation is established between the two conversion matrices R_σ, R_ε.

$$\mathbf{R}_\sigma = \mathbf{R}_\varepsilon^{-T} \quad \mathbf{R}_\varepsilon = \mathbf{R}_\sigma^{-T} \tag{4.1.15}$$

Using this, the stress strain relationship equation in the local coordinate system can be expressed as the MCS stress and strain as follows:

$$\left\{ \begin{array}{l} \boldsymbol{\sigma}_{x'y'z'} = \mathbf{D}_{x'y'z'} \boldsymbol{\varepsilon}_{x'y'z'} \\ \boldsymbol{\sigma}_{x'y'z'} = \mathbf{R}_\sigma \boldsymbol{\sigma}_{XYZ} \\ \boldsymbol{\varepsilon}_{x'y'z'} = \mathbf{R}_\varepsilon \boldsymbol{\varepsilon}_{XYZ} \end{array} \right\} \Rightarrow \mathbf{R}_\sigma \boldsymbol{\sigma}_{XYZ} = \mathbf{D}_{x'y'z'} \mathbf{R}_\sigma^{-T} \boldsymbol{\varepsilon}_{XYZ} \tag{4.1.16}$$

Rearranging the equation above gives the constitutive equation of the MCS XYZ, as shown in equation (4.1.17).

$$\boldsymbol{\sigma}_{XYZ} = \left[\mathbf{R}_\sigma^T \mathbf{D}_{x'y'z'}^{-1} \mathbf{R}_\sigma \right]^{-1} \boldsymbol{\varepsilon}_{XYZ} \tag{4.1.17}$$

Defining interface direction

The axial direction vectors $\mathbf{n}$, $\mathbf{s}$, $\mathbf{t}$ of the local coordinate system $x'y'z'$ defined in the MCS XYZ are defined by the dip angle α_1 and dip direction α_2. Figure 4.1.3 displays the definition of the two angles.

Figure 4.1.3 MCS according to dip angle and dip direction

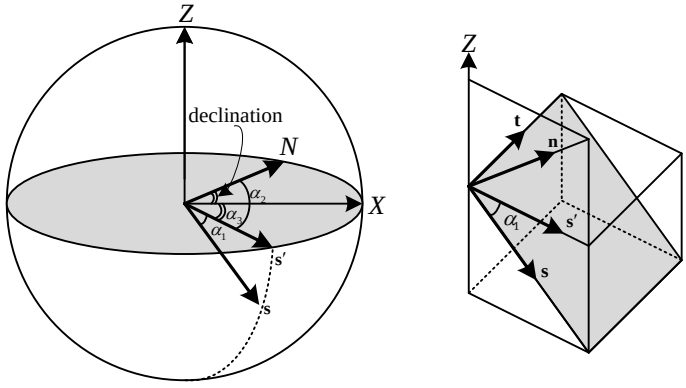

α_1 is the angle between the MCS Z axis and the sliding plane corresponding to the $y'-z'$ plane of the local coordinate system with reference to the Y axis, and α_2 is the angle of rotation for the y' axis of the sliding plane in the Z axis direction, with reference to the $\mathbf{N}$ axis of the $X-Y$ plane. Here, α_1 needs to be in the $[0^\circ, 180^\circ]$ domain, and α_2 needs to be in the $[0^\circ, 360^\circ]$ domain.

Generally, reference axes $\mathbf{N}$ and X of the sliding plane and horizontal plane are not the same. Hence the auxiliary angle α_3, which subtracts the declination corresponding to the angle between the reference axes of the two planes from α_2, is used when composing the actual transformation matrix.

$$\alpha_3 = \alpha_2 - declination \tag{4.1.18}$$

From the definition above, the vectors $\mathbf{n}$, $\mathbf{s}$, $\mathbf{t}$ that form the equations (4.1.13) and (4.1.14) for 3D element transformation matrices can be obtained. Here, $\mathbf{n}$ is the normal vector of the inclined plane and $\mathbf{s}$ and $\mathbf{t}$ are vectors on the inclined plane that are perpendicular to it.

3D:

$$\mathbf{n} = \begin{bmatrix} \sin\alpha_1 \cdot \cos\alpha_3 \\ -\sin\alpha_1 \cdot \sin\alpha_3 \\ \cos\alpha_1 \end{bmatrix}, \quad \mathbf{s} = \begin{bmatrix} \cos\alpha_1 \cdot \cos\alpha_3 \\ -\cos\alpha_1 \cdot \sin\alpha_3 \\ -\sin\alpha_1 \end{bmatrix}, \quad \mathbf{t} = \begin{bmatrix} \sin\alpha_3 \\ \cos\alpha_3 \\ 0 \end{bmatrix} \tag{4.1.19}$$

Meanwhile, because the MCS axes of 2D elements are different from that of 3D elements in FEA NX, the definition of the axial direction vector and dip angle of the local coordinate system changes. The dip angle α_1 is defined as the angle between the MCS Y axis and x' axis of the local coordinate system. However, because the rotation angle of the vertical axis Y is not considered, the dip direction α_2 and declination is not used. The figure below displays the definition of the axis direction vector and dip angle of the 2D local coordinate system $x'y'z'$.

Figure 4.1.4 Definition of dip angle and dip direction on 2D MCS

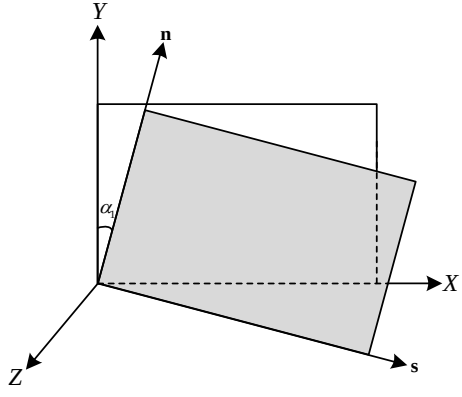

From the definition above, the vectors $\mathbf{n}$, $\mathbf{s}$, $\mathbf{t}$ that form the equations (4.1.13) and (4.1.14) for 2D element transformation matrices can be obtained:

2D:

$$\mathbf{n}=\begin{bmatrix}\sin\alpha_1\\ \cos\alpha_1\\ 0\end{bmatrix}, \mathbf{s}=\begin{bmatrix}\cos\alpha_1\\ -\sin\alpha_1\\ 0\end{bmatrix}, \mathbf{t}=\begin{bmatrix}0\\ 0\\ -1\end{bmatrix} \tag{4.1.20}$$

1.4 Elastic Material of Interface Affiliated Elements

Interface affiliated elements (interface, shell interface, pile elements) are models used to simulate interface behavior. The linear stiffness matrix used for these elements are applied such that the elements are separated or do not penetrate each other.

The linear stiffness matrix for interface, pile elements are expressed as equation (4.1.21) and the added rotational DOF form for shell interface elements is expressed as equation (4.1.22).

$$\mathbf{D}=\begin{bmatrix}k_n & 0 & 0\\ 0 & k_t & 0\\ 0 & 0 & k_t\end{bmatrix} \tag{4.1.21}$$

$$\mathbf{D}=\begin{bmatrix}k_n & 0 & 0 & 0\\ 0 & k_t & 0 & 0\\ 0 & 0 & k_t & 0\\ 0 & 0 & 0 & k_n t^3/12\end{bmatrix} \tag{4.1.22}$$

k_n : Normal stiffness

k_t : Tangential stiffness

t : Thickness of shell interface element

Precautions need to be taken on the units for the stiffness above. For example, when the SI system of units is used, the units for stiffness are N/m^3, not the units for the modulus of elasticity N/m^2 .
Equation (4.1.23) is recommended for calculating the stiffness, where the modulii of elasticity around the target element is divided by the characteristic length. Here, the characteristic length (l_{ch}) is recommended for the thickness of line interface, shell interface, and pile elements. The use of the square root of the element area ($\sqrt{A}$) is recommended for the plane interface.

$$k_n=\alpha\frac{E}{l_{ch}}, \quad k_t=\beta k_n \ \ or \ \ \beta\frac{G}{l_{ch}} \tag{4.1.23}$$

α , β : Scale factor

E , G : Modulus of elasticity, Shear modulus

The scale factor in the equation above needs to be selected empirically depending on the analysis. If the scale factor is too large, numerical problems can occur. If it is too small, accurate result values for the relative displacement of the interface element cannot be obtained. A value of '0.1 ~ 10' is recommended.

1.5 Nonlinear Elastic Behavior of Truss/Embedded Truss

The Coulomb friction model is provided for as the nonlinear material model for interface, shell interface elements, and the details are explained in Chapter 2. For pile elements, the multiple curve input or a value to simulate perfectly plastic behavior is used as the nonlinear material model.
FEA NX supports the following nonlinear elastic behavioral models for truss or embedded truss elements:

- Compression only behavior
- Gap behavior
- Tension only behavior
- Hook behavior
- User defined nonlinear elastic behavior

Figure 4.1.5 Various nonlinear elastic behavioral models

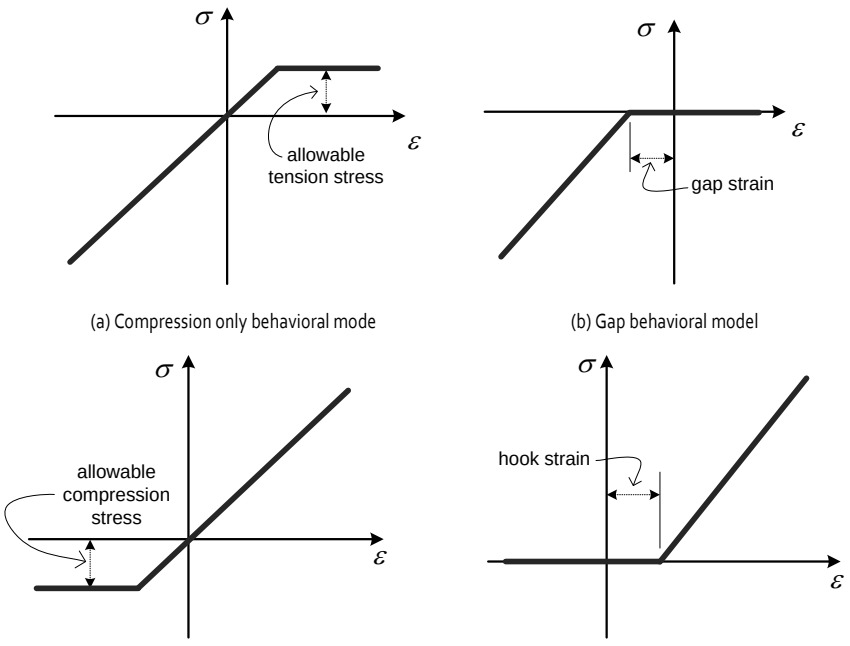

(a) Compression only behavioral mode

(b) Gap behavioral model

(c) Tension only behavioral model

(d) Hook behavioral model

Gaps and hooks have inputs with a length unit. Internally, the gap strain and hook strain are calculated using the element length.

1.6 Nonlinear Elastic Behavior of Elastic Link Elements

FEA NX supports the following nonlinear elastic behavioral models for elastic link elements:

- General behavior
- Tension only behavior
- Compression only behavior
- User defined nonlinear elastic behavior

Tension only, compression only and user defined nonlinear elastic behavior are defined in a similar way as the nonlinear elastic behavior of truss and embedded truss in section 1.4. However, whilst the behavior of truss and embedded truss elements are represented using the stress strain relationship, elastic link elements do not have sectional properties and hence, their behavior is defined using the force displacement relationship shown in Figure 4.1.6, not the stress strain concept. Because tension only and compression only behaviors do not require separate inputs for allowable strength and allowable displacement, a user defined function needs to be used for application.

Figure 4.1.6 Tension only and compression only behavior of elastic link elements

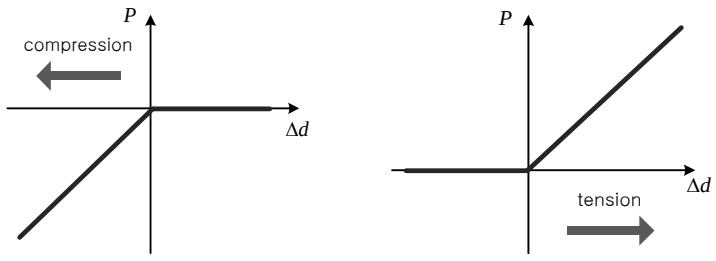

(a) Tension only (b) Compression only

In Figure 4.1.6, Δd represents the relative displacement between connected nodes and P represents the internal member forces.

1.7 Jardine

Jardine[1] suggested the use of material models that define nonlinear behavior to consider the nonlinear behavior that occurs in small strain states for clay.

The Jardine model is a nonlinear elastic model that can simulate nonlinear behavior at small strain states, and the Tresca model is used for plastic analysis when the stress of the material is larger than the input shear strength. Here, the behavior is completely plastic and the stiffening behavior is not considered.

[1] Jardine, R. J., Symes, M. J. and Burland, J. B. "The measurement of soil stiffness in the triaxial apparatus," Geotechnique 34, No. 3, 323-340, 1984.

Nonlinear elastic behavior

The Jardine model derives the nonlinear formula based on the relationship between the secant modulus of elasticity and axial strain measured from the undrained triaxial compression test. The undrained triaxial compression test applies an incremental load in the axial direction of a cylindrical sample, and the stress along the circumferential side is maintained.

The secant modulus of elasticity (E_u) can be directly calculated from the measured value from the triaxial compression test.

$$E_u = \frac{\sigma_a - \sigma_{a;0}}{\varepsilon_a} \tag{4.1.23}$$

ε_a : Axial strain
σ_a : Axial stress
$\sigma_{a;0}$: Initial(when $\varepsilon_a = 0$) axial stress

Because the Jardine model assumes the nonlinear relationship between the secant modulus of elasticity and axial strain, the modulus of elasticity in the elastic region can be defined using the following equation:

$$E_u = G + (F - G)\cos\left[\alpha\left\{\log\frac{\varepsilon_a}{A}\right\}^{\gamma}\right] \tag{4.1.25}$$

A : Strain at maximum stiffness
F : Maximum stiffness value
G : Average stiffness value

Figure 4.1.7 Jardine parameters

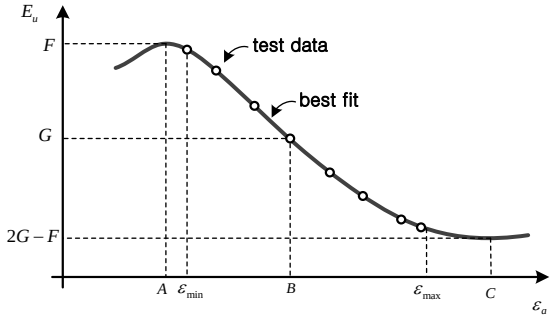

A , F , G can be directly computed from the experimental stiffness-strain curve, and the B , C parameters needed for computing α , γ in the following equation are assumed to be the strain at the average stiffness and minimum stiffness. In this case, the average stiffness becomes equation (4.1.25) where $\pi / 2$ input is for the cosine term, and the minimum stiffness is where π is input.

$$\gamma = \frac{\log 2}{\log\left[\frac{\log(C/A)}{\log(B/A)}\right]} \tag{4.1.26}$$

$$\alpha = \frac{\pi/2}{\left[\log(B/A)\right]^{\gamma}} \tag{4.1.27}$$

F , G do not need to be the same as the experimental maximum, average stiffness. F is the maximum value of the trend line that best fits the data. When the strain is outside the range of the maximum strain ($\varepsilon_{\max}$) and minimum strain ($\varepsilon_{\min}$), the tangent modulus of elasticity is assumed as a constant value.

The general value of $\varepsilon_{\min}$ represents the minimum strain of the experimental data values. A value that is stable in the plastic region needs to be selected for $\varepsilon_{\max}$. If $\varepsilon_{\max}$ the value is too large, a negative (-) elastic tangent stiffness is computed, which can cause numerical instability. Hence, the $\varepsilon_{\max}$ value is generally defined to be smaller than C .

The equivalent stiffness of the Jardine model is as follows:

$$\varepsilon_{eq} = \sqrt{\frac{2}{3}\left[\left(\varepsilon_1-\varepsilon_2\right)^2+\left(\varepsilon_2-\varepsilon_3\right)^2+\left(\varepsilon_3-\varepsilon_1\right)^2\right]} \tag{4.1.28}$$

ε_1 , ε_2 , ε_3 : Major strain at the elastic state

Here, ε_{eq} can be calculated as $\sqrt{3}\varepsilon_a$ at the stress state of the undrained triaxial test ($\varepsilon_1 = \varepsilon_a$, $\varepsilon_2 = \varepsilon_3 = -1/2\ \varepsilon_a$).

The tangent modulus of elasticity E_{ut} can be expressed in the same way as equation (4.1.25), and expressing this as a relationship equation with ε_{eq} is as follows:

$$E_u = f_1\left(\varepsilon_{eq}\right) = G + (F-G)\cos\left(\alpha I^{\gamma}\right) \tag{4.1.29}$$

$$E_{ut} = f_2\left(\varepsilon_{eq}\right) = G + (F-G)\cos\left(\alpha I^{\gamma}\right) - \frac{(F-G)\alpha\gamma I^{\gamma-1}}{2.303}\sin\left(\alpha I^{\gamma}\right) \tag{4.1.30}$$

And,

$$I = \log\left(\frac{\varepsilon_{eq}}{\sqrt{3}A}\right) \tag{4.1.31}$$

The equivalent linear strain considering the boundary range $\varepsilon_{\max}$ and $\varepsilon_{\min}$ is as follows.

$$\varepsilon_{eq\min} = \varepsilon_{\min}\sqrt{3}\ ,\ \varepsilon_{eq\max} = \varepsilon_{\max}\sqrt{3} \tag{4.1.32}$$

The tangent modulus of elasticity is assumed to be a constant value outside the boundary range, and the general form of E_u can be expressed as follows:

$$E_u = \begin{cases} f_1\left(\varepsilon_{eq\min}\right) & \varepsilon_{eq} \le \varepsilon_{eq\min} \\ f_1\left(\varepsilon_{eq}\right) & \varepsilon_{eq\min} < \varepsilon_{eq} \le \varepsilon_{eq\max} \\ f_2\left(\varepsilon_{eq\max}\right) + \left(f_1\left(\varepsilon_{eq\max}\right) - f_2\left(\varepsilon_{eq\max}\right)\right)\dfrac{\varepsilon_{eq\max}}{\varepsilon_{eq}} & \varepsilon_{eq} > \varepsilon_{eq\max} \end{cases} \tag{4.1.33}$$

The computed average tangent stiffness from equation (4.1.33) is used when calculating the increment strain through recursive calculations. When calculating the actual stiffness, the secant stiffness equation (4.1.24) is used for accurate computation.

The relationship between the tangent and secant modulus of elasticity in the triaxial test is as follows:

$$E_{ut} = \frac{d\sigma_a}{d\varepsilon_a} = \frac{d\left(E_u\varepsilon_a\right)}{d\varepsilon_a} \tag{4.1.34}$$

The axial incremental stress $\Delta\sigma_a$ due to the axial incremental strain $\Delta\varepsilon_a$, found from the relationship between the given axial strain and secant modulus of elasticity, can be expressed as follows:

$$\Delta\sigma_a = \int_{\varepsilon_a^0}^{\varepsilon_a^0+\Delta\varepsilon_a} E_{ut}\,d\varepsilon_a = \left[E_u\varepsilon_a\right]_{\varepsilon_a^0}^{\varepsilon_a^0+\Delta\varepsilon_a} = E_u\left(\varepsilon_a^0 + \Delta\varepsilon_a\right) - E_u^0\varepsilon_a^0 \tag{4.1.35}$$

To express the relationship between incremental stress and incremental strain linearly, the average modulus of elasticity E_{ut} is used, and can be expressed as follows.

$$\overline{E}_{ut} = \frac{E_u\varepsilon_{eq} - E_u^0\varepsilon_{eq}^0}{\varepsilon_{eq} - \varepsilon_{eq}^0} \tag{4.1.36}$$

ε_{eq} : Renewed equivalent strain

E_u : Secant stiffness, computed from equation (4.1.33)

The 3D material stiffness matrix can be expressed as follows, using the average modulus of elasticity:

$$\mathbf{D} = \frac{\overline{E}_{ut}}{(1+\nu)(1-2\nu)} \begin{bmatrix} 1-\nu & \nu & \nu & 0 & 0 & 0 \\ \nu & 1-\nu & \nu & 0 & 0 & 0 \\ \nu & \nu & 1-\nu & 0 & 0 & 0 \\ 0 & 0 & 0 & \frac{1-2\nu}{2} & 0 & 0 \\ 0 & 0 & 0 & 0 & \frac{1-2\nu}{2} & 0 \\ 0 & 0 & 0 & 0 & 0 & \frac{1-2\nu}{2} \end{bmatrix} \tag{4.1.37}$$

1.8 D-min

The D-min model is a sectioned linear model applied to general rocks (hard rock, soft rock etc.), proposed by Japan Central Research Institute of Electric Power Industry (CRIEPI), Hayashi, Hibino. Sectioned linear models have different stiffnesses for each construction step, but are normalized such that the stiffness has a fixed value within a construction step.

It is assumed that the modulus of elasticity decreases and the Poisson's ratio increases as the Mohr circle approaches the failure envelope. Hence, the relative distance between the Mohr circle and failure envelope determines the modulus of elasticity and Poisson's ratio of each section. The material property values of this model are constant for each load step and so, repeated analysis is not required for each load step.

The failure envelope equation can be expressed as follows:

$$\left(\frac{\tau}{\tau_R}\right)^a = 1 - \frac{\sigma}{\sigma_t} \tag{4.1.38}$$

σ : Hydrostatic stress

τ : Shear stress

a : Mohr circle coefficient

σ_t : Tensile strength

τ_R : Shear strength

The relationship between the failure envelope and Mohr circle is expressed in Figure 4.1.8

Figure 4.1.8 Failure envelope and Mohr circle of D-min model

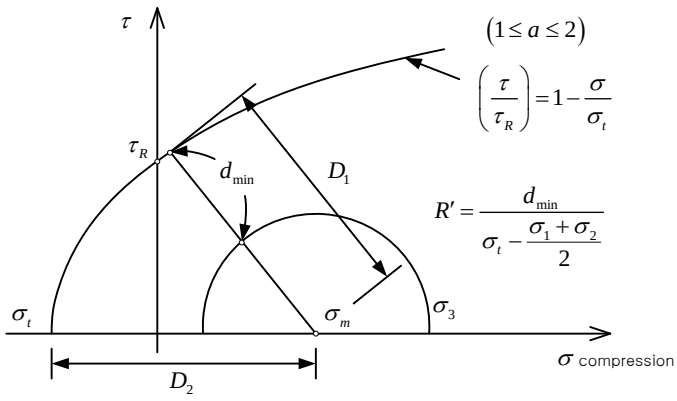

Failure is determined using the buffer index (R), as shown in Figure 4.1.8. If the buffer index is larger than '1', it is in the elastic region and if the buffer index is less than 'o', failure is assumed.

$$R = k \cdot R' \quad (0.0 \le R \le 1.0) \tag{4.1.39}$$

Here, the modified buffer index is:

$$R' = \frac{d_{\min}}{\sigma_t - \frac{\sigma_1 + \sigma_3}{2}} \tag{4.1.40}$$

$d_{\min}$: Minimum distance between failure envelope and Mohr circle

k : Buffer index from user input variable

The factor of safety (F_s) is as follows:

$$F_s = \frac{\min(D_1, D_2)}{\left(\frac{\sigma_1 - \sigma_3}{2}\right)} \tag{4.1.41}$$

Here, the buffer index is computed at the integral point, and this can be used to compute the modulus of elasticity and Poisson's ratio of the next step:

$$E = R^m(E_i - E_{cr}) + E_{cr}$$
$$\nu = R^n(\nu_i - \nu_{cr}) + \nu_{cr} \qquad (4.1.42)$$

E_i : Initial modulus of elasticity

E_{cr} : Critical modulus of elasticity

m : Nonlinear material coefficient

ν_i : Initial Poisson's ratio

ν_{cr} : Critical Poisson's ratio

n : Nonlinear material coefficient

The Mohr circle coefficient (a) and buffer index (k) increases with the increase in initial modulus of elasticity (E_i). The relationship between the Mohr circle coefficient (a) of various rocks, buffer index (k) and initial modulus of elasticity (E_i) is shown below in table 4.1.2. The data is based on the triaxial compression test and was put together by the Japan Road Traffic Information Center in 1986.

Table 4.1.2 Parameters based on initial Elasticity modulus (JARTIC, 1986)

Initial Elasticity modulus (E_i , kgf/cm^2)	**Buffer index (k)**	**Mohr circle coefficient (a)**
$100 \le E_i < 1,000$	2.0	1.0
$1,000 \le E_i < 10,000$	4.0	2.0
$10,000 \le E_i < 100,000$	6.0	3.0
$100,000 \le E_i$	10.0	4.0

1.9 Hyperbolic Model (Duncan-Chang)

Ground stress-strain behavior becomes nonlinear as it approaches the failure criterion, and this can be simulated by modifying the foundation modulus. The function proposed by Duncan and Chang[2] is used to calculate the foundation modulus. The stress-strain curve of the function is a hyperbola and the foundation modulus is a function of confining stress and shear stress. It is very useful because nonlinear material models only need material properties that can be easily obtained from the triaxial compression test or literature,

The Duncan and Change nonlinear stress-strain curve displays a hyperbolic form between the axial strain space generated by shear stress $\sigma_1 - \sigma_3$. Three foundation modulus are needed depending on the stress state and stress path; the initial modulus E_i , tangent modulus E_t , and unloading-reloading modulus E_{ur} . (Refer to Figure 4.1.9)

[2] Duncan, J. M., and Chang, C.-Y. "Nonlinear Analysis of Stress and Strains in Soils," J. Soil Mech. Found. Div., ASCE 96, 5 (1970), 1629-1653.

Figure 4.1.9 Nonlinear stress-strain behavior

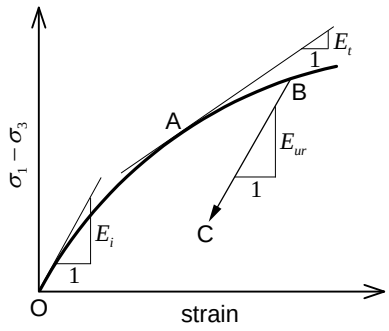

The modluii and coefficient of the nonlinear elastic model can be obtained from the graph with a vertical axis of the ratio between modulus of elasticity and atmospheric pressure (E/p_a) or ratio between bulk modulus and atmospheric pressure (B_m/p_a), and a horizontal axis of the ratio between maximum confining pressure and atmospheric pressure (σ_3/p_a) in log scale, as shown in Figure 4.1.10. The initial loading coefficient (K) can be obtained when the vertical axis is E/p_a at the point where $\sigma_3/p_a = 1$ and slope at this point can be used to calculate the coefficient n for the initial stiffness. The bulk modulus index m can be found from the slope when the vertical axis is B_m/p_a .

Figure 4.1.10 Determination of nonlinear ground material properties

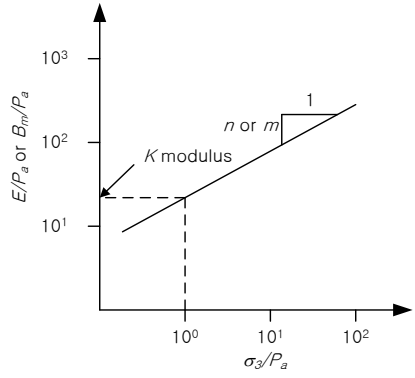

The bulk modulus B_m is defined by equation (4.1.43).

$$B_m = \frac{(\Delta\sigma_1 + \Delta\sigma_2 + \Delta\sigma_3)/3}{\Delta\varepsilon_v} \qquad (4.1.43)$$

$\Delta\sigma$: Amount of principal stress change,

$\Delta\varepsilon_v$: Amount of principal stress change,

Initial modulus

When the ground experiences a '0(zero)'shear stress (when $\sigma_1 - \sigma_3 = 0$), the stress-strain behavior is calculated using the initial modulus E_i . This initial tangent modulus is controlled by the confining stress σ_3 and can be calculated using equation (4.1.44).

$$E_i = K_L p_a \left(\frac{\sigma_3}{p_a} \right)^n \tag{4.1.44}$$

E_i : Initial tangent modulus, a function of confining stress

K_L : Loading coefficient

p_a : Atmospheric pressure

σ_3 : Confining stress

n : Index for defining the effects of confining stress on initial modulus

If the index n is 1.0, the initial modulus E_i is directly proportional to the confining stress. If it is '0(zero)', E_i is unrelated to the confining stress.

If the confining stress is in the tensile state, the initial modulus can be '0 (zero)' or '-(negative)'. To prevent this, FEA NX sets a lower bound for the confining stress. The set value is $0.01 p_a$.

Tangent modulus

The ground is known to follow the load path when it experiences a larger shear stress than it has experienced before. The constitutive behavior is dominated by the tangent modulus E_t when the load path is followed. This tangent modulus can be defined as a function of the ground material properties, triaxial deviatoric stress $\sigma_1 - \sigma_3$ and confining stress σ_3 of a Duncan-Chang model.

$$E_t = \left[1 - \frac{R_f (\sigma_1 - \sigma_3)(1 - \sin\phi)}{2c\cos\phi + 2\sigma_3 \sin\phi} \right]^2 E_i \tag{4.1.45}$$

E_t : Tangent modulus

E_i : Initial tangent modulus

ϕ : Internal friction angle of the ground

c : Cohesion of the ground

R_f : Ratio between maximum shear stress and asymptote of the hyperbola (generally a value of 0.75 ~ 1)

Here, the minimum value of E_t can be restricted. The basic minimum tangent modulus is p_a. If this value is too small, it can cause convergence problems.

Unloading-reloading modulus

Nonlinear models use the unloading-reloading modulus E_{ur} when the ground is unloading from a large shear stress state. This coefficient is calculated in a similar manner to the initial modulus, except that the unloading-reloading coefficient number K_{ur} is used instead of K_L.

$$E_{ur} = K_{ur} p_a \left(\frac{\sigma_3}{p_a} \right)^n \tag{4.1.46}$$

Unlike the tangent modulus, this modulus is not affected by the shear stress. If the unloading-reloading coefficient number K_{ur} is not defined, it is defined to be the same as the loading coefficient number K_L.

Friction Angle

The friction angle can be defined by incremental form according to the confining pressure.

$$\phi = \phi_0 - \Delta\phi \lg\left(\frac{\sigma_3}{p_a} \right) \tag{4.1.47}$$

Poisson's ratio

The Poisson's ratio of nonlinear models are either set as a constant unrelated to the stress state or calculated from the bulk modulus of the soil depending on the confining stress. For the latter case, the bulk modulus can be found using equation (4.1.47).

$$B_m = K_b p_a \left(\frac{\sigma_3}{p_a} \right)^m \tag{4.1.48}$$

B_m : Bulk modulus

K_b : Bulk modulus number

m : Bulk modulus index

The relationship between the Poisson's ratio and bulk modulus can be defined from the elastic theory, as shown in equation (4.1.48).

$$B_m = \frac{E}{3(1-2\nu)} \tag{4.1.49}$$

If the Poisson's ratio in the equation above is '0(zero)', $B_m = E/3$ and if the Poisson's ratio is 0.49, $B_m = 17E$, the calculated Poisson's ratio is limited to '0 ~ 0.49'.

And the Poisson's ratio in Duncan-Chang model can be defined by the experimental constant not the bulk modulus.

$$\nu_t = \frac{G - F\lg\left(\frac{\sigma_3}{p_a}\right)}{\left\{1 - \frac{D(\sigma_1-\sigma_3)}{K\,p_a\left(\frac{\sigma_3}{p_a}\right)^m\left[1-\frac{R_f}{(\sigma_1-\sigma_3)_f}(\sigma_1-\sigma_3)\right]}\right\}^2} \tag{4.1.50}$$

Failure region

The failure condition of a nonlinear elastic model cannot be defined. However, to show that the shear region is large for this material, the failure region is defined as the region that satisfies the following condition:

$$\frac{\sigma_1-\sigma_3}{2} - \frac{\sigma_1+\sigma_3}{2}\sin\phi \geq R_f c\cos\phi \tag{4.1.51}$$

The failure ratio R_f in the Duncan-Chang equation is used as shown in equation (4.1.50):

$$(\sigma_1-\sigma_3)_f = R_f\,(\sigma_1-\sigma_3)_{ult} \tag{4.1.52}$$

The ultimate strength $(\sigma_1-\sigma_3)_{ult}$ term represents the asymptote which the hyperbolic stress-strain curve approaches at high strains. Also, $(\sigma_1-\sigma_3)_f$ is the deviatoric strain at failure.

Section 2

Plastic Material Properties

FEA NX includes various plastic material models to simulate actual ground and structural phenomena. This section briefly introduces the plastic theory used and the properties of each material model. The table below lists the available plastic materials for each element.

Table 4.2.1 Available plastic materials for each element type

Failure condition	Element type								
	Truss	Beam	Interface	Geogrid	Plane Stress	Shell	Plane strain	Axisymmetric Solid	Solid
von Mises	v				v	v	v	v	v
Tresca							v	v	v
Mohr-Coulomb							v	v	v
Drucker-Prager							v	v	v
Strain-Softening							v	v	v
Modified Cam Clay							v	v	v
Jointed Rock							v	v	v
Modified Mohr Coulomb							v	v	v
Hoek Brown							v	v	v
Generalized Hoek Brown							v	v	v
Modified UBCSAND							V	V	V
Sekiguchi-Ohta (Inviscid)							V	V	V
Soft Soil							V	V	V
Hardening Soil with Small strain stiffness							V	V	V

Generalized SCLAY1S			V	V	V
CWFS			V	V	V
Inverse Rankine		V			
GeoGrid		V			
Coulomb Friction	V				
Janssen	V				

2.1 Failure Criterion and Invariance

Principal stress invariance

Principal stress invariance is a convenient method of expressing the yield function. The stress induced at an arbitrary point within the material can be expressed using the following equation, which uses the direction vector n_j that defines the principal stress direction:

$$\left(\sigma_{ij} - \sigma\delta_{ij}\right)n_j = 0 \tag{4.2.1}$$

δ_{ij} : Kronecker delta

$n_j \neq 0$ in the equation (4.2.1) above, and the necessary and sufficient condition for equation (4.2.1) is as follows:

$$\left|\sigma_{ij} - \sigma\delta_{ij}\right| = 0 \tag{4.2.2}$$

The matrix equation (4.2.2) can be expressed as a cubic equation for principal stress, as shown below:

$$\sigma^3 - I_1\sigma^2 + I_2\sigma - I_3 = 0 \tag{4.2.3}$$

Here,

$$\begin{aligned} I_1 &= \sigma_x + \sigma_y + \sigma_z = \sigma_{ii} \\ I_2 &= \left(\sigma_x\sigma_y + \sigma_y\sigma_z + \sigma_z\sigma_x\right) - \left(\tau_{xy}^2 + \tau_{yz}^2 + \tau_{zx}^2\right) = \frac{1}{2}\left(I_1^2 - \sigma_{ij}\sigma_{ji}\right) \\ I_3 &= \begin{vmatrix} \sigma_x & \tau_{xy} & \tau_{xz} \\ \tau_{yx} & \sigma_y & \tau_{yz} \\ \tau_{zx} & \tau_{zy} & \sigma_z \end{vmatrix} = \frac{1}{3}\sigma_{ij}\sigma_{jk}\sigma_{ki} - \frac{1}{2}I_1\sigma_{ij}\sigma_{ji} + \frac{1}{6}I_1^3 \end{aligned} \tag{4.2.4}$$

I_1, I_2, I_3 can be expressed using the principal stresses σ_1, σ_2, σ_3 as follows.

$$\begin{aligned} I_1 &= \sigma_1 + \sigma_2 + \sigma_3 \\ I_2 &= \sigma_1\sigma_2 + \sigma_2\sigma_3 + \sigma_3\sigma_1 \\ I_3 &= \sigma_1\sigma_2\sigma_3 \end{aligned} \tag{4.2.5}$$

Deviatoric stress invariance

The stress tensor σ_{ij} can be divided into the hydrostatic pressure and invariant stress components, as shown below:

$$\sigma_{ij} = s_{ij} + \sigma_m \delta_{ij} \tag{4.2.6}$$

Here, $\sigma_m = (\sigma_x + \sigma_y + \sigma_z)/3 = I_1/3$ and represents the average stress. Also, $s_{ij} = \sigma_{ij} - \sigma_m \delta_{ij}$ is the deviatoric stress and represents the pure shear state.

The deviatoric stress invariance can be expressed as shown below:

$$\left| s_{ij} - s\delta_{ij} \right| = 0 \tag{4.2.7}$$

Equation (4.2.7) can be expressed as follows:

$$s^3 - J_1 s^2 + J_2 s - J_3 = 0 \tag{4.2.8}$$

Here,

$$\begin{aligned} J_1 &= s_{ii} = s_x + s_y + s_z = 0 \\ J_2 &= \frac{1}{2} s_{ij} s_{ji} \\ &= \frac{1}{6}\left[(\sigma_x - \sigma_y)^2 + (\sigma_y - \sigma_z)^2 + (\sigma_z - \sigma_x)^2 \right] + \tau_{xy}^2 + \tau_{yz}^2 + \tau_{zx}^2 \\ J_3 &= \frac{1}{3} s_{ij} s_{jk} s_{ki} = \begin{vmatrix} s_x & \tau_{xy} & \tau_{xz} \\ \tau_{yx} & s_y & \tau_{yz} \\ \tau_{zx} & \tau_{zy} & s_z \end{vmatrix} \end{aligned} \tag{4.2.9}$$

J_1, J_2, J_3 can be expressed using the deviatoric principal stresses s_1, s_2, s_3 as follows:

$$\begin{aligned} J_1 &= s_1 + s_2 + s_3 = 0 \\ J_2 &= \frac{1}{2}\left(s_1^2 + s_2^2 + s_3^2 \right) = \frac{1}{6}\left[(\sigma_1 - \sigma_2)^2 + (\sigma_2 - \sigma_3)^2 + (\sigma_3 - \sigma_1)^2 \right] \\ J_3 &= \frac{1}{3}\left(s_1^3 + s_2^3 + s_3^3 \right) = s_1 s_2 s_3 \end{aligned} \tag{4.2.10}$$

I_1, I_2, I_3, J_1, J_2, J_3 are all scalar invariants, which have properties independent of the coordinate axes. To conveniently express the yield function geometrically, I_1, J_2, J_3 invariants are often used.

Geometric meaning of the three stress invariants

Figure 4.2.1 Stress state definition in principal stress space

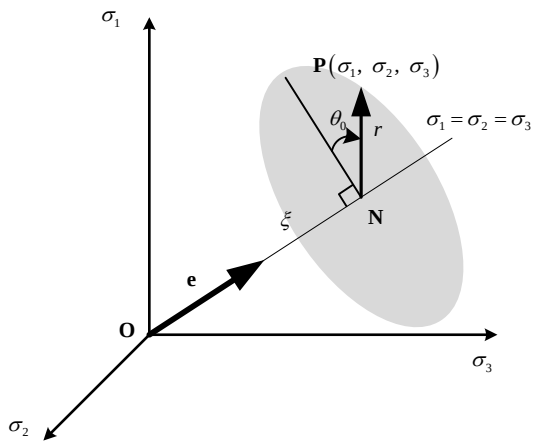

Vector $\mathbf{OP}$ can be defined when point $\mathbf{P}(\sigma_1, \sigma_2, \sigma_3)$ is expressed as an arbitrary stress state in the principal stress space, as shown in Figure 4.2.1. Vector $\mathbf{OP}$ can be divided into vector $\mathbf{ON}$, which follows the hydrostatic pressure axis; and vector $\mathbf{NP}$, which exists in the deviatoric plane perpendicular to the hydrostatic pressure axis. Their size is as follows:

$$\begin{aligned} |\mathbf{ON}| &= \xi = \frac{1}{\sqrt{3}} I_1 \\ |\mathbf{NP}| &= r = \sqrt{2J_2} \end{aligned} \tag{4.2.11}$$

Vector $\mathbf{NP}$ needs to be rotated by θ_0 in the σ_1 axis to define point $\mathbf{P}$ on the deviatoric plane. Here, θ_0 is called the similarity angle and its equation is as follows:

$$\theta_0 = \frac{1}{3}\cos^{-1}\left(\frac{3\sqrt{3}}{2}\frac{J_3}{J_2^{3/2}}\right) \tag{4.2.12}$$

Here, θ_0 has the following range:

$$0 \le \theta_0 \le \frac{\pi}{3} \tag{4.2.13}$$

For numerical analysis, it is more convenient to use Lode's angle θ rather than θ_0 and it can be defined using the following equation:

$$\theta = \frac{1}{3}\sin^{-1}\left(-\frac{3\sqrt{3}}{2}\frac{J_3}{J_2^{3/2}}\right) \tag{4.2.14}$$

Here, $\theta = \theta_0 - \frac{\pi}{6}$ and has the following range:

$$-\frac{\pi}{6} \le \theta \le \frac{\pi}{6} \tag{4.2.15}$$

It is often more convenient to express the principal stress as an invariant stress when defining the yield function of the material, and it can be rearranged using Lode's angle to give the following equation:

$$\begin{Bmatrix}\sigma_1\\ \sigma_2\\ \sigma_3\end{Bmatrix} = \frac{2\sqrt{J_2}}{\sqrt{3}}\begin{Bmatrix}\sin\left(\theta+\frac{2}{3}\pi\right)\\ \sin(\theta)\\ \sin\left(\theta+\frac{4}{3}\pi\right)\end{Bmatrix} + \frac{I_1}{3}\begin{Bmatrix}1\\1\\1\end{Bmatrix} \tag{4.2.16}$$

2.2 Formulation of Plastic Behavior

Plastic materials display permanent deformation on structures even after the external load is removed, unlike elastic materials. To express such behavioral properties, strain is formulated following additive decomposition, which divides strain into elastic and plastic components, as shown below:

$$\boldsymbol{\varepsilon} = \boldsymbol{\varepsilon}^{el} + \boldsymbol{\varepsilon}^{pl} \tag{4.2.17}$$

- $\boldsymbol{\varepsilon}$: Total strain
- $\boldsymbol{\varepsilon}^{el}$: Elastic strain
- $\boldsymbol{\varepsilon}^{pl}$: Plastic strain

Because Hook's law defines the relationship between deformation and stress in the elastic region, applying this to equation (4.2.17) and rearranging gives the following equation for stress:

$$\boldsymbol{\sigma} = \mathbf{D}\boldsymbol{\varepsilon}^{el} = \mathbf{D}(\boldsymbol{\varepsilon} - \boldsymbol{\varepsilon}^{pl}) \tag{4.2.18}$$

$\boldsymbol{\sigma}$: Stress vector

$\mathbf{D}$: Material stiffness matrix

The failure criterion defines the plasticity criteria and can be defined differently depending on the material properties such as steel or concrete. The material failure criterion can be modeled in function form using various experiments on the material. Generally, this function has variables that represent stress and hardening, and can be expressed as follows:

$$f(\boldsymbol{\sigma}, \kappa) = 0 \tag{4.2.19}$$

f : Yield function

κ : Hardening parameter

If the yield function f is equal to or smaller than '0'(zero), plastic flow does not occur and if f is larger than '0', plastic flow occurs.

Plastic flow rule

Material failure induces plastic flow, and this plastic flow causes stress redistribution to maintain the equilibrium state of the material. The plastic flow calculation is done in nonlinear form and the increment form is generally used for formulation. The general values used for calculating the plastic flow in plasticity analysis for materials are the incremental stress direction and plastic strain increment direction. The incremental stress direction is as follows:

$$\mathbf{n}_i = \frac{\partial f_i}{\partial \boldsymbol{\sigma}} \tag{4.2.20}$$

$\mathbf{n}$: Gradient vector representing the stress increment direction perpendicular to the failure surface

i : Number of yield functions

The plastic strain increment can be divided into the size and directional components using Koiter's law as follows:

$$\dot{\varepsilon}^p = \sum_{i=1}^{n} \dot{\lambda}_i \frac{\partial g_i}{\partial \boldsymbol{\sigma}} = \sum_{i=1}^{n} \dot{\lambda}_i \mathbf{m}_i \tag{4.2.21}$$

Here, g_i is the plastic potential function, which can be expressed as $g_i(\boldsymbol{\sigma}, \kappa)$ using stress and hardening variable κ , generally obtained from material tests. $\dot{\lambda}_i$ is the plastic multiplier, and it needs to satisfy the following Kuhn-Tucker condition:

$$f \le 0\,,\ \dot{\lambda}_i \ge 0\,,\ \dot{\lambda}_i f = 0 \tag{4.2.22}$$

From the conditions above, plastic flow does not occur when the yield function f is smaller than 0 and $\dot{\lambda}_i$ is always 0. When plastic flow occurs ($\dot{\lambda}_i$ is larger than 0), the yield function is always 0. $\mathbf{m}$ is the vector that defines the plastic strain increment in equation (4.2.21). Here, the method of defining the plastic strain increment by $\partial f / \partial \boldsymbol{\sigma}$, which uses the yield function f and not the plastic potential function g, is called the associated flow rule and the method which uses the plastic potential function to define the plastic strain increment direction by $\partial g / \partial \boldsymbol{\sigma}$ is called the non-associated flow rule. Using the non-associated flow rule on a material model can suppress the excessive cubical expansion phenomena due to the discord between the stress direction and strain direction. However, the amount of calculation increases because the stiffness matrix is asymmetric and an asymmetric solver needs to be used.

The hardening variable κ used for strain hardening can be defined using the dimensionless equivalent plastic strain as shown below:

$$\kappa = \sqrt{\frac{2}{3}\left(\boldsymbol{\varepsilon}^{\mathrm{p}}\right)^{\mathrm{T}} \mathbf{Q}\, \boldsymbol{\varepsilon}^{\mathrm{p}}} \tag{4.2.23}$$

Here,

$$\boldsymbol{\varepsilon}^{p} = \begin{Bmatrix} \varepsilon_{xx}^{p} \\ \varepsilon_{yy}^{p} \\ \varepsilon_{zz}^{p} \\ \gamma_{xy}^{p} \\ \gamma_{yz}^{p} \\ \gamma_{zx}^{p} \end{Bmatrix}, \quad \mathbf{Q} = \begin{bmatrix} 1 & 0 & 0 & 0 & 0 & 0 \\ 0 & 1 & 0 & 0 & 0 & 0 \\ 0 & 0 & 1 & 0 & 0 & 0 \\ 0 & 0 & 0 & 1/2 & 0 & 0 \\ 0 & 0 & 0 & 0 & 1/2 & 0 \\ 0 & 0 & 0 & 0 & 0 & 1/2 \end{bmatrix} \tag{4.2.24}$$

Stress Return Method

► Implicit backward Euler method

Figure 4.2.2 Implicit backward Euler method

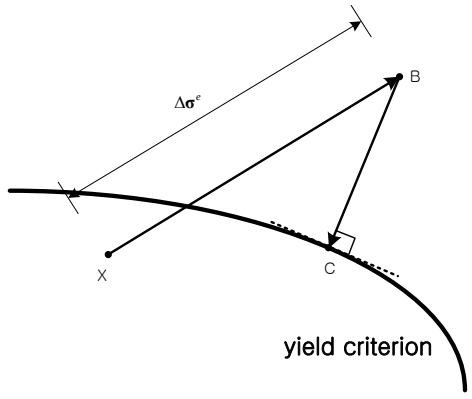

The Implicit backward Euler method can be expressed using the following equation:

$$\boldsymbol{\sigma}_C = \boldsymbol{\sigma}_B - \Delta\lambda \mathbf{D}\mathbf{m}_C \tag{4.2.25}$$

Because the unknown C values exist on both sides of equation (4.2.25), the concept of residual vectors $\mathbf{r}$ is introduced to find the value using repeated analysis:

$$\mathbf{r} = \boldsymbol{\sigma}_c - \left(\boldsymbol{\sigma}_B - \Delta\lambda \mathbf{D}\mathbf{m}_C\right) \tag{4.2.26}$$

The residual vector $\mathbf{r}$ converges to 0 when the final stress state lies on the failure surface. The new residual vector $\mathbf{r}_{new}$ for recursive calculations using the 1st order Taylor expansion can be defined using the following equation:

$$\mathbf{r}_{new} = \mathbf{r}_{old} + \dot{\boldsymbol{\sigma}} + \dot{\lambda}\mathbf{D}\mathbf{m} + \Delta\lambda \mathbf{D}\frac{\partial \mathbf{m}}{\partial \boldsymbol{\sigma}}\dot{\boldsymbol{\sigma}} \tag{4.2.27}$$

Because the residual vector is $\mathbf{r}_{new} = 0$ for the converged final stress, substituting this into equation (4.2.27) and rearranging for $\dot{\boldsymbol{\sigma}}$ gives equation (4.2.28).

$$\dot{\boldsymbol{\sigma}} = -\left(\mathbf{I} + \Delta\lambda \mathbf{D}\frac{\partial \mathbf{m}}{\partial \boldsymbol{\sigma}}\right)^{-1}\left(\mathbf{r}_{old} + \dot{\lambda}\mathbf{D}\mathbf{m}\right) = -\mathbf{R}^{-1}\left(\mathbf{r}_{old} + \dot{\lambda}\mathbf{D}\mathbf{m}\right) \tag{4.2.28}$$

Also, using the 1st order Taylor expansion on the yield function gives the following equation.

$$f_{new} = f_{old} + \frac{\partial f}{\partial \boldsymbol{\sigma}}\dot{\boldsymbol{\sigma}} + \frac{\partial f}{\partial \boldsymbol{\kappa}}\dot{\boldsymbol{\kappa}} = f_{old} + \mathbf{n}^T\dot{\boldsymbol{\sigma}} + h\dot{\lambda} = 0 \tag{4.2.29}$$

Substituting equation (4.2.29) into equation (4.2.28) and rearranging for $\dot{\lambda}$ gives the following equation:

$$\dot{\lambda} = \frac{f_{old} - \mathbf{n}^T\mathbf{R}^{-1}\mathbf{r}_{old}}{h + \mathbf{n}^T\mathbf{R}^{-1}\mathbf{Dm}} \tag{4.2.30}$$

► Cutting Plane Method

Figure 4.2.3 Cutting Plane Method

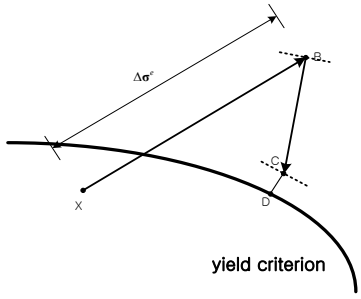

The cutting plane method can be defined as follows with reference to Figure 4.2.3:

$$\boldsymbol{\sigma}_C = \boldsymbol{\sigma}_X + \Delta\boldsymbol{\sigma}^e - \Delta\lambda\mathbf{Dm} \tag{4.2.31}$$

Defining the stress return direction above at point B in the perpendicular direction modifies equation (4.2.31) as follows:

$$\boldsymbol{\sigma}_C = \boldsymbol{\sigma}_B - \Delta\lambda\mathbf{Dm}_B \tag{4.2.32}$$

Also, using the 1st order Taylor expansion on the incremental function gives the following equation.

$$f_C = f_B + \frac{\partial f}{\partial \boldsymbol{\sigma}}\Delta\boldsymbol{\sigma} + \frac{\partial f}{\partial \boldsymbol{\kappa}}\Delta\boldsymbol{\kappa} = f_B - \Delta\lambda\mathbf{n}_B\mathbf{Dm} - \Delta\lambda h = 0 \tag{4.2.33}$$

Hence, the plastic multiplier increment $\Delta\lambda$ is as follows $\Delta\lambda$:

$$\Delta\lambda = \frac{f_B}{\mathbf{n}_B\mathbf{Dm}_B + h} \tag{4.2.34}$$

Constitutive equation

The plastic constitutive equation can be composed as follows. The small stress increment is determined by the elastic part of the strain increment vector.

$$\dot{\boldsymbol{\sigma}} = \mathbf{D}\left(\dot{\boldsymbol{\varepsilon}} - \dot{\boldsymbol{\varepsilon}}^{p}\right) = \mathbf{D}\dot{\boldsymbol{\varepsilon}} - \dot{\lambda}\mathbf{D}\mathbf{m} \tag{4.2.35}$$

Because the current stress always needs to be positioned on the failure surface, the consistency condition $\dot{\lambda}\,\dot{f} = 0$ needs to be satisfied. Rearranging equation (4.2.35) for the small strain increment gives the following equation (4.2.36) for the small stress increment:

$$\dot{\boldsymbol{\sigma}} = \left(\mathbf{D} - \frac{\mathbf{D}\mathbf{m}\mathbf{n}^{\mathrm{T}}\mathbf{D}}{h + \mathbf{n}^{\mathrm{T}}\mathbf{D}\mathbf{m}}\right)\dot{\boldsymbol{\varepsilon}} = \mathbf{D}^{\mathbf{ep}}\dot{\boldsymbol{\varepsilon}} \tag{4.2.36}$$

The $\mathbf{D}^{\mathbf{ep}}$ in equation (4.2.36) is called the continuum tangent stiffness matrix,

When using the consistent tangent stiffness matrix for the Newton-Raphson recursive formula, it converges faster than when equation (4.2.36) is used because of the 2nd order convergence property. This 2nd order convergence property can be obtained from the following process. First, differentiating equation (4.2.25) gives the following equation:

$$\dot{\boldsymbol{\sigma}} = \mathbf{D}\dot{\boldsymbol{\varepsilon}} - \dot{\lambda}\mathbf{D}\mathbf{m} - \Delta\lambda\mathbf{D}\frac{\partial \mathbf{m}}{\partial \boldsymbol{\sigma}}\dot{\boldsymbol{\sigma}} - \Delta\lambda\mathbf{D}\frac{\partial \mathbf{m}}{\partial \kappa}\frac{\partial \kappa}{\partial \lambda}\dot{\lambda} \tag{4.2.37}$$

Here, $\dot{\lambda}$ is the change in $\Delta\lambda$.

Equation (4.2.37) can be rearranged as follows:

$$\mathbf{A}\dot{\boldsymbol{\sigma}} = \mathbf{D}\dot{\boldsymbol{\varepsilon}} - \dot{\lambda}\mathbf{D}\bar{\mathbf{m}} \tag{4.2.38}$$

Here, $\mathbf{A} = \mathbf{I} + \Delta\lambda\mathbf{D}\frac{\partial \mathbf{m}}{\partial \boldsymbol{\sigma}}$, $\bar{\mathbf{m}} = \mathbf{m} + \Delta\lambda\mathbf{D}\frac{\partial \mathbf{m}}{\partial \kappa}\frac{\partial \kappa}{\partial \lambda}$

If $\mathbf{H} = \mathbf{A}^{-1}\mathbf{D}$, equation (4.2.38) can be arranged as follows.

$$\dot{\boldsymbol{\sigma}} = \mathbf{H}\left(\dot{\boldsymbol{\varepsilon}} - \dot{\lambda}\bar{\mathbf{m}}\right) \tag{4.2.39}$$

If equation (4.2.39) is rearranged for the total strain term using the consistency condition, the following equation can be obtained:

$$\dot{\boldsymbol{\sigma}} = \left(\mathbf{H} - \frac{\mathbf{H}\bar{\mathbf{m}}\mathbf{n}^{\mathrm{T}}\mathbf{H}}{h + \mathbf{n}^{\mathrm{T}}\mathbf{H}\bar{\mathbf{m}}} \right) \dot{\boldsymbol{\varepsilon}} = \mathbf{C}^{\mathrm{ep}} \dot{\boldsymbol{\varepsilon}} \tag{4.2.40}$$

The $\mathbf{D}^{\mathrm{ep}}$ in equation (4.2.36) is the continuum tangent stiffness matrix, and the $\mathbf{C}^{\mathrm{ep}}$ in equation (4.2.40) is the consistent tangent stiffness matrix.

2.3 von-Mises

The von Mises failure condition assumes that failure occurs when the 2nd order invariant of deviatoric stress J_2 reaches a certain value. This condition is often used to simulate plastic behavior of metallic materials. The perfect plastic failure condition that does not consider hardening can be expressed using the following equation:

$$f(\boldsymbol{\sigma}) = \sqrt{3J_2} - \sigma_y = \sqrt{\frac{3}{2}\boldsymbol{\sigma}_{dev} : \boldsymbol{\sigma}_{dev}} - \sigma_y = 0 \tag{4.2.41}$$

$\boldsymbol{\sigma}_{dev}$: Deviatoric stress

σ_y : Failure stress

Because only the deviatoric stress is used to express the failure condition, it is appropriate in expressing the ductile materials where failure occurs regardless of hydrostatic pressure. The radius of the von Mises failure surface in 3D stress state is $\sqrt{2/3}\sigma_y$, and surface is expressed as a cylinder parallel to the hydrostatic axis.

Figure 4.2.4 von Mises failure surface in principal stress coordinate system

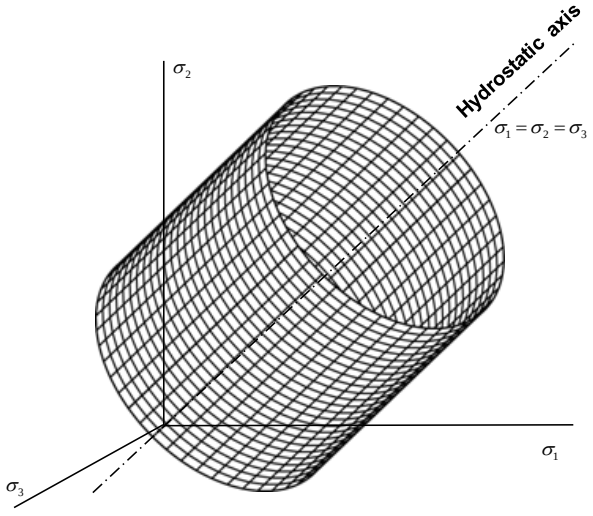

Figure 4.2.5 von Mises failure surface shape in the meridian plane for $\theta = -\frac{\pi}{6}$

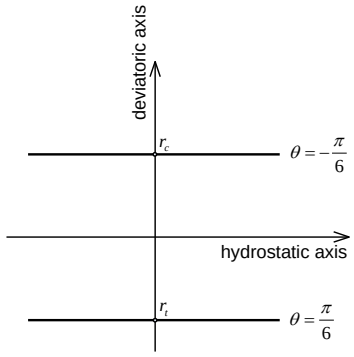

The associated plastic flow is assumed for the von Mises failure condition. The plastic strain variation is as follows:

$$d\boldsymbol{\varepsilon}^{pl} = d\lambda \frac{\partial f}{\partial \boldsymbol{\sigma}} = d\lambda \frac{\sqrt{3}}{\sqrt{2\boldsymbol{\sigma}_{dev} : \boldsymbol{\sigma}_{dev}}} \boldsymbol{\sigma}_{dev} \tag{4.2.42}$$

Hardening factor

FEA NX supports isotropic, kinematic and combined hardening model in von-Mises yield function. In the case of isotropic hardening, the central axis of initial yield surface isn't change since it supposes that the initial yield surface expands uniformly.

$$f(\boldsymbol{\sigma}, \mathbf{q}) = \sqrt{3J_2} - \sigma_y(\mathbf{q}) = \sqrt{\frac{3}{2}\boldsymbol{\sigma}_{dev} : \boldsymbol{\sigma}_{dev}} - \sigma_y(\mathbf{q}) = 0 \tag{4.2.43}$$

Figure 4.2.5-1 Change of the yield surface of isotropic hardening model

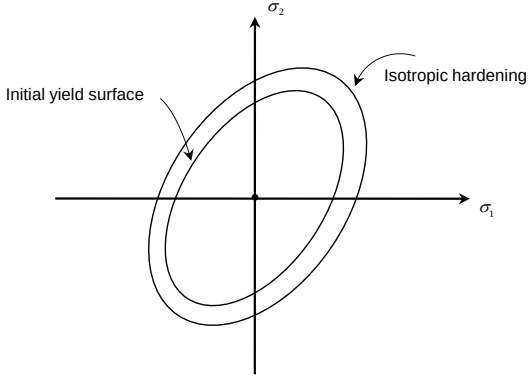

The hardening factor of isotropic hardening model consists of effective plastic strain such as $\mathbf{q} = \{e_p\} = \{\lambda\}$. The yield stress due to hardening is given by the function of effective plastic strain, $\sigma_y(e_p)$ and directly uses the hardening function, $h_y(e_p)$.

The combined hardening model supposes that expansion and movement of the yield surface occurs simultaneously by plastic deformation. In the combined hardening model, the yield surface is defined by yield stress and back stress as follows:

$$f(\boldsymbol{\sigma}, \mathbf{q}) = \sqrt{\frac{3}{2}\boldsymbol{\Sigma}_{dev} : \boldsymbol{\Sigma}_{dev}} - \sigma_y(\mathbf{q}) = 0 \tag{4.2.44}$$

$\boldsymbol{\Sigma}_{dev}$: $\boldsymbol{\sigma}_{dev} - \boldsymbol{\alpha}$

$\boldsymbol{\alpha}$: back stress

Figure 4.2.5-2 Change of the yield surface of combined hardening model

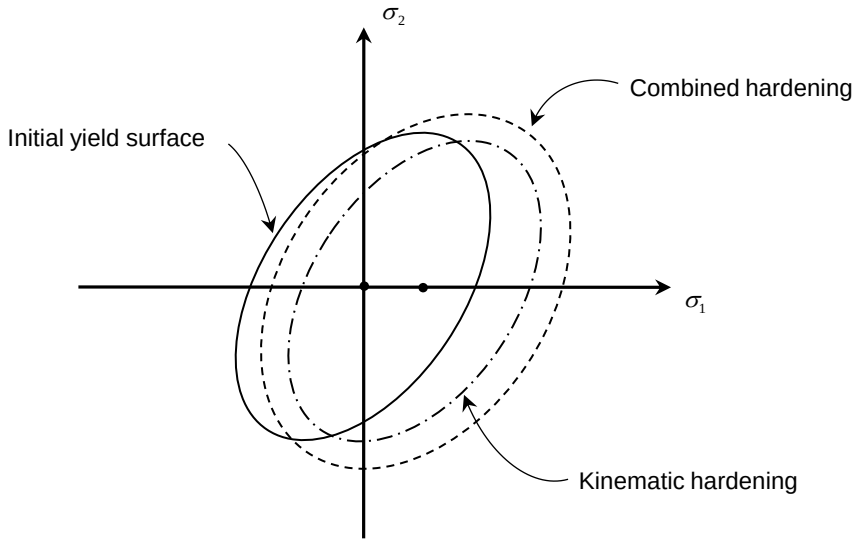

The hardening factors of combined hardening model are effective plastic strain and back stress.

$$\mathbf{q} = \begin{Bmatrix} e_p \\ \boldsymbol{\alpha} \end{Bmatrix} \tag{4.2.45}$$

The yield stress is calculated from hardening function using the combined variable λ_c as follows:

$$\sigma_y = \lambda_c h_y(0) + (1-\lambda_c) h_y(e_p) \tag{4.2.46}$$

In case of the combined variable, $\lambda_c = 0$, it is isotropic hardening and kinematic hardening when $\lambda_c = 1$. The plastic strain of combined hardening and the change rate of back stress which follows hardening rule of Ziegler can be expressed using the following equation:

$$d\boldsymbol{\varepsilon}^{pl} = d\lambda \frac{\sqrt{3}}{\sqrt{2\boldsymbol{\Sigma}_{dev} : \boldsymbol{\Sigma}_{dev}}} \boldsymbol{\Sigma}_{dev} \tag{4.2.47}$$

$$d\boldsymbol{\alpha} = \lambda_c \frac{dh_y}{de_p} d\boldsymbol{\varepsilon}^{pl} \tag{4.2.48}$$

Hardening curve

The hardening curve is a material property which expresses plastic property of material. It is generally obtained from test and uniaxial tension/compression test or pure shear test is widely used. The hardening curve in FEA NX consists of inputting true stress-plastic strain curve and the conversion process from test result is as follows:

If you know load-displacement curve, true strain and true stress can be calculated using the following equation.

$$\varepsilon = \log\left(\frac{L_0 + d}{L_0}\right) = \log\left(\frac{L}{L_0}\right), \ \sigma = \frac{Pe^{\varepsilon}}{A_0} \tag{4.2.49}$$

L_0, L : Length of before/after deformation

A_0 : Area of before deformation

If you know engineering stress-strain, it can be calculated as follows:

$$\varepsilon = \log(1 + \varepsilon_E), \ \sigma = \sigma_E e^{\varepsilon} \tag{4.2.50}$$

ε_E, σ_E : Engineering strain/stress

Since the plastic strain begins to occur from the moment that the material yield, it can be calculated ad follows:

$$e_p = \varepsilon - \varepsilon^{el} = \varepsilon - \frac{\sigma}{E} \tag{4.2.51}$$

E : Elastic modulus

2.4 Tresca

The Tresca criterion was originally developed to be used on failure conditions of metallic materials. In geotechnical analysis it is often used to simulate the ground material behavior for undrained conditions. The failure condition for this criterion can be expressed using the uniaxial compression strength, as shown below.

$$|\sigma_3 - \sigma_1| = \sigma_y \tag{4.2.52}$$

σ_y : uniaxial compression strength

Equation (4.2.52) can be expressed using the stress invariant term J_2 and θ_0, as shown in equation (4.2.53). $(0^\circ \le \theta_0 \le 60^\circ)$

$$\sigma_1 - \sigma_3 = \frac{1}{\sqrt{3}}\sqrt{J_2}\left[\cos\theta_0 - \cos\left(\theta_0 + \frac{2}{3}\pi\right)\right] = \sigma_y \tag{4.2.53}$$

Rearranging this equation:

$$f(J_2, \theta_0) = 2\sqrt{J_2}\sin\left(\theta_0 + \frac{1}{3}\pi\right) - \sigma_y = 0 \tag{4.2.54}$$

Or, it can be expressed using the terms I_1, J_2, θ as follows. $\left(-\frac{\pi}{6} \le \theta \le \frac{\pi}{6}\right)$

$$\begin{aligned} f(J_2, \theta_0) &= \frac{2}{\sqrt{3}}\sqrt{J_2}\left[\sin\left(\theta + \frac{2}{3}\pi\right) - \sin\left(\theta + \frac{4}{3}\pi\right)\right] - \sigma_y \\ &= 2\sqrt{J_2}\cos\theta - \sigma_y = 0 \end{aligned} \tag{4.2.55}$$

The effects of hydrostatic pressure on the failure plane are not considered for this criterion and so, it is unrelated to I_1. The Tresca failure criterion is a hexagonal column parallel to the hydrostatic axis in the principal stress space, as shown in Figure 4.2.6, and is expressed as a regular hexagon in the deviatoric plane, as shown in Figure 4.2.7(a).

According to the experimental results, the shear strength of the saturated soil is unrelated to I_1 for undrained loading. The Tresca model can obtain appropriate results under these conditions:

Figure 4.2.6 Tresca failure surface shape in principal stress space

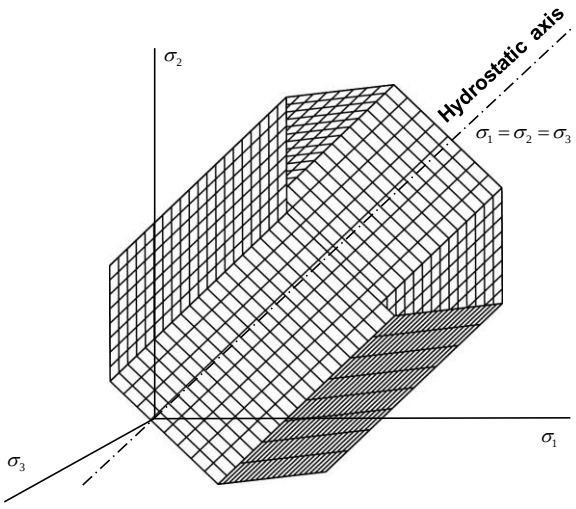

Figure 4.2.7 Tresca failure surface shape in π plane and meridian plane

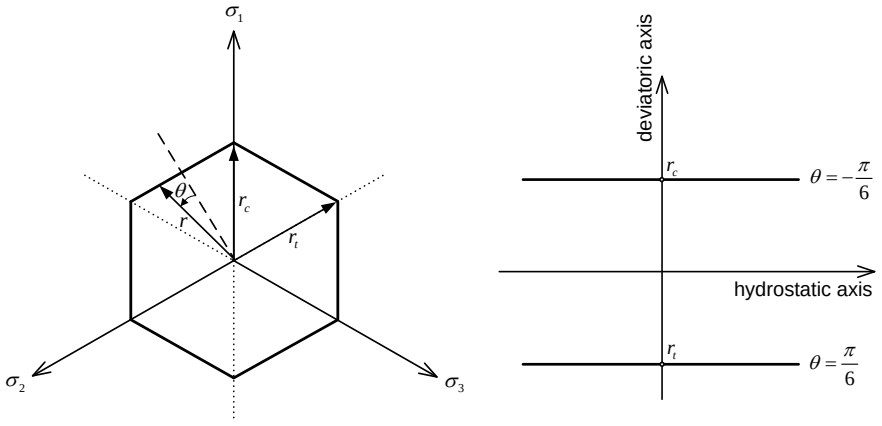

(a) Failure surface shape in π plane (b) Failure surface shape in the meridian plane for $\theta = -\frac{\pi}{6}$

If the von Mises and Tresca criteria are congruent for $r_c(\theta_0 = 0^\circ)$ and $r_t(\theta_0 = 60^\circ)$, the von Mises surface becomes a circle that circumscribes the Tresca hexagon (Figure 4.2.7(a)) in the deviatoric plane. In this case, the expected maximum difference in failure stress occurs along $(\theta_0 = 30^\circ)$, and the failing shear stress ratio between the von Mises and Tresca criteria is $2/\sqrt{3} = 1.15$. If the two criteria are conformed for simple shear,

the von Mises circle inscribes the Tresca hexagon, and the maximum error between the two criteria occur along $(\theta_0 = 0^\circ)$ and $(\theta_0 = 60^\circ)$.

Figure 4.2.8 von Mises and Tresca failure surface shape

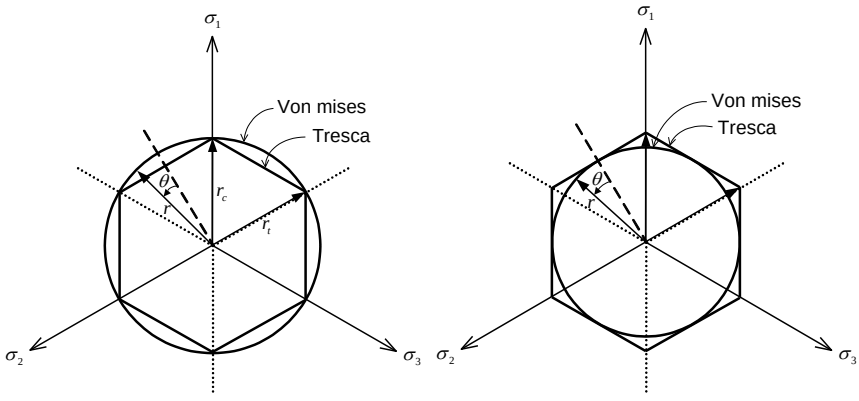

(a) Relation with Tresca-Circumscription in π plane

(b) Relation with Tresca-Inscription in π plane

2.5 Mohr-Coulomb

The Mohr-Coulomb model is used to simulate most terrain and it displays sufficiently reliable results for general nonlinear analysis of the ground.

Figure 4.2.9 Yield function of Mohr-Coulomb model

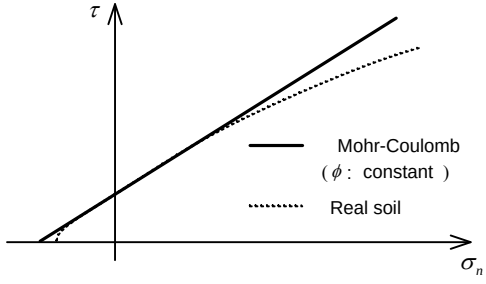

FEA NX can simulate changes in the modulus of elasticity and cohesion with height for a Mohr-Coulomb model using equation (4.1.4). If the amount of cohesion change with height is '0(zero)', a constant value is used. If the amount of change is not '0(zero)', the cohesion can be calculated with respect to a reference height using equation (4.2.56).

$$\begin{aligned} c &= c_{ref} + \left(y_{ref} - y\right)c_{inc} && \left(y \le y_{ref}\right) \\ c &= c_{ref} && \left(y > y_{ref}\right) \end{aligned} \qquad (4.2.56)$$

c_{ref} : Input cohesion value

c_{inc} : Cohesion increment with respect to depth

y_{ref} : Depth at which c_{ref} is measured

The y in equation (4.2.56) represents the integral position of the element. If the integral position is located higher than y_{ref}, the cohesion can be smaller than 'o'. To prevent this, the cohesion value is not decreased any further and the c_{ref} value is used.

Yield function of Mohr-Coulomb model

According to Mohr(1900), failure can be expressed using the following equation:

$$|\tau| = c - \sigma_n \tan\phi \tag{4.2.57}$$

c : Cohesion

ϕ : Internal friction angle

Here, the limit shear stress τ of an arbitrary plane is only related to the normal stress σ_n of the same plane. Equation (4.2.57) shows that material failure occurs at the stress state where the largest Mohr circle comes across the Coulomb friction failure envelope. It also shows that the intermediate principal stress $\sigma_2 (\sigma_1 \geq \sigma_2 \geq \sigma_3)$ does not have an effect on the failure condition.

Hence, the yield function of the Mohr-Coulomb failure plane is as follows:

$$f = |\tau| + \sigma_n \tan\phi - c = 0 \tag{4.2.58}$$

The failure criterion of equation (4.2.58) is called the Mohr-Coulomb criterion and it is the most widely used method for ground materials due to its simplicity and accuracy.

Expressing the Mohr-Coulomb criterion using principal stress terms $(\sigma_1 \geq \sigma_2 \geq \sigma_3)$, equation (4.2.58) can be rearranged into the following equation:

$$\begin{aligned} \frac{\sigma_1 - \sigma_3}{2} &= -\frac{\sigma_1 + \sigma_3}{2}\sin\phi + c\cos\phi \\ \sigma_1 \frac{1+\sin\phi}{2c\cos\phi} - \sigma_3 \frac{1-\sin\phi}{2c\cos\phi} &= 1 \\ \frac{\sigma_1}{f_t'} - \frac{\sigma_3}{f_c'} &= 1 \end{aligned} \tag{4.2.59}$$

$f_c' = \frac{2c\cos\phi}{1-\sin\phi}$: Uniaxial compressive strength when maximum principal stress is 0

$f_t' = \frac{2c\cos\phi}{1+\sin\phi}$: Uniaxial tensile strength when minimum principal stress is 0

Equation (4.2.59) provides convenience when defining material properties because it uses the uniaxial compressive and tensile strengths.

Figure 4.2.10 Geometric diagram of principal stresses

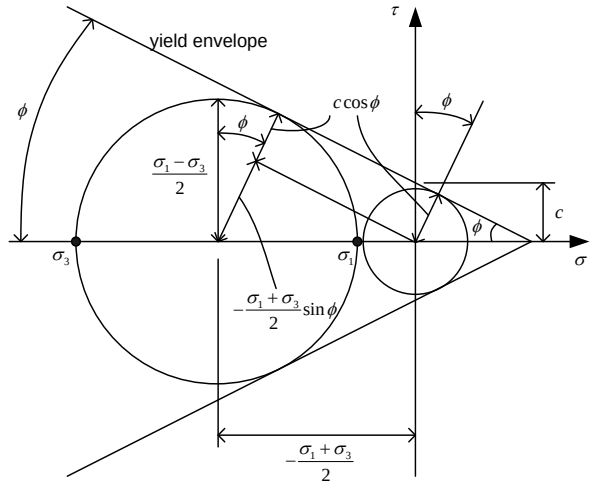

Equation (4.2.58) can be expressed using terms I_1, J_2 and θ, which are often used in numerical analysis.

$$f(I_1, J_2, \theta) = -\frac{1}{3}I_1\sin\phi + \sqrt{J_2}\left(\cos\theta + \frac{1}{\sqrt{3}}\sin\theta\sin\phi\right) - c\cos\phi = 0 \qquad (4.2.60)$$

Assuming associated flow for the plastic potential function gives the following equation:

$$g(I_1, J_2, \theta) = -\frac{1}{3}I_1\sin\psi + \sqrt{J_2}\left(\cos\theta + \frac{1}{\sqrt{3}}\sin\theta\sin\psi\right) - c\cos\psi = 0 \qquad (4.2.61)$$

The Mohr-Coulomb criterion is an irregular hexagonal pyramid with a straight meridian in the principal stress space, as shown in Figure 4.2.11, and the deviatoric shape in the π plane $(\sigma_1 + \sigma_2 + \sigma_3 = 0)$ is an irregular hexagon. To draw the irregular hexagon, the lengths r_{t0} and r_{c0} are required and can be expressed as follows:

$$r_{t0} = \frac{2\sqrt{6}c\cos\phi}{3+\sin\phi} \tag{4.2.62}$$

$$r_{c0} = \frac{2\sqrt{6}c\cos\phi}{3-\sin\phi} \tag{4.2.63}$$

The r_{t0} / r_{c0} from equations (4.2.62) and (4.2.63) is as follows:

$$\frac{r_{t0}}{r_{c0}} = \frac{3-\sin\phi}{3+\sin\phi} \tag{4.2.64}$$

Because the deviatoric sections of the Mohr-Coulomb failure surface are all geometrically similar, the ratio r_t / r_c is always constant for an arbitrary deviatoric section.

$$\frac{r_t}{r_c} = \frac{r_{t0}}{r_{c0}} = \frac{3-\sin\phi}{3+\sin\phi} \tag{4.2.65}$$

If the tensile strength is input, the tensile principal stress of the Mohr-Coulomb cannot surpass the input tensile strength. FEA NX applies a complex of the Mohr-Coulomb failure function and the tensile Rankine failure function to consider Mohr-Coulomb failure with allowed tensile strength.

In the Mohr-Coulomb model tensile strength can be considered based on two types: Pressure and Rankine.

- In the first "pressure type" method, the average of the principal stresses can not exceed the tensile strength:

$$\frac{\sigma_1+\sigma_2+\sigma_3}{3} < \sigma_t$$

- For Rankine type the maximum principal stress should not exceed the tensile strength.

$$\sigma_1 < \sigma_t$$

For more information on the Rankine model, see Section 2.14.

Figure 4.2.11 Mohr-Coulomb failure surface shape in principal stress space

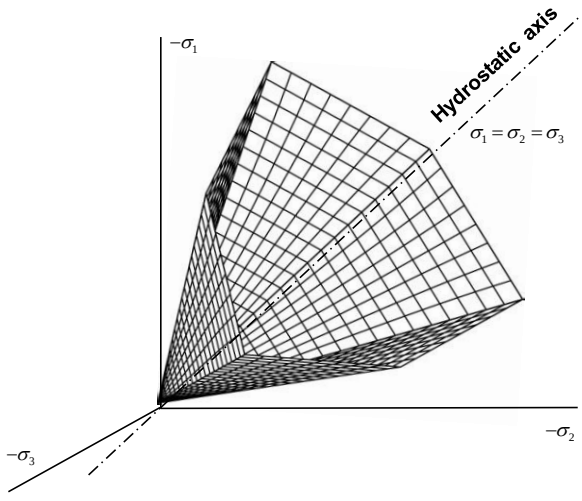

Figure 4.2.12 Mohr-Coulomb failure surface shape in π plane and meridian plane

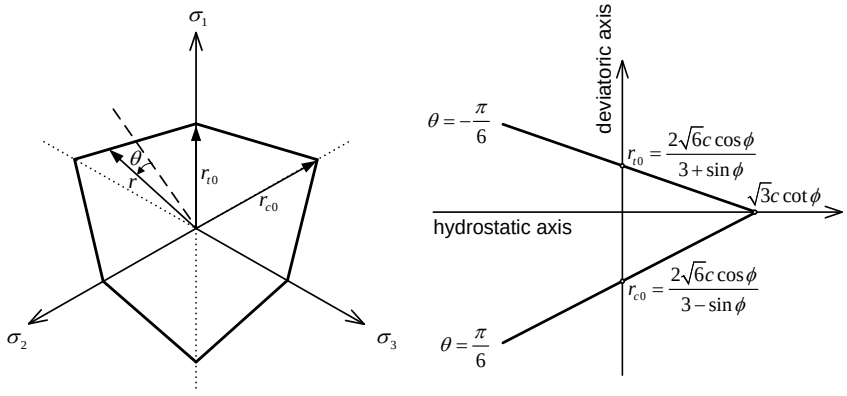

(a) Failure surface shape in π plane (b) Failure surface shape in the meridian plane for $\theta = -\frac{\pi}{6}$

As shown in Figure 4.2.12(b), $\tan\phi$ corresponding to the slope of the straight failure surface of the Mohr-Coulomb failure criterion does not change with the confining pressure (or hydrostatic pressure). Hence, the criterion is accurate when the confining stress is within a limited range, but it does not agree with actual physical phenomena when the confining stress is larg enough to cause compressive failure. However, this criterion gives highly accurate results within the confining stress ranges of the field and it is easy to use. Hence, it is the most widely used failure model.

2.6 Drucker-Prager

The Drucker-Prager model[3] was developed to solve the numerical problems that occur on the corners of the yield shape of the Mohr-Coulomb model. This model is an expansion of the von Mises model and because the function is defined such that the deviatoric stress can increase or decrease depending on hydrostatic pressure, it is also called the Extended von Mises criterion.

Yield function of Drucker-Prager model

Thye Drucker-Prager failure criterion (f) and plastic potential function(g) can be expressed using the stress invariant terms I_1 and J_2 as follows:

$$f(I_1, J_2) = \sqrt{3J_2} - \alpha I_1 - \beta c = 0$$
$$g(I_1, J_2) = \sqrt{3J_2} - \gamma I_1 = 0 \qquad (4.2.66)$$

Here, α , β , γ are as follows:

[3] Drucker, D. C. and Prager, W. "Soil mechanics and plastic analysis for limit design," Quarterly of Applied Mathematics, vol. 10, no. 2, 1952, pp. 157–165.

$$\alpha = \frac{2\sin\phi}{3-\sin\phi}, \quad \beta = \frac{6\cos\phi}{3-\sin\phi}, \quad \gamma = \frac{2\sin\psi}{3-\sin\psi} \tag{4.2.58}$$

The Drucker-Prager failure surface can be expressed in the principal stress space, as shown in Figure 4.2.13. This failure surface has a conical shape with the hydrostatic axis ($\sigma_1 = \sigma_2 = \sigma_3$) as its center. The Drucker-Prager failure surface can be thought of as a Mohr-Coulomb failure surface with no edges, or it can be thought of as the expanded form of the von Mises failure surface for materials that depend on hydrostatic pressure, such as soil. If it is assumed to circumscribe the outer boundary of the Mohr-Coulomb failure surface, then α and β can be expressed as follows.

$$\alpha = \frac{\tan\phi}{\left(9+12\tan^2\phi\right)^{1/2}}, \quad \beta = \frac{3}{\left(9+12\tan^2\phi\right)^{1/2}} \tag{4.2.68}$$

Figure 4.2.13 Drucker-Prager failure surface shape in principal stress space

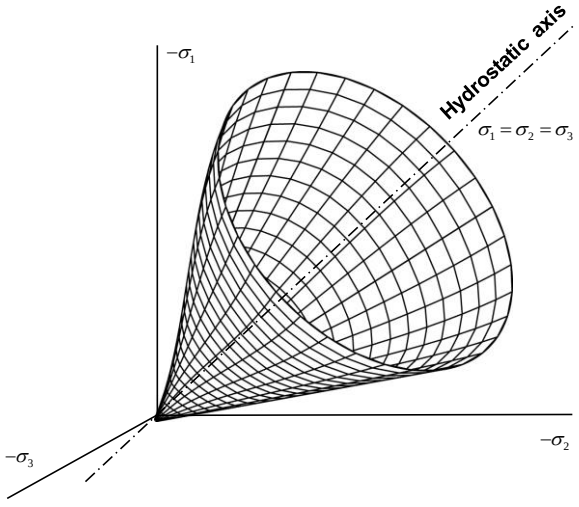

Figure 4.2.14 Drucker-Prager failure surface shape in π plane and meridian plane

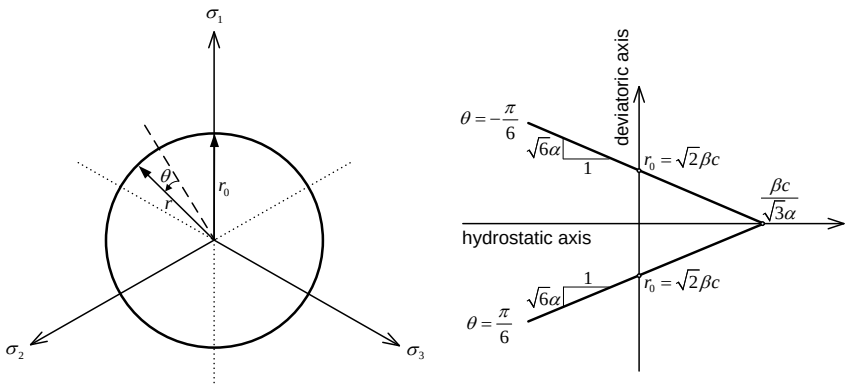

(a) Failure surface shape in π plane (b) Failure surface shape in meridian plane

2.7 Strain Softening

FEA NX provides the strain softening model with the stress-strain curve shown in Figure 4.2.15. This stress-strain curve is composed of 3 linear sections. The linear sections are the elastic section to peak shear strength, the strain softening section from peak to residual shear strength, and the constant residual shear strength section.

Figure 4.2.15 Strain softening composition relationship

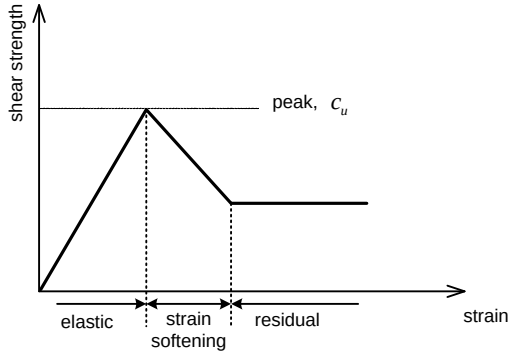

Failure criterion

The strain softening model of FEA NX is an elastic-soft plastic model that uses the von Mises model. The softening behavior is isotropic softening behavior and is formulated based on the strain softening theory. The yield function of the strain softening model can be expressed using the shear stress and shear strength terms, as shown in equation (4.2.69).

$$f = \sqrt{3J_2} - \sqrt{3}C_u(\kappa) \tag{4.2.69}$$

Here, the shear strength C_u can be expressed using the softening coefficient κ as shown in Figure 4.2.15 using equation (4.2.70):

$$C_u = \begin{cases} C_u & \text{when} \quad \kappa = 0 \\ C_u - R\kappa & \text{when} \quad 0 < \kappa < \kappa_{res} \\ C_{res} & \text{when} \quad \kappa > \kappa_{res} \end{cases} \tag{4.2.70}$$

C_u : Maximum cohesive shear strength

C_{res} : Residual cohesive shear strength

κ : Softening coefficient

κ_{res} : Softening coefficient at intersection of residual strength line and softening line

R : Softening rate

The softening coefficient κ is a control variable that controls the plastic softening behavior and is calculated from the principal plastic strain. The principal plastic strain of the von Mises model is as follows:

$$\boldsymbol{\varepsilon}^{\mathrm{p}} = \lambda \mathbf{m} = \lambda \frac{1}{2\sigma_e} \begin{Bmatrix} 2\sigma_1 - \sigma_2 - \sigma_3 \\ -\sigma_1 + 2\sigma_2 - \sigma_3 \\ -\sigma_1 - \sigma_2 + 2\sigma_3 \end{Bmatrix} \tag{4.2.71}$$

Here,

$$\sigma_e = \sqrt{\frac{1}{2}\boldsymbol{\sigma}^T \mathbf{P} \boldsymbol{\sigma}}, \quad \boldsymbol{\sigma} = \begin{Bmatrix} \sigma_{xx} \\ \sigma_{yy} \\ \sigma_{zz} \\ \tau_{xy} \\ \tau_{yz} \\ \tau_{zx} \end{Bmatrix}, \quad \mathbf{P} = \begin{bmatrix} 2 & -1 & -1 & 0 & 0 & 0 \\ -1 & 2 & -1 & 0 & 0 & 0 \\ -1 & -1 & 2 & 0 & 0 & 0 \\ 0 & 0 & 0 & 6 & 0 & 0 \\ 0 & 0 & 0 & 0 & 6 & 0 \\ 0 & 0 & 0 & 0 & 0 & 6 \end{bmatrix} \tag{4.2.72}$$

The softening coefficient κ can be calculated from the following equation and the κ - C_u relationship is shown in Figure 4.2.16.

$$\kappa = \sqrt{\frac{2}{3}\left(\boldsymbol{\varepsilon}^{\mathrm{p}}\right)^{\mathrm{T}} \mathbf{Q}\, \boldsymbol{\varepsilon}^{\mathrm{p}}} \tag{4.2.73}$$

Figure 4.2.16 Definition of softening behavior

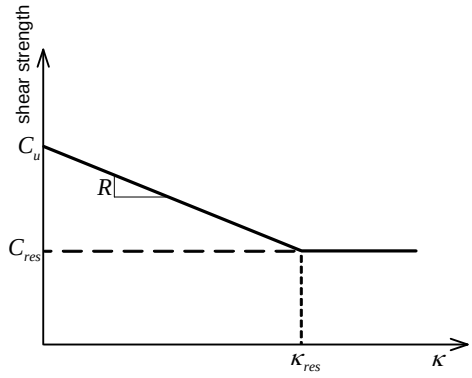

2.8 Modified Cam-Clay

Simulating clay like materials as elastic-plastic hardening materials is a widely used concept (Britto and Gunn[4]). The Modified Cam-clay model provided in FEA NX is also based on the elastic-plastic hardening theory.

Formulation of the Modified Cam-clay model in FEA NX uses all effective stresses and is materialized using nonlinear elastic and the implicit backward Euler method (R.I. Borja[5]). Nonlinear elastic behavior represents the increase in bulk modulus when pressure is applied to the material. Also, the associated flow rule is used and the failure surface can increase or decrease depending on hardening/softening behavior.
Figure 4.2.17(a) displays the relationship between the ground volume change and hydrostatic pressure using the normal consolidation line and over-consolidation line, or swelling line. If the stress increases and surpasses the hydrostatic pressure, the volume change follows the over-consolidation line. If the increase in hydrostatic pressure is enough, the volume change passes through the intersection of the normal and over-consolidated lines and follows the normal consolidation line.

Rotating Figure 4.2.17(a) in the counter clockwise direction by 90°shows similarities with the elastic-plastic hardening stress-strain curve in Figure 4.2.17(b). In other words, the overconsolidation line corresponds to the initial linear elastic section and the normal consolidation line corresponds to the hardening plastic stress-strain relationship.

[4] Britto, A. M., Gunn, M. J. Critical state soil mechanics via finite elements, Ellishorwood Limited, 1987.

[5] Borja, R. I., "Cam-clay plasticity, Part II: Implicit integration of constitutive equation based on a nonlinear elastic stress predictor," Computer Methods in Applied Mechanics and Engineering, Vol. 88, Issue 2, 1991, pp. 225-240.

Figure 4.2.17 Similarity between volume-hydrostatic pressure and stress-strain relationships

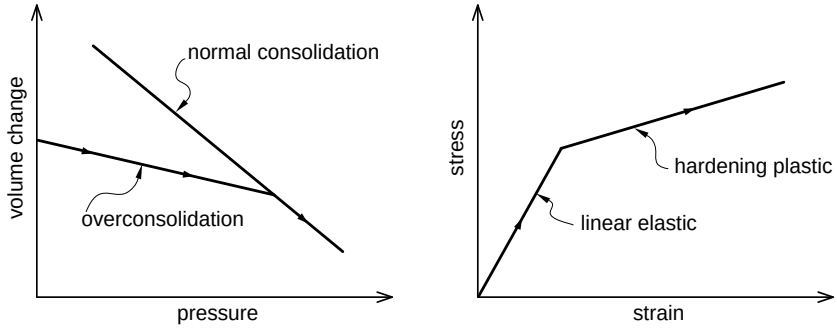

(a) Volume-hydrostatic pressure relationship (b) Stress-strain relationship

Figure 4.2.18 displays the pressure, volume and critical state line relationship. M is defined as the slope of the critical state line in Figure 4.2.18(a) projected onto the $p'-q$ plane, as shown in Figure 4.2.18(b).

Figure 4.2.18 Critical state line

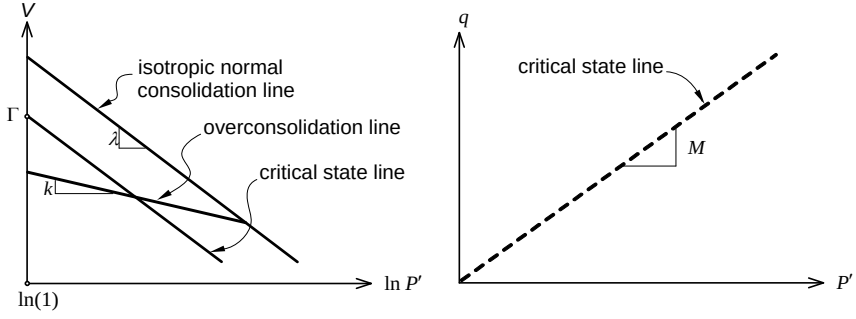

(a) Pressure and specific volume relationship (b) Critical state line

Table 4.2.2 Modified Cam-clay material properties

Symbol	Significance
κ	Slope of over-consolidation line
λ	Slope of normally consolidation line
M	Slope of critical state line

The material properties of the ground are generally obtained from 1D consolidation experiments. The compression index C_c and recompression index C_s are generally obtained from the void ratio, e and $\log_{10}(p)$ graph. The compression index and recompression index have the following equation using the slope of normal consolidation line λ and slope of over-consolidation line κ :

$$\lambda = \frac{C_c}{2.303} \quad , \quad \kappa = \frac{C_s}{2.303} \tag{4.2.74}$$

The slope of the critical state line M can be estimated from the relationship with the effective shear resistance angle (shear resistance angle from drained tests).

$$M = \frac{6\sin\phi}{3-\sin\phi} \tag{4.2.75}$$

ϕ : Internal friction angle, calculated from triaxial compression test

Γ can be calculated using the following equation, after the specific volume N of the normal consolidation line at $p = 1.0$ is found from Figure 4.2.18(a).

$$\Gamma = N - (\lambda - \kappa)\ln 2 \tag{4.2.76}$$

The yield function of Modified Cam-clay is as follows, and it displays an elliptic shape:

$$\begin{aligned} f(\boldsymbol{\sigma}) &= \frac{q^2}{M^2} + p'(p' - p_c') = 0 \\ p' &= -\frac{1}{3}\sigma'_{kk}\,\delta_{ij} \\ q &= \sqrt{\frac{3}{2}\mathbf{s}:\mathbf{s}} \\ s_{ij} &= \sigma'_{ij} - \frac{1}{3}\sigma'_{kk}\,\delta_{ij} \end{aligned} \tag{4.2.77}$$

p_c' : Pre-consolidation pressure

M : Slope of critical state line

σ'_{ij} : Effective stress

Figure 4.2.19 Yield function of Modified Cam-clay model

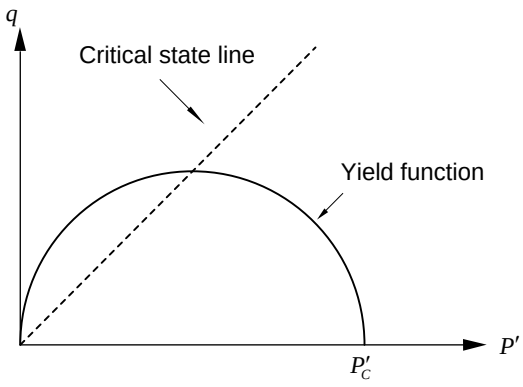

When the ground reaches the critical state, the following relationship is satisfied:

$$q = Mp' \tag{4.2.78}$$

The size of the Modified Cam-clay model failure surface is determined by p'_C . In other words, increasing p'_C increases the failure surface and can simulate hardening behavior, and reducing p'_C can simulate softening behavior. The hardening/softening equation for Modified Cam-clay models can be obtained from the following process:

Firstly, the volumetric strain change and its relationship with the specific volume change are defined by the following equation:

$$d\varepsilon_v = \frac{dV}{V} = \frac{dv}{1+e} \tag{4.2.79}$$

e : Void ratio

v : Specific volume

ε_v : Volumetric strain

Also, the additive decomposition of strain is assumed for the Modified Cam-clay model as shown below:

$$d\varepsilon_v = d\varepsilon_v^e + d\varepsilon_v^p \tag{4.2.80}$$

The following equation can be obtained from equations (4.2.79) and (4.2.80).

$$dv = (1+e)\,d\varepsilon_v = (1+e)(d\varepsilon_v^e + d\varepsilon_v^p) = dv^e + dv^p$$
$$dv^p = dv - dv^e \tag{4.2.81}$$

The v and p_c' relationship can be rearranged using Figure 4.2.20.

Figure 4.2.20 Pressure and specific volume relationship

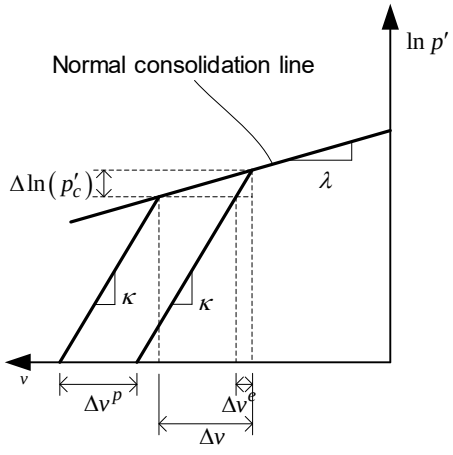

$$dv^e = -\kappa d\ln(p_c') = -\kappa\frac{dp_c'}{p_c'}$$
$$dv = -\lambda d\ln(p_c') = -\lambda\frac{dp_c'}{p_c'} \tag{4.2.82}$$

Rearranging equations (4.2.81) and (4.2.82) are as follows:

$$dv^p = dv - dv^e = -(\lambda-\kappa)\frac{dp_c'}{p_c'}$$
$$\frac{dp_c'}{p_c'} = -\frac{1+e}{\lambda-\kappa}d\varepsilon_v^p \tag{4.2.83}$$

Integrating equation (4.2.83) gives the following hardening/softening equation:

$$p_c' = p_{c0}'\exp(-\frac{1+e}{\lambda-\kappa}\Delta\varepsilon_v^p) \tag{4.2.84}$$

Also, Modified Cam-clay material models have the following nonlinear elastic properties:

$$K = \frac{1+e}{\kappa} p', \; G = \frac{3(1-2\nu)}{2(1+\nu)} K \tag{4.2.85}$$

K : Bulk modulus

G : Shear modulus

e : Void ratio

However, the effective pressure is unknown when calculating the initial stress state and so, the given linear elastic modulus is used.

To use the Modified Cam-clay model, the initial void ratio, in-situ stress and initial pre-consolidation pressure p'_c is required. FEA NX uses a direct input value or a value automatically calculated from in-situ stresses and over-consolidation ratio (OCR) for the pre-consolidation pressure p'_c . The user needs to input the initial void ratio.

The over-consolidation ratio (OCR) is defined using equation (4.2.86). The $p'_{\max}$ is the maximum effective hydrostatic pressure on the material, and p'_v is the initial effective hydrostatic pressure. Generally, the maximum effective normal stress experienced by the ground is determined from oedometer tests.

$$OCR = \frac{p'_{\max}}{p'} \tag{4.2.86}$$

For a clear explanation, it is assumed that the shear stress does not exist and the gravitational direction is the y axis. Then, the in-situ stress becomes equation (4.2.87).

$$\boldsymbol{\sigma}'_0 = \{\sigma'_{X0} \quad \sigma'_{Y0} \quad \sigma'_{Z0} \quad 0 \quad 0 \quad 0\}^T \tag{4.2.87}$$

To calculate p'_c , first use the OCR and equations (4.2.88) and (4.2.89) to calculate $p'_{\max}$ and $q_{\max}$.

$$\boldsymbol{\sigma}'_{\max} = \{\mathrm{OCR}\sigma'_{X0} \quad \mathrm{OCR}\sigma'_{Y0} \quad \mathrm{OCR}\sigma'_{Z0} \quad 0 \quad 0 \quad 0\}^T \tag{4.2.88-a}$$

$$\boldsymbol{\sigma}'_{\max} = \{\mathrm{OCR}\sigma'_{Y0}K_0 \quad \mathrm{OCR}\sigma'_{Y0} \quad \mathrm{OCR}\sigma'_{Y0}K_0 \quad 0 \quad 0 \quad 0\}^T \tag{4.2.88-b}$$

$$\begin{aligned} p'_{\max} &= \frac{1}{3}\left(\sigma'_{x\max} + \sigma'_{y\max} + \sigma'_{z\max}\right) \\ q'_{\max} &= \frac{1}{\sqrt{2}}\sqrt{\left(\sigma'_{x\max} - \sigma'_{y\max}\right)^2 + \left(\sigma'_{y\max} - \sigma'_{z\max}\right)^2 + \left(\sigma'_{z\max} - \sigma'_{x\max}\right)^2} \end{aligned} \tag{4.2.89}$$

The K_0 condition is also applied to equation (4.2.88-b). K_0 can be estimated from the internal friction angle using the following equation:

$$K_0 = \frac{\sigma'_h}{\sigma'_v} = 1 - \sin\phi' \tag{4.2.90}$$

σ'_h : Horizontal direction effective stress

FEA NX uses equation (4.2.77) to calculate p'_c. If the user inputs the p'_c value directly, FEA NX tests whether the input value and in-situ stress state satisfy equation (4.2.77) and adjusts the value when it is not satisfactory.

2.9 Jointed Rock

General ground surface strata have brittle fracture surfaces, and these are called 'joints' for rock models. The material models that reflect these properties are called jointed rock models.

Jointed rock models are transversely isotropic perfectly plastic material models. The material can have transversely isotropic properties depending on the rock layer characteristics in the elastic region. In other words, rock layers have isotropic properties in the layer direction, but have anisotropic properties in the normal direction to the layer. The perfectly plastic behavior is based on the Coulomb friction function in the major joint direction. Hence, perfect plasticity occurs in the major joint direction when maximum shear stress is reached. The major joint direction can be defined in a maximum of 3 directions and the first major joint direction is equal to the transversely isotropic material direction.

Orthotropic elastic material stiffness

The elastic material behavior of jointed rock models are already explained for transversely isotropic elastic materials above.

Plastic behavior in 3 directions

The yield function in the major joint direction i can be defined using equation (4.2.82):

$$f_i = \sqrt{\tau_s^2 + \tau_t^2} + \sigma_n \tan\phi_i - c_i \tag{4.2.91}$$

Figure 4.2.21 Yield criterion for individual planes

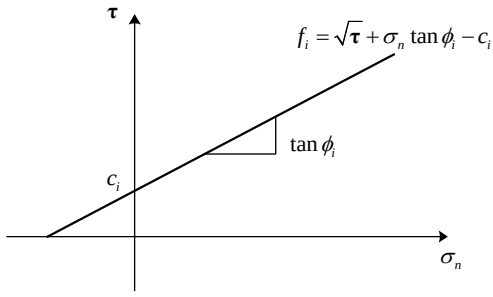

To examine the plasticity condition for each failure surface, stress transformation to the local coordinate system (n , s , t) is required.

$$\boldsymbol{\sigma}_{nst} = \mathbf{T}_i^T \boldsymbol{\sigma}_{XYZ} \tag{4.2.92}$$

$\boldsymbol{\sigma}_{nst}$: Stress in local coordinate system

$\boldsymbol{\sigma}_{XYZ}$: Stress in material coordinate system

$\mathbf{T}_i$: Transformation matrix in the i active plane

The general 3D transformation matrix that considers the dip angle and dip direction is as follows:

$$\mathbf{T}_i^T = \begin{bmatrix} n_x^2 & n_y^2 & n_z^2 & 2n_x n_y & 2n_y n_z & 2n_z n_x \\ n_x s_x & n_y s_y & n_z s_z & n_x s_y + n_y s_x & n_z s_y + n_y s_z & n_z s_x + n_x s_z \\ n_x t_x & n_y t_y & n_z t_z & n_y t_x + n_x t_y & n_y t_z + n_z t_y & n_z t_x + n_x t_z \end{bmatrix} \tag{4.2.93}$$

Here, the 3D $\mathbf{n}_i$, $\mathbf{s}_i$, $\mathbf{t}_i$ is as follows:

$$\mathbf{n}_i = \begin{bmatrix} \sin\alpha_1 \cdot \cos\alpha_3 \\ -\sin\alpha_1 \cdot \sin\alpha_3 \\ \cos\alpha_1 \end{bmatrix}, \mathbf{s}_i = \begin{bmatrix} \cos\alpha_1 \cdot \cos\alpha_3 \\ -\cos\alpha_1 \cdot \sin\alpha_3 \\ -\sin\alpha_1 \end{bmatrix}, \mathbf{t}_i = \begin{bmatrix} \sin\alpha_3 \\ \cos\alpha_3 \\ 0 \end{bmatrix} \tag{4.2.94}$$

Expressing the local coordinate system by rotation in the GCS is as follows:

Figure 4.2.22 MCS from dip angle and dip direction

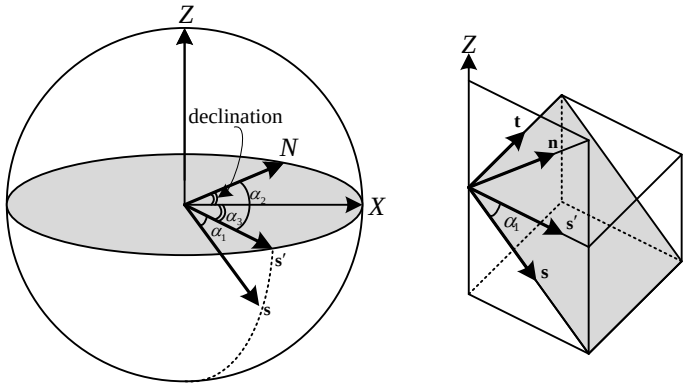

2.10 Modified Mohr-Coulomb

The Modified Mohr-Coulomb model is the expanded version of the Mohr-Coulomb model, and is a specialized model for silt or sand. Modified Mohr-Coulomb models are complex material models which combine nonlinear elastic and plastic models.

Nonlinear elastic

The Modified Mohr-Coulomb model defines the elastic region as nonlinear elastic and the power-law is used to obtain the elastic volumetric stress-strain relationship. In other words, the tangent compression modulus is expressed as a water supply form of the current hydrostatic pressure, as shown below:

$$K_t = K_{ref}\left(\frac{p}{p_{ref}}\right)^{1-m} \tag{4.2.95}$$

K_{ref} : Reference coefficient of compressibility

p_{ref} : Reference pressure

m : Rational number, '0.5' used for sand $0 < m < 1$

The following equation can be expressed by considering the tensile pressure (p_t):

$$K_t = K_{ref}\left(\frac{p + p_t}{p_{ref}}\right)^{1-m} \tag{4.2.96}$$

Here, the tensile pressure is a numerical invention used to consider the tensile stress when an in-situ pressure of '0' is assumed. However, actual soil analysis nearly always considers non-zero in-situ stresses.
The equation (4.2.96) above is derived as the volumetric stress-strain relationship, as shown in the equation (4.2.97):

$$\left(\frac{p+p_t}{p_{ref}}\right)^{m-1} dp = K_{ref}\, d\varepsilon_V^e \tag{4.2.97}$$

Integrating equation (4.2.97) and rearranging gives equation (4.2.98):

$$p = -p_t + \left(\left(p_0 + p_t \right)^m - m p_{ref}^{m-1} K_{ref} \Delta\varepsilon_V^e \right)^{\frac{1}{m}} = F\left(\Delta\varepsilon_V^e\right) \tag{4.2.98}$$

Yield function

The failure surface of the Modified Mohr-Coulomb model is a decoupled double hardening model, where shear failure and compressive failure do not affect each other. This coupled failure surface has the following equation in the $p-q$ space:

$$\begin{aligned} f_1 &= \frac{q}{R_1(\theta)} - \frac{6\sin\phi}{3-\sin\phi}\left(p+\Delta p\right) = 0 \\ f_2 &= \left(p+\Delta p\right)^2 + \alpha\left(\frac{q}{R_2(\theta)}\right)^2 - p_c^2 = 0 \end{aligned} \tag{4.2.99}$$

f_1 : Shear yield function

f_2 : Compressive yield function

Figure 4.2.23 Shape of yield function in p-q plane

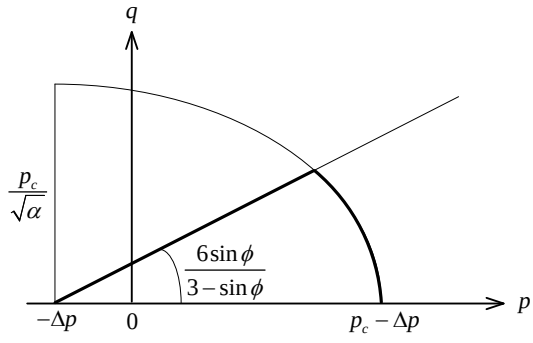

Figure 4.2.24 Shape of yield function in deviatoric plane

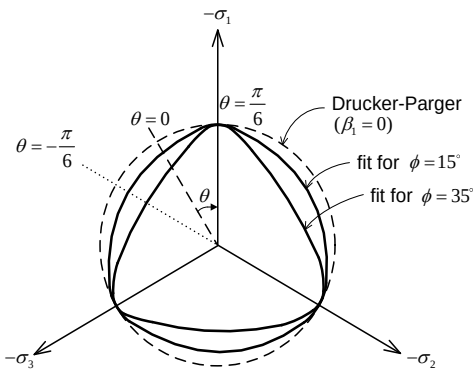

The functions $R_1(\theta)$, $R_2(\theta)$ of equation (4.2.99) model the strength difference between triaxial compression and triaxial tension as a function of θ. The Modified Mohr-Coulomb model can be expressed in the same way as a Mohr-Coulomb model using functions $R_1(\theta)$, $R_2(\theta)$ in the deviatoric plane.

A relationship like the one found in equation (4.2.100) is derived to fit the triaxial tensile Mohr-Coulomb model.

$$R_1(\theta) = \left(\frac{1 - \beta_1 \sin 3\theta}{1 - \beta_1} \right)^n \tag{4.2.100}$$

Here, n = -0.229 .

β_1 is coupled with the friction angle, as shown in equation (4.2.101).

$$\beta_1 = \frac{\left(\frac{3 + \sin\phi}{3 - \sin\phi} \right)^{-\frac{1}{n}} - 1}{\left(\frac{3 + \sin\phi}{3 - \sin\phi} \right)^{-\frac{1}{n}} + 1} \tag{4.2.101}$$

Here, $\beta_1 \le 0.7925$.

The maximum value of β_1 is the friction angle (ϕ) 46.55°. Also, the shape of the compression cap can be modified using $R_2(\theta)$. $R_2(\theta)$ is the same as equation (4.2.102) below.

$$R_2(\theta) = \left(\frac{1 - \beta_2 \sin 3\theta}{1 - \beta_2} \right)^2 \tag{4.2.102}$$

Here, n = -0.229 and the cap is circular when the basic value '0' is used for β_2.

Flow rule

The plastic potential function in the $p-q$ plane can be expressed as follows. For the Modified Mohr-Coulomb model, it is applied to 2 faces that consider shear and compression.

$$\begin{aligned} q_1 &= q - \frac{6\sin\psi}{3-\sin\psi}\left(p+\Delta p\right) \\ q_2 &= \left(p+\Delta p\right)^2 + \alpha q^2 - p_c^2 \end{aligned} \tag{4.2.103}$$

Here, the dilatancy angle ψ can be expressed using the friction angle ϕ, as shown in equation (4.2.104).

$$\sin\psi = \frac{\sin\phi - \sin\phi_{cv}}{1-\sin\phi\sin\phi_{cv}} \tag{4.2.104}$$

$\sin\phi_{cv}$: Friction angle when volume is constant

Hardening behavior

Two types of shear and compression hardening behavior are applied in the Modified Mohr-Coulomb model. The shear hardening behavior is determined by the friction angle and can be expressed as the following equation. If the shear hardening occurs, the dilatancy angle is recalculated by the Row's rule[6] (4.2.104).

$$\sin\phi = \sin\phi(\kappa) \tag{4.2.105}$$

$$\kappa = \sqrt{\frac{2}{3}\boldsymbol{\gamma}_{\mathbf{p}} \cdot \boldsymbol{\gamma}_{\mathbf{p}}} \tag{4.2.106}$$

κ : Equivalent deviatoric plastic strain

$\boldsymbol{\gamma}_{\mathbf{p}}$: Deviatoric plastic strain

The compression hardening behavior is expressed by the pre-consolidation stress as the following equation.

$$P_c = p_{ref}\left(\left(\frac{P_{c0}}{p_{ref}}\right)^m + \frac{m}{\Gamma}\Delta\varepsilon_v^p\right)^{\frac{1}{m}} \tag{4.2.107}$$

P_c : Pre-consolidation stress

[6] ROWE, P. W. The stress-dilatancy relation for static equilibrium of an assembly of particles in contact. Proc. Roy. Soc. London A269 (1962), 500-527.

P_{c0} : Pre-overburden pressure

Γ : Compression cap hardening parameter

2.11 Hoek-Brown

Hoek and Brown[7] suggested the use of the equivalent continuum concept to define the stress reduction phenomena due to failure of jointed rocks. Hoek and Brown first suggested a failure function to separate intact rock and broken rock. After the failure is defined, the stress reduction phenomena were simulated by decreasing the particular coefficient values that define the failure function. This method suggested by Hoek and Brown defines the uniaxial compressive strength, which cannot be considered in the existing Mohr-Coulomb method. This allows for the accurate and simple representation of rock behavior.

Yield function

The failure criterion suggested by Hoek and Brown is as follows. The intermediate principal stress (σ_2) term is ignored in this failure criterion.

$$\sigma_1 = \sigma_3 + \sqrt{m\sigma_c\sigma_3 + s\sigma_c^2}$$
$$\sigma_1 \geq \sigma_2 \geq \sigma_3 \qquad (4.2.108)$$

σ_c : Uniaxial compressive strength

m , s : Empirical coefficient for defining rock failure

The yield function (f) can be expressed using the stress invariant as follows:

$$f = 4J_2\cos^2\theta + m\sigma_c\sqrt{2}\left(-\frac{\sin\theta}{\sqrt{3}} + \cos\theta\right) + m\sigma_c\frac{I_1}{3} - s\sigma_c^2 = 0 \qquad (4.2.109)$$

I_1 : First order invariant

J_2 : Second order invariant

σ_c : Uniaxial compressive strength of the rock ($-\pi/6 \leq \theta \leq \pi/6$)

In the principal stress space, the Hoek-Brown model has a diverging hexagonal pyramid shape along the hydrostatic axis and its deviatoric plane shape is expressed as an angular hexagonal shape made up of 6 curved surfaces. This hexagonal shape has an edge where the curved surfaces meet, and this creates difficulties. To solve this problem, FEA NX processes these edges as curved surfaces using the modified Hoek-Brown criterion suggested by Wan[8].

---

[7] Hoek, E. and Brown, E. T., "Empirical strength criterion for rock masses," Journal of Geotechnical and Geoenvironmental Engineering, Vol. 106, Issue GT9, 1980.

[8] Wan, R. "Stress return solution algorithm for generalized Hoek-Brown plasticity model," Proceedings of the 8th

$$f = q^2 g^2(\theta) + \sigma_c^* q g(\theta) + 3\sigma_c^* p - s\sigma_c^2 = 0 \quad (4.2.110)$$

Here, $\sigma_c^* = m\sigma_c / 3$, $q = \sqrt{3J_2}$, $p = I_1 / 3$ and the $g(\theta)$ used to define the deviatoric plane shape is as follows:

$$g(\theta) = \frac{4(1-e^2)\cos^2(\pi/6+\theta) + (1-2e)^2}{2(1-e^2)\cos^2(\pi/6+\theta) + (2e-1)D} \quad (4.2.111)$$

Here, $D = \sqrt{4(1-e^2)\cos^2(\pi/6+\theta) + 5e^2 - 4e}$

Figure 4.2.25 displays the shape of the Hoek-Brown model in the stress space.

Figure 4.2.25 Hoek-Brown failure surface

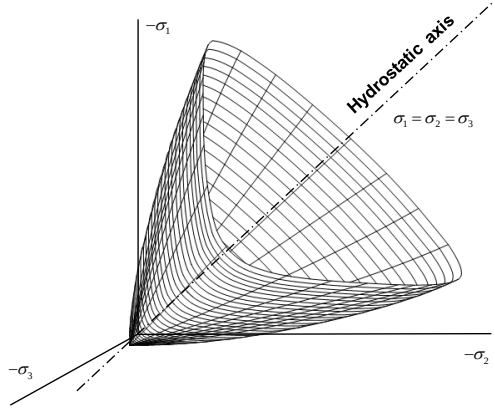

2.12 Coulomb Friction

The Coulomb friction model assumes that the frictional force is proportional to the size of the value obtained by multiplying the coefficient of friction and the tangent direction force. FEA NX defines the yield function of the model using the equation below:

$$f = \sqrt{\mathbf{t}_t^2} + t_n \tan\phi(\kappa) - c(\kappa) = 0 \quad (4.2.112)$$

$\mathbf{t}_t$: Lateral direction force

t_n : Normal direction force

ϕ : Internal friction angle

International Conference of the Association for Computer Methods and Advances in Geomechanics, Morgantown, USA, 1994, pp. 719-724.

C : Cohesion

κ : Size of plastic relative displacement

In FEA NX, the internal friction angle and cohesion can be set as a functional value that depends on the plastic relative displacement.

The equation above can be expressed as Figure 4.2.26. FEA NX supports additional tensile strength inputs to express brittle behavior in the tensile direction.

Figure 4.2.26 Coulomb friction function

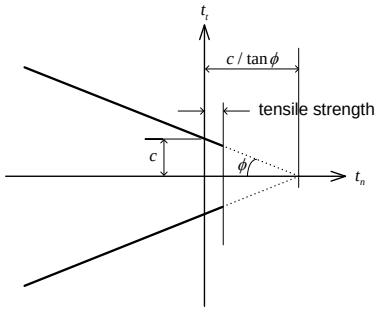

The plastic relative displacement $\Delta\dot{\mathbf{u}}^p$ can be defined using the plastic multiplier, which represents size and plastic direction components as shown below:

$$\Delta\dot{\mathbf{u}}^p = \dot{\lambda}\frac{\partial g}{\partial \mathbf{t}}$$
$$g = \sqrt{\mathbf{t}_t^2} + t_n \tan\psi \qquad (4.2.113)$$

ψ : Dilatency angle

$\dot{\lambda}$: Plastic multiplier

2.13 Janssen

Here, the plastic multiplier can be calculated from the map regression method.
The Janssen model, which is applied to the rotational DOF of shell interface elements, simulates the nonlinear elastic relationship between the moment and rotational displacement. FEA NX provides for the Coulomb friction model and Janssen model for shell interface elements. The Coulomb friction model is used to define the normal and lateral direction forces.

$$m_y = \begin{cases} 0 \;\&\; t_x = t_y = t_z = 0 & if\ \Delta u_x \geq 0 \\ \dfrac{K_n b^3}{12}\Delta\phi_y & if\ \Delta\phi_y \leq \dfrac{2t_x}{K_n b^2} \quad , \quad t_x = K_x b \Delta u_x \\ \dfrac{\Delta\phi_y}{|\Delta\phi_y|}\dfrac{|t_x| b}{2}\left[1 - \sqrt{\dfrac{8|t_x|}{9|\Delta\phi_y| K_n b^2}}\right] & if\ \Delta\phi_y > \dfrac{2t_x}{K_n b^2} \end{cases} \tag{4.2.114}$$

t_x / Δu_x : Normal interface traction / Normal relative displacement

t_y , t_z : Tangential interface traction

m_y , $\Delta\phi_y$: Axial moment / rotation angle

b : Thickness of shell interface element

K_n : Tangential stiffness

Only perfectly plastic behavior is supported for Coulomb friction models used on shell interface elements.

2.14 Rankine/Inverse Rankine

Geogrids are reinforcing structures used to strengthen the ground and have only the tensile only structural behavioral properties. When selecting the geogrid element in FEA NX, the inverse Rankine model applied on a truss elements is used for 2D models and the inverse Rankine model applied on a plane stress element is used for 3D models. Here, the allowable compressive strength is '0(zero)'. The inverse Rankine model only needs to be computed using the opposite sign from the Rankine model defined below.

The Rankine material failure assumes that failure occurs when the maximum principal stress ($\sigma_{\max}$) reaches the tensile strength and the yield function is as follows:

$$f = \sigma_{\max} - \sigma_t(\kappa) = 0 \tag{4.2.115}$$

Expressing equation (4.2.115) using the invariants I_1, J_2, θ are as follows.

$$f = \frac{2}{\sqrt{3}}\sqrt{J_2}A(\theta) + \frac{I_1}{3} \tag{4.2.116}$$

Here, $A(\theta)$ is

$$A(\theta)=\begin{cases}\dfrac{\sqrt{3}}{2}\cos\theta-\dfrac{1}{2}\sin\theta & \text{for } \sigma_1\\ \sin\theta & \text{for } \sigma_2\\ -\dfrac{\sqrt{3}}{2}\cos\theta+\dfrac{1}{2}\sin\theta & \text{for } \sigma_3\end{cases} \tag{4.2.117}$$

Figure 4.2.27 displays the 3D shape of the inverse Rankine model in the stress space. The shape is a right triangle in the deviatoric plane (π plane) as shown in Figure 4.2.28, and it can be defined as a linear function about the hydrostatic axis in the meridian plane.

Figure 4.2.27 Rankine failure surface shape in principal stress space

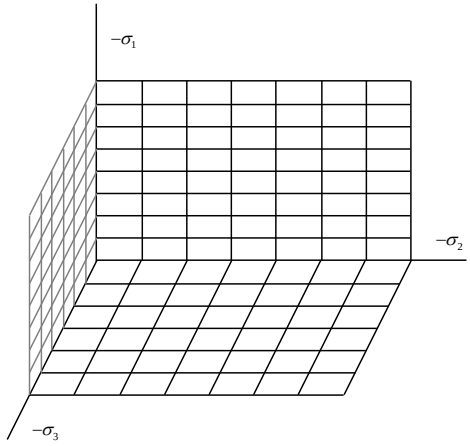

Figure 4.2.28 Rankine failure surface shape in deviatoric plane (π plane) and meridian plane

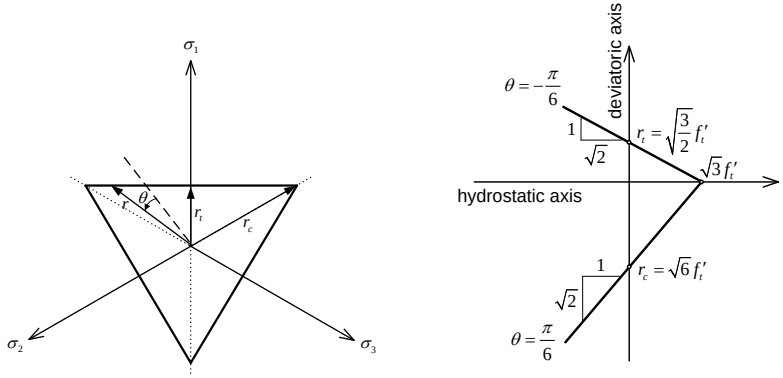

(a) Failure surface shape in deviatoric plane (π plane) (b) Failure surface shape in meridian plane for $\theta=-\frac{\pi}{6}$

2.15 Modified UBCSAND

The Modified UBCSAND model is developed to simulate liquefaction phenomenon using plastic theory based on effective stress. It is extended to enable implicit nonlinear analysis for 3D stress state based on the constitutive model[9, 10] developed to simulate liquefaction phenomenon with explicit method for 2D stress state. Basically, in the elastic domain, it represents a nonlinear elastic behavior that elastic modulus changes with respect to pressure. A plastic behavior is determined by three yield functions of shear, compression and pressure off. In particular, the shear yield function is able to consider the effect of material densification for cyclic loading. The Modified UBCSAND model is implemented as the implicit backward Euler method to maximize convergence and efficiency and uses a consistent tangent stiffness matrix

Nonlinear elasticity

In elastic zone, it represents a nonlinear elastic properties that elastic modulus changes with respect to effective pressure (p').

$$G^e = K_G^e p_{ref} \left(\frac{p' + p_t}{p_{ref}} \right)^{ne} \tag{4.2.118}$$

K_G^e : Elastic shear modulus number

p_{ref} : Reference pressure

ne : Elastic shear modulus exponent

p_t : Allowable tension pressure

Here, the allowable tension pressure is calculated automatically based on the cohesion and maximum friction angle. Assuming that Poisson's ratio doesn't change according to the pressure and isotropic properties are maintained, the bulk modulus is determined as follows:

$$K^e = \frac{2(1+\nu)}{3(1-2\nu)} G^e \tag{4.2.119}$$

Shear yield function

The Modified UBCSAND model represents a plastic shear behavior using Mohr-Coulomb yield function.

---

[9] Beaty, M. and Byrne, PM., "An effective stress model for predicting liquefaction behaviour of sand," In Geotechnical earthquake engineering and soil dynamics III, Americal Society of Civil Engineers, Geotechnical Special Publication 75(1), 1998, pp. 766-777.

[10] Puebla, H., Byrne, PM., and Phillips, R., "Analysis of CANLEX liquefaction embankments: protype and centrifuge models," Canadian Geotechnical Journal, 34, 1997, pp 641-657.

$$f_s = R_{mc}\sqrt{3J_2} + \frac{1}{3}I_1 \tan\phi_m - c = 0 \tag{4.2.120}$$

ϕ_m : Mobilized friction angle

Here, R_{mc} which expresses the shape of π plane is as follows:

$$R_{mc} = \frac{1}{\sqrt{3}\cos\phi_m}\sin\left(\Theta + \frac{\pi}{3}\right) + \frac{1}{3}\cos\left(\Theta + \frac{\pi}{3}\right)\tan\phi_m$$
$$\Theta = \frac{3\sqrt{3}}{2}\frac{J_3}{J_2^{3/2}} \tag{4.2.121}$$

Shear flow rule

The flow rule utilizes the following plastic potential based on the non-associated plastic flow rule[11]. Therefore, the non-associated matrix operation is performed in case of using the Modified UBCSAND model.

$$g_s = \sqrt{(\varepsilon c \tan\psi_m)^2 + 3R_{mw}{}^2 J_2} + \frac{I_1}{3}\tan\psi_m$$
$$R_{mw} = \frac{4\left(1-e^2\right)\cos^2\Theta + (2e-1)^2}{2\left(1-e^2\right)\cos\Theta + (2e-1)\sqrt{4\left(1-e^2\right)\cos^2\Theta + 5e^2 - 4e}} R_{mc}\left(\frac{\pi}{3}, \phi_m\right) \tag{4.2.122}$$

ψ_m : Mobilized dilatancy angle

The size of dilatancy angle changes with the similar form to the stress-dilatancy angle theory[12] for the variation of mobilized friction angle

$$\sin\psi_m = \sin\phi_m - \sin\phi_{cv} \tag{4.2.123}$$

ϕ_{cv} : Constant volume friction angle

In other words, the plastic deformation describes shrinkage when mobilized friction angle is smaller than constant volume friction angle whereas it describes swelling when mobilized friction angle is larger than constant volume friction angle

[11] Menetrey, P. and Willam, KJ, "Triaxial failure criterion for concrete and its generalization," ACI Structural Journal, 92:3, 1995, pp. 11-18.

[12] Rowe, P.W., "Stress-dilatancy relation for static equilibrium of an assembly of particles in contact," Proceedings of the Royal Society of London, Mathematical and Physical Scieces, Series A, 269, 1962. pp-500-557.

Figure 4.2.29 Swelling/Shrinkage according to the direction of plastic strain

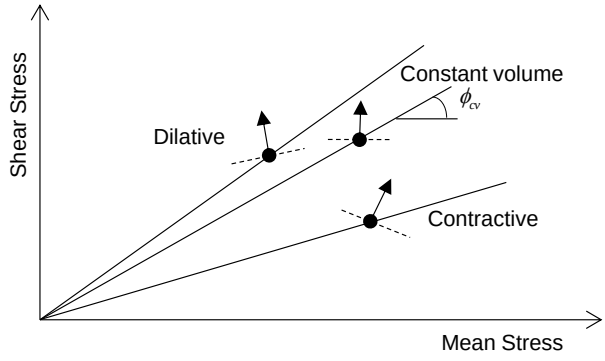

Hardening shear behavior

The hardening rule for the variation of maximum plastic shear strain is represented by the variation of stress ratio.

$$\eta = \sin\phi_m$$
$$f_s(\phi_m, \sigma) = 0 \tag{4.2.124}$$

The hardening phenomenon is determined respectively for two shear yield functions. The primary yield surface is used when the present stress ratio is the maximum stress ratio of material. On the other hand, the secondary yield surface is activated when the present stress ratio is smaller than the maximum value of material. At this time, if the stress ration exceeds the previous maximum value, the primary yield surface is activated again.

The secondary yield surface is introduced to simulate the increase of plastic stiffness for cyclic loading. Therefore, the plastic strain by secondary yield surface is smaller than by the primary yield surface. This phenomenon is called the densification of soil. On the other hand, if the load is unloading, the material maintains elastic state and the stress ratio decreases.

The hardening rule of primary yield surface is expressed with the following equation:

$$\Delta \sin\phi_m = \frac{G^p}{p'}\Delta\kappa_s = K_G^p\left(\frac{p'}{p_{ref}}\right)^{np-1}\left\{1-\left(\frac{\sin\phi_m}{\sin\phi_p}\right)R_f\right\}^2\Delta\kappa_s$$
$$\Delta\kappa_s = \left|\Delta\varepsilon_1^p - \Delta\varepsilon_3^p\right| \tag{4.2.125}$$

K_G^p : Plastic shear modulus number

p_{ref} : Reference pressure

np : Plastic shear modulus exponent

ϕ_p : Peak friction angle

R_f : Failure ratio

$\Delta\varepsilon_1^P, \Delta\varepsilon_3^P$: Min./Max. plastic strain of principal axis

Figure 4.2.30 Plastic shear hardening behavior

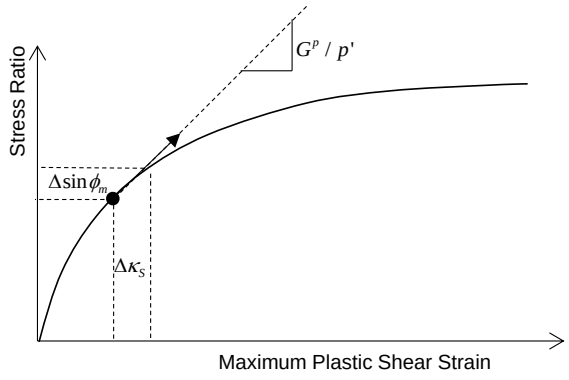

Considering the densification of soil due to cyclic loading, the hardening rule of secondary yield surface is as follows:

$$\Delta \sin\phi_m = K_{G,2}^p \left(\frac{p'}{p_{ref}} \right)^{np-1} \left\{ 1 - \left(\frac{\sin\phi_m}{\sin\phi_p} \right) R_f \right\}^2 \Delta\kappa_s$$
$$K_{G,2}^p = K_G^p \left(4 + \frac{n-1}{2} \right) F_{dens} \qquad (4.2.126)$$

$K_{G,2}^p$: Cyclic plastic shear modulus number

n : Number of half cycles

F_{dens} : Soil densification fitting factor

As the mobilized friction angle for cyclic loading closes to the maximum mobilized friction angle, the plastic shear modulus decreases and finally it closes to the perfect plastic state. In this case, the ground is determined with liquefaction. In case of reaching liquefaction, some residual hardening stiffness can be given through F_{post} .

$$K_{G,post}^p = K_G^p F_{post} \qquad (4.2.127)$$

F_{post} : Post liquefaction fitting factor

Cap yield function, flow rule and hardening behavior

The cap yield function is same with that of Modified Mohr-Coulomb model (4.2.99). It uses the associated plastic flow rule and the hardening model can be expressed with the following equation in the form what the size of compression limit increases for the plastic volumetric strain.

$$\Delta p_c = K_B^p p_{ref} \left(\frac{p'}{p_{ref}} \right)^{mp} \Delta \varepsilon_v^p \qquad (4.2.128)$$

K_B^p : Plastic bulk modulus number

mp : Plastic shear modulus exponent

Pressure cut-off yield function and flow rule

The pressure cut-off yield function can be considered additionally to add the condition what the effective pressure is always larger than specified value ($f_{pr} = p_{cut} - p'$). It uses the associated plastic flow rule and the pressure cut-off yield function does not have hardening behavior.

2.16 Sekiguchi-Ohta (Inviscid)

The Sekiguchi-Ohta model is widely used in Japan and still improved since it is developed by Sekiguchi and Ohta[13]. There are Inviscid and Viscid type. The Inviscid type is plastic model without time dependency. Although it shares several characteristic with Cam-Clay[14] model, there is a difference that the irreversible diliatancy[15] is strictly described considering the K_0 stress state of normally consolidation. However, it causes a numerical problem because the plastic flow value is only undetermined under the preconsolidation stress state. In FEA NX, it resolves numerical problem in the preconsolidation stress using the algorithms[16] which calculates the specificity vertex using the crossing of the two yield function.

Nonlinear elastic

Similarly to the Modified Cam-Clay model of FEA NX, it shows the nonlinear elastic characteristic what the elastic modulus changes with the effective stress (p) in the elastic range.

$$K = \frac{1+e_0}{\kappa} p \,,\; G = \frac{3(1-2\nu)}{2(1+\nu)} K \qquad (4.2.129)$$

---

[13] Sekiguchi, H. and Ohta, H., "Induced anisotropy and time dependency in clays", 9th ICSMFE, Tokyo, Constitutive equations of Soils, 1977, 229-238

[14] Roscoe, K. H., Schofield, A. N. and Thurairajah, A., "Yielding of Clays in States Wetter than Critical", Geotech., 1963, Vol. 13, No. 3, pp. 211-240

[15] Ohta, H., Sekiguchi, H., "Constitutive equations consdiering anisotropy and stress reorientation in clay", Proceedings of the 3rd International Conference on Numerical in Geomechanics., 1979, pp. 475-484

[16] Pipatpongsa, T., Iizula, A., Kobayashi, I., Ohta, H., "Fem formulation for analysis of soil constitutive model with a corner on the yield surface", Journal of Structural Engineering, Vol. 48, pp. 185-194

K : Bulk modulus

e_0 : Initial void ratio

κ : Slope of overconsolidation line

ν : Poisson's ratio

G : Shear modulus

Yield function

The yield function of Sekiguchi-Ohta (Inviscid) model is as follows:

$$f = MD\ln\left(\frac{p}{p_c}\right) + D\bar{\eta} = 0 \tag{4.2.130}$$

M : Slope of critical state line

D : Dilatancy modulus

p_c : Preconsolidation pressure

$\bar{\eta}$: Generalized relative stress ratio

The generalized relative stress ratio ($\bar{\eta}$) which is the value for the degree of volume expansion is expressed as follows:

$$\bar{\eta} = \sqrt{\frac{3}{2}\left(\frac{s_{ij}}{p} - \frac{s_{cij}}{p_c}\right)\left(\frac{s_{ij}}{p} - \frac{s_{cij}}{p_c}\right)} \tag{4.2.131}$$

s_{ij} : Stress deviator tensor

s_{cij} : Preconsolidation stress deviator tensor of K_0 state

In the above equation, it can be found that $\bar{\eta}$ is affected by the preconsolidation pressure and each component of stress deviator tensor. Through this, it describes strictly the dilatancy effect than Cam-Clay model which considers only the preconsolidation pressure and the present stress deviator tensor.

The dilatancy modulus (D) has the relation with slope of critical state line (M), slope of normally consolidation line (λ), slope of overconsolidation line (κ) and initial void ratio as follows:

$$MD = \lambda^* - \kappa^* \tag{4.2.132}$$

Here, $\lambda^* = \lambda/(1+e_0)$, $\kappa^* = \kappa/(1+e_0)$. The dilatancy modulus (D) is calculated internally in FEA NX.

Figure 4.2.31 displays the yield function in principal stress space. As described before, it can be found that the yield function of Sekiguchi-Ohta model has the specificity which causes a numerical problem in the preconsolidation stress.

Figure 4.2.31 Yield function in principal stress space

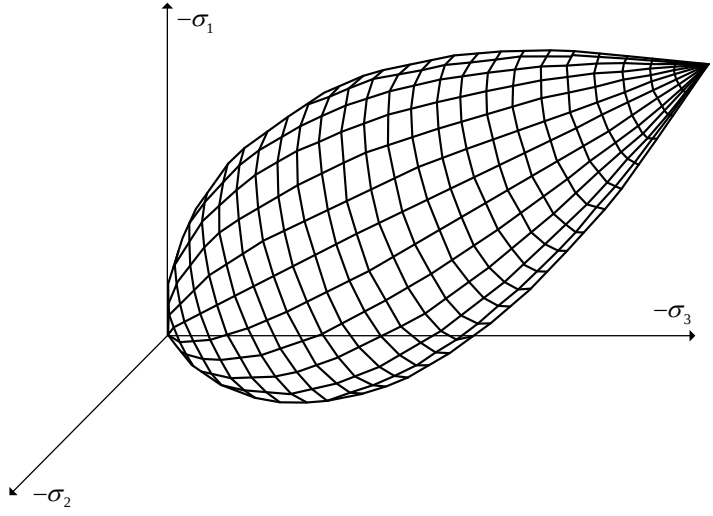

Hardening behavior

The preconsolidation stress (p_c) is used as a parameter of isotropic hardening and defined as follows:

$$p_c = p_{c0} \exp\left[\frac{\varepsilon_v^p - \varepsilon_{v0}^p}{\lambda^* - \kappa^*}\right] \tag{4.2.133}$$

p_{c0} : Initial preconsolidation pressure

ε_v^p : Plastic volumetric strain

ε_{v0}^p : Initial plastic volumetric strain

2.17 Generalized Hoek-Brown

The Hoek-Brown failure criterion for rock masses is widely accepted and has been applied. While, in general, it has been found to be satisfactory, there are some uncertainties and inaccuracies that have made the criterion inconvenient to apply and to incorporate into numerical models. In particular, the difficulty of finding an acceptable equivalent friction angle and cohesive strength for a given rock mass has been a problem since the publication of the criterion in 1980. The Generalized Hoek-Brown model resolves all these issues and sets out a recommended sequence of calculations for applying the criterion. In order to link the empirical criterion to geological observations by means of one of the available rock mass classification schemes, the Rock Mass Rating is used[17].

Yield function

The non-linear Generalized Hoek-Brown criterion for rock masses defines material strength in terms of major and minor principal stresses as:

$$f_{HB} = (\sigma_1 - \sigma_3) - \sigma_{ci}\left(-\frac{m_b}{\sigma_{ci}}\sigma_1 + s\right)^a \qquad \sigma_1 \geq \sigma_2 \geq \sigma_3 \tag{4.2.134}$$

σ_{ci} : Uniaxial compressive strength

m_b , s , a : Parameter for defining rock mass failure

Here, m_b , s , a can be expressed with the parameters related to the geological strength index(GSI) and the disturbance factor(D).

$$m_b = m_i \exp\left(\frac{GSI-100}{28-14D}\right),\ s = \exp\left(\frac{GSI-100}{9-3D}\right),\ a = \frac{1}{2} + \frac{1}{6}\left(e^{-GSI/15} - e^{-20/3}\right) \tag{4.2.135}$$

GSI : Geological strength index

m_i : Intact rock material property

D : Disturbance factor (D=0 for undisturbed rock masses, D=1 for very disturbed rock masses)

Flow rule

If the flow rule is used same as the yield function of Generalized Hoek-Brown, the corner from hexagon should be handled. However, this difficulty is removed by using the flow rule of conical shape such as Drucker-Prager model.

---

[17] Hoek E., C. Carranza-Torres, and B. Corkum. 2002. Hoek-Brown criterion – 2002 edition. In Proceedings of the 5th North American Rock Mechanics Symposium and the 17th Tunnelling Association of Canada: NARMS-TAC 2002, Toronto, Canada, eds. R.E. Hammah et al, Vol. 1, pp. 267-273.

$$g_{HB} = \sqrt{S} + \frac{I_1}{3}\tan\psi \tag{4.2.136}$$

Here, $S = 3R_{mw}{}^2 J_2$, $R_{mw} = \frac{1-\sin\psi/3}{2\cos\psi}$ and ψ is dilatancy angle.

Figure 4.2.32 shows the shape in stress space of the Generalized Hoek-Brown model. The tensile stress is the following equation.

$$\sigma_t = \frac{s\sigma_{ci}}{m_b} \tag{4.2.137}$$

Figure 4.2.32 Hoek-Brown failure surface in the principal stress space

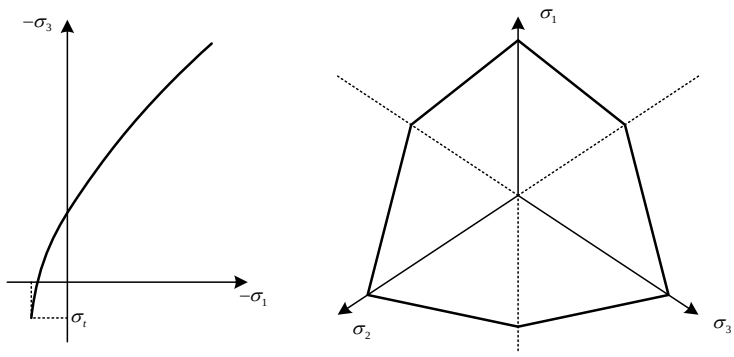

2.18 Soft Soil

The Soft Soil model is suitable for simulation of normally consolidated or near normally consolidated clay soils. Although this model is replaced by the advanced constitute model that simulates the hardening behavior better or the Soft Soil Creep model that simulates the secondary consolidation, the Soft Soil model is better capable to model the compression behavior of very soft soils. The Soft Soil model uses the yield surface of Modified Mohr Coulomb model to resolve the convergence problem due to the discontinuity of yield function. The main features of this model are the stress-dependent nonlinear elastic behavior, the hardening behavior through pre-consolidation stress and the failure by shear stress.

Nonlinear elastic

The Soft Soil model has the nonlinear elastic characteristic which has the logarithmically relationship between volumetric strain and mean effective pressure. This is the same stress-dependent stiffness with Modified Cam-Clay.

The bulk modulus K and the shear modulus G have the following relationship for the effective stress p .

$$K = \frac{(1+e_0)}{\kappa} p \ , \ G = \frac{3(1-2\nu)}{2(1+\nu)} K \tag{4.2.138}$$

e_0 : Initial void ratio

κ : Slope of over-consolidation line

ν : Poisson's ratio

If the tensile strength Δp is considered from the above equation, the bulk modulus can be expressed as follows:

$$K = \frac{(1+e_0)}{\kappa}(p + \Delta p) \tag{4.2.139}$$

By using the cohesion C and the friction angle ϕ , the tensile strength Δp can be calculated as follows:

$$\Delta p = \frac{C}{\tan\phi} \tag{4.2.140}$$

Yield function and flow rule

The Soft Soil model uses the yield function of Modified Mohr Coulomb model. The yield function and flow rule of Soft Soil model are same with the equation (4.2.99) and (4.2.103) respectively. For more details, please refer to the '2.10 Modified Mohr-Coulomb'.

Hardening behavior

Even though the Soft Soil model has each yield function of shear and compression, the hardening behavior occurs for the compression yield function. Same as the Modified Cam-Clay model, the compression hardening behavior is defined by the pre-consolidation stress which is the function of plastic strain.

$$p_c = p_{c0} \exp\left[\frac{\varepsilon_v^p - \varepsilon_{v0}^p}{\lambda^* - \kappa^*}\right] \tag{4.2.141}$$

p_{c0} : Initial pre-consolidation stress

ε_v^p : Plastic volumetric strain

ε_{v0}^p : Initial plastic volumetric strain

2.19 Hardening Soil with small strain stiffness

The Hardening Soil with small strain stiffness model is a modification of the Modified Mohr-Coulomb model that considers the increased stiffness of soils at small strains. This behavior is described in this model using an additional strain-history parameter and two additional material parameters.
As the sign convention for stresses and strains is displayed that compression is negative and tensile is positive, it assume that $\sigma_1 \geq \sigma_2 \geq \sigma_3$ for the principal stresses and $\varepsilon_1 \geq \varepsilon_2 \geq \varepsilon_3$ for the principal strains. For example, the relationship of $\sigma_1 = \sigma_2 \geq \sigma_3$ is established in case of triaxial tests.

Nonlinear elastic

In the Modified Mohr-Coulomb model, the following characteristics are used to the stress dependent value.

$$E_{50} = E_{50}^{ref}\left(\frac{-\sigma_1 + p_x}{p^{ref} + p_x}\right)^m, E_{ur} = E_{ur}^{ref}\left(\frac{-\sigma_1 + p_x}{p^{ref} + p_x}\right)^m, E_{oed} = E_{oed}^{ref}\left(\frac{-\sigma_3 + p_x}{p^{ref} + p_x}\right)^m \quad (4.2.142)$$

$$p_x = c\cot\phi$$

c : Cohesion

p^{ref} : Reference stress for stiffnesses

ϕ : Friction angle

m : Power law for stress dependent stiffness

E_{50}^{ref} : Reference secant stiffness in standard drained triaxial test

E_{oed}^{ref} : Reference tangent stiffness for primary oedometer loading

E_{ur}^{ref} : Reference unloading / reloading stiffness

As the stiffness modulus can be changed according to the stress, this model shows the nonlinear elastic characteristic what the elastic modulus changes.

Yield function, plastic potential function and flow rule

T. Schanz, P.A. Vermeer and P.G. Bonnier[18] have developed the Hardening Soil model based on the hyperbolic relationship between deviatoric stress and vertical strain in the triaxial test, and suggested the shear & compressive yield function as the following equation.

[18] Schanz T., Vermeer P.A., Bonnier P.G. (1999). The hardening-soil model: Formulation and verification. Beyond 2000 in Computational Geotechnics, Balkema, Rotterdam. pp. 281-290.

$$f_s = \frac{q_a}{E_{50}}\frac{q}{q_a - q} - \frac{2q}{E_{ur}} - \gamma_p = 0 \qquad , q_a := \frac{q_f}{R_f} \text{ and } \gamma_p := \varepsilon_1^p - \varepsilon_2^p - \varepsilon_3^p$$

$$f_c = \frac{\tilde{q}^2}{\alpha^2} + \left(p + p_x\right)^2 - \left(p_c + p_x\right)^2 \qquad , \tilde{q} := \frac{1}{\delta}\sigma_1 + \left(1 - \frac{1}{\delta}\right)\sigma_2 - \sigma_3 \qquad (4.2.143)$$

$$\delta = \frac{3 - \sin\phi}{3 + \sin\phi}$$

q : Deviatoric stress

q_a , q_f : Asymptotic & ultimate deviatoric stress

E_{50} : Confining stress dependent stiffness modulus for primary loading

E_{ur} : Young's modulus for unloading and reloading

γ^p : Hardening parameter (plastic shear strain)

R_f : Failure ratio q_f / q_a

f_s, f_c : Shear & compressive yield function

p_c : Pre-consolidation stress

If $\varepsilon_v^{\,p} = 0$, the above shear yield function can be considered the strain relationship as the following equation.

$$0 = \varepsilon_1 - \varepsilon_1^{\,e} - \varepsilon_1^{\,p}, \leftarrow \varepsilon_1 = \frac{q_a}{2E_{50}}\frac{q}{q_a - q}, \quad \varepsilon_1^{\,e} = \frac{2q}{E_{ur}}, \quad \varepsilon_1^{\,p} = \gamma_p \qquad (4.2.144)$$

The yield function of Modified Mohr-Coulomb model consists of the shear, compressive and tensile yield function as the following equation.

$$f_{13} = \frac{2q_a}{E_i}\frac{(\sigma_1 - \sigma_3)}{q_a - (\sigma_1 - \sigma_3)} - \frac{2(\sigma_1 - \sigma_3)}{E_{ur}} - \gamma_p = 0 \qquad , E_i := \frac{2E_{50}}{2 - R_f}$$

$$q_a := \frac{1}{R_f}q_f \,, \qquad q_f := \frac{2\sin\phi}{1 - \sin\phi}\left(-\sigma_1 + c\cot\phi\right) \qquad (4.2.145)$$

$$f_c = \frac{q^2}{\alpha^2} + \left(p + c\cot\phi\right)^2 - \left(p_c + c\cot\phi\right)^2 = 0$$

$$f_t = -p - p_t$$

f_{13} : Shear yield function ($\sigma_1 \geq \sigma_2 \geq \sigma_3$)

f_c : Compressive yield function

f_t : Tensile yield function

p_c : Pre-consolidation stress

α : Cap parameter

p_t : Tensile strength

The maximum shear stress q_f is calculated by the Mohr-Coulomb criteria, and the Mohr-Coulomb model is used in case of $q_f < (\sigma_1 - \sigma_3)$.

α is an auxiliary model parameter which control the value of compressive yield function in p-q space. It is decided by considering the stress ratio in the normally consolidated state ($K0nc$) and the friction angle.

The plastic potential function uses the Mohr-Coulomb criteria for shear, and the yield function for compressive and tensile as the following equation.

$$\begin{aligned} g_{13} &= \frac{(\sigma_1 - \sigma_3)}{2} + \frac{(\sigma_1 + \sigma_3)}{2}\sin\psi_m \\ g_c &= \frac{q^2}{\alpha^2} + \left(p + c\cot\phi\right)^2 \\ g_t &= -p \end{aligned} \tag{4.2.146}$$

g_{13} : Shear plastic potential function (in case of $\sigma_1 \geq \sigma_2 \geq \sigma_3$)

g_c : Compressive plastic potential function

g_t : Tensile plastic potential function

ψ_m : Mobilized dilatancy angle

The mobilized dilatancy angle ψ_m can be obtained from the following equation, and it is limited to satisfy the condition $0 \leq \psi_m \leq \psi$ considering physical behavior.

$$\sin\psi_m = \frac{\sin\phi_m - \sin\phi_{cv}}{1 - \sin\phi_m \sin\phi_{cv}} \quad ,\sin\phi_m = \frac{\sigma_1 - \sigma_3}{-(\sigma_1 + \sigma_3) + 2c\cot\phi} \quad ,\sin\phi_{cs} = \frac{\sin\phi - \sin\psi}{1 - \sin\phi\sin\psi} \tag{4.2.147}$$

ϕ_m : Mobilized friction angle

ϕ_{cs} : Critical state friction angle

ψ : Dilatancy angle

The mobilized friction angle and the critical state friction angle are consistent with the Rowe theory as described by T. Schanz, P.A. Vermeer and P.G. Bonnier.

Hardening behavior

The Modified Mohr-Coulomb model shows hardening behavior while increasing the effective plastic strain and it reaches the perfect plastic state in case of $q_f < (\sigma_1 - \sigma_3)$ as mentioned in the previous yield function.

In the process of compressive hardening, the pre-consolidation stress p_c is defined as below:

$$p_c^{n+1} = \left(p_c^{ref} + p_x\right)\left(\left(\frac{p_c^n + p_x}{p_c^{ref} + p_x}\right)^{1-m} + \frac{1-m}{p_c^{ref} + p_x} H \Delta\varepsilon_v^p\right)^{\frac{1}{1-m}} - p_x \qquad (4.2.148)$$

$$H = -\frac{K_s^{ref} K_c^{ref}}{K_s^{ref} - K_c^{ref}}, \qquad K_s^{ref} = \frac{E_{ur}^{ref}}{3(1-2v)}, \qquad K_c^{ref} = \frac{E_{oed}^{ref}}{3(1-2v)}$$

p_c^{ref} : Reference pre-consolidation stress

$\Delta\varepsilon_v^p$: Plastic volumetric strain

Hardening Soil with small strain stiffness

The Hardening Soil with small strain stiffness model is implemented by using the Modified Mohr-Coulomb model and Small strain overlay[19] model, and needed two additional parameters as below:

G_0^{ref} : Initial or very small-strain shear modulus

$\gamma_{0.7}$: Shear strain at which the shear modulus is about 70% of the initial small-strain shear modulus

The strain range in which soils can be considered truly elastic is very small. With increasing strain range, soil stiffness decrease nonlinearly as the following graph.

[19] Benz, T. "Small strain stiffness of soil and its numerical consequences", PhD thesis, University Stuttgart, 2007.

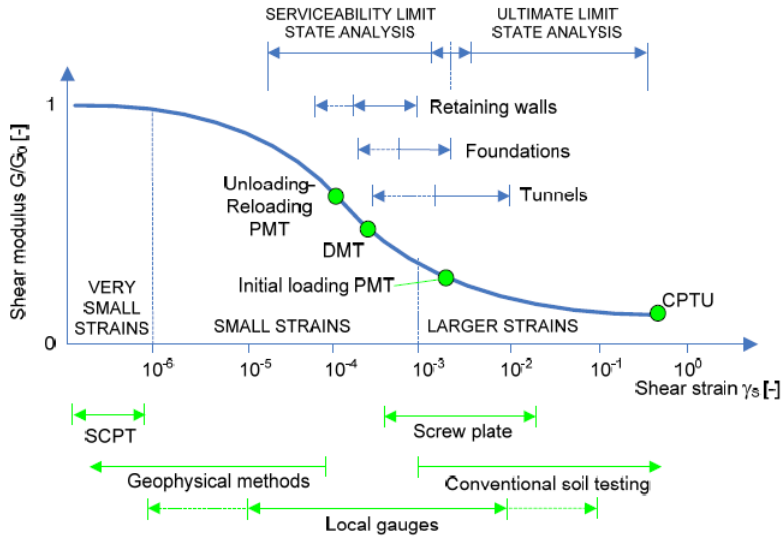

Figure 4.2.33 Characteristic stiffness-strain behavior of soil with the ranges for typical geotechnical structures and different tests

To reflect the above characteristics, the Hardening Soil with small strain stiffness model uses the modified Hardin & Drnevich relationship[20] as the following equation.

$$\frac{G_s}{G_0} = \frac{1}{1 + a\left|\frac{\gamma}{\gamma_{0.7}}\right|} \quad ,a = 0.385 \tag{4.2.149}$$

G_s : Shear modulus

G_0 : Initial shear modulus

γ : Shear strain

$\gamma_{0.7}$: Shear strain at which the shear modulus is about 70% of the small-strain shear modulus

Once the direction of loading is reversed, the stiffness regains a maximum recoverable value which is in the order of the initial soil stiffness. Then, while loading in the reversed direction is continued, the stiffness decreases again.

To reflect the above characteristics, the Hardening Soil with small strain stiffness model writes the history of strain in the internal model, and follows Masing's rule as follows:

[20] B.O. Hardin, V.P. Drnevich, "Shear modulus and damping in soils: Design equations and curves", Journal of the Soil Mechanics and Foundations Division, 98(SM7):667-692, 1972.

► The shear modulus in unloading is equal to the initial tangent modulus for the initial loading curve.

► The shape of the unloading and reloading curves is equal to the initial loading curve, but twice its size. Masing's rule can be fulfilled by using twice of the initial loading $\gamma_{0.7}$ for the reloading $\gamma_{0.7}$.

The initial shear modulus G_0 is calculated by the following equation.

$$G_0 = G_0^{ref}\left(\frac{-\sigma_1 + c\cot\phi}{p^{ref} + c\cot\phi}\right)^m \tag{4.2.150}$$

And the hysteresis shear strain (γ_H) is defined as the following equation.

$$\gamma_H = \sqrt{3}\frac{\|\Delta\mathbf{eH}\|}{\|\Delta\mathbf{e}\|}, \quad \|\Delta\mathbf{e}\| = \sqrt{\Delta\mathbf{e}:\Delta\mathbf{e}} \tag{4.2.151}$$

$\mathbf{H}$: Strain hysteresis tensor (for more details, refer to Benz[19])

$\Delta\mathbf{e}$: Incremental shear strain

In the numerical analysis, the following incremental equation is used with the tangential stiffness of modified Hardin & Drnevich relationship.

$$G^{n+1} = \frac{G_0}{\gamma_H^{n+1} - \gamma_H^n}\left(\frac{\gamma_H^{n+1}}{1 + a\frac{\gamma_H^{n+1}}{\gamma_{0.7}}} - \frac{\gamma_H^n}{1 + a\frac{\gamma_H^n}{\gamma_{0.7}}}\right), a = 0.385 \tag{4.2.152}$$

2.20 Generalized SCLAY1S

Soft clay in its natural state has a significant anisotropy in the interior soil particle fabric by deposition and consolidation[21]. Also as the strain is continuously generated, the degree of anisotropy is changed whereby the interior soil particles are rearranged and contact between the particles is changed. The Generalized SCLAY1S model of FEA NX is rooted in the SCLAY1[22] model which considered the change due to the initial stress induced anisopropy of the soft clay and anisotropy of rotational hardening.

---

[21] S.J. Wheeler, M. Cudny, H.P. Neher, C. Wlitafsky, "Some developments in constitutive modelling of soft clays", Proceedings of the International Workshop on Geotechnics of Soft Soils-Theory and Practice, Noordwijkerhoud, the Netherlands, 2003, pp. 17-19.

[22] S.J. Wheller, A. Naatanen, M. Karstunen, M. Lojander "An anisotropic elastoplastic model for soft clays", Canadian Geotechnical Journal, 40.2., 2003., pp. 403-418.

On the other hand, the structure of the soil particle is composed of two parts[23]: bonding as well as fabric. The fabric is composed of spatial arrangement of particles and inter-particle contact, and the bonding is weakened gradually as the plastic straining is caused by the forces acting between the particles. The phenomenon that the bonding is weakened gradually by the plastic straining is called destructuration, and SCLAY1S model considers the destructuration phenomenon of the SCLAY1 model additionally.
The initial SCLAY1(S) model was the model assumed the triaxial stress state, and later it is improved by the model considering the general stress state. The Generalized SCLAY1S model is that the shape of yield function is complicated and needs more variables to represent the hardening behavior. However, It has a advantage that it can simulate the behavior of the general stress state strictly as well as the triaxial stress state.
In the SCLAY1S model, ignoring the initial anisotropy and bonding, and in case of assuming a related material constant to 0, it can be found that the Modified Cam Caly model and the yield function are matched exactly.

Nonlinear elastic

The Generalized SCLAY1S model of FEA NX does the stress-dependent non-linear elastic behavior like Modified Cam Clay, Sekiguchi-Ohta, Soft-Soil models. This being so, the detailed description and formulas will be omitted. (Refer to the equation 4.2.139)

Yield function and plastic potential function

As the Generalized SCLAY1S model follows the associated flow rule, it is equal to the yield function and plastic potential function.
The yield function of the SCLAY1 model simplified of the triaxial stress state is represented about the effective stress, and the signs of the stress is that compression is (+) and tensile is (-).

$$f = \left(q - \alpha p'\right)^2 - \left(M^2 - \alpha^2\right)\left(p'_c - p'\right)p' = 0$$
$$p' = \frac{1}{3}\sigma'_{kk}\,\delta_{ij},\; q = \sqrt{\frac{3}{2}\mathbf{s}:\mathbf{s}} \qquad (4.2.153)$$
$$s_{ij} = \sigma'_{ij} - \frac{1}{3}\sigma'_{kk}\,\delta_{ij}$$

p : Pressure

q : Shear stress

p_c : Preconsolidation pressure

M : Slope of critical state line

α : Degree of anisotropy

[23] J.B. Burland, "On the compressibility and shear strength of natural clays", Geotechnique, 40.3, 1990, pp. 329-378.

Substituting o to the degree of anisotropy α and summarizing the equation in the equation (4.2.153), it can be found that the yield function of the Modified Cam Clay is equal to the equation (4.2.77). In other words, the SCLAY1 model is the generalized model considering the degree of anisotropy from the Modified Cam Clay model.

Figure 4.2.34 Yield function of triaxial stress state

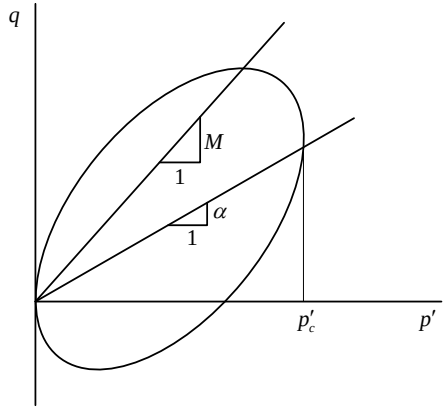

The generalized yield function in the general stress state is represented as follows.

$$f = \frac{3}{2}\left[(\mathbf{s} - p'\boldsymbol{\alpha}_d) : (\mathbf{s} - p'\boldsymbol{\alpha}_d)\right] - \left(M^2 - \frac{3}{2}(\boldsymbol{\alpha}_d : \boldsymbol{\alpha}_d)\right)(p'_c - p')\,p' = 0 \tag{4.2.154}$$

Here, the deviatoric fabric tensor $\boldsymbol{\alpha}_d$ of the soil particle is represented by the fabric tensor $\boldsymbol{\alpha}^*$ in the same form of the deviatoric stress tensor.

$$\alpha_{d,ij} = \alpha^*_{ij} - \frac{1}{3}\alpha^*_{ij}\delta_{ij} \tag{4.2.155}$$

The fabric tensor $\boldsymbol{\alpha}^*$ has the following properties.

$$\alpha^*_{kk}\delta_{ij} = 1 \tag{4.2.156}$$

The degree of anisotropy α meaning the slope of the yield function in the simplified of the triaxial stress state is defined by the deviatoric fabric tensor $\boldsymbol{\alpha}_d$ as follows.

$$\alpha^2 = \frac{3}{2}(\boldsymbol{\alpha}_d : \boldsymbol{\alpha}_d) \tag{4.2.157}$$

And preconsolidation stress p'_c in the generalized SCLAY1S model considered bonding of the soil particle is represented as follows.

$$p'_c = (1+x)\, p'_{ci} \tag{4.2.158}$$

p'_{ci} : Preconsolidation pressure of the intrinsic yield function

x : Degree of bonding

Here, the intrinsic yield function has the same stress in the same fabric, the void ratio, the slope and the limit state but is the conceptional yield function[24] having smaller preconsolidation stress. The detailed description about the intrinsic yield function and the degree of bonding can be seen part of the hardening behavior.
On the other hand, the Generalized SCLAY1S model of FEA NX is under the allowable tensile pressure to handle the convergence problem in case of occurring tensile to materials like Modified Cam Clay, Sekiguchi-Ohta models.

$$f = \frac{3}{2}\left[(\mathbf{s} - p'\boldsymbol{\alpha}_d) : (\mathbf{s} - p'\boldsymbol{\alpha}_d)\right] - \left(M^2 - \frac{3}{2}(\boldsymbol{\alpha}_d : \boldsymbol{\alpha}_d)\right)(p'_c - p')(p' + p'_t) = 0 \tag{4.2.159}$$

Isotropic hardening law

The Generalized SCLAY1S model has three kinds of the hardening laws. Here, the isotropic hardening law is the hardening law which the general soft clay has, and it is equal to the law of the Modified Cam Clay, Sekiguchi-Ohta models. The following is the equation representing the general isotropic hardening law.

$$dp'_c = \frac{(1+e)\, p'_c}{\lambda - \kappa} d\varepsilon_v^p \tag{4.2.160}$$

p'_c, dp'_c : Preconsolidation pressure and the change rate of the preconsolidation pressure

$d\varepsilon_v^p$: The change rate of the volumetric plastic strain

λ : The gradient of the normal consolidation line

κ : The gradient of the over-consolidation line

e : The void raio

[24] M. Karstunen, C. Wiltafsky, H. Krenn, F. Scharinger, H.F. Schweiger, "Modelling the behaviour of an embankment on soft clay with different constitutive models", International journal for numerical and analytical methods in geomechanics, 30.10, 2006, pp. 953-982.

The isotropic hardening behavior of the Generalized SCLAY1S model is equal to the equation (4.2.160) but the using material constants are changed and the object of hardening turns to the preconsolidation stress of the intrinsic yield function.

$$dp'_{ci} = \frac{(1+e)\,p'_{ci}}{\lambda_i - \kappa} d\varepsilon_v^p \tag{4.2.161}$$

λ_i : The gradient of reconstituted soil(or intrinsic) normal consolidation line

Figure 4.2.35 Compression line of natural and reconstituted soil

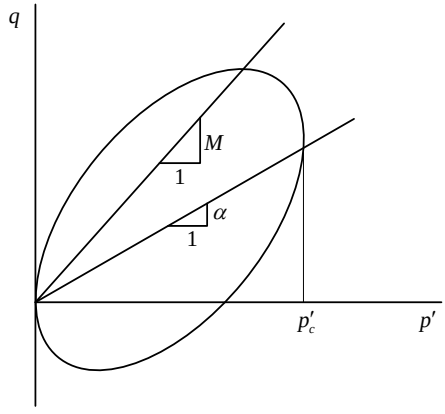

The reconstituted soil without bonding and the natural soil having the initial bonding follow the intrinsic compression line of the picture 4.2.35 and the general compression line respectively. The general compression line generates the yielding at the bigger effective pressure than the reconstituted soil, and converges to the compression line of reconstituted soil as the bonding decreases gradually. At this time, generally the gradient of the post-yield compression curve λ has a lot bigger value than the gradient of the reconstituted soil line λ_i , but is is due to the destructuration that the bonding of natural soil reduces gradually.

Rotational hardening law

The rotational hardening law simulates the behavior changing the degree of anisotropy as the plastic strain changes, but it causes the hardening so that the anisotropy disappears as the plastic strain increases.
The rotational hardening law in the simplified of the triaxial stress state is represented as follows.

$$d\alpha = \mu\left[\left(\frac{3}{4}\eta - \alpha\right)\left\langle d\varepsilon_v^p \right\rangle + \beta\left(\frac{1}{3}\eta - \alpha\right)\left|d\varepsilon_d^p\right|\right] \tag{4.2.162}$$

$\alpha, d\alpha$: Degree of anisotropy and the change rate of the degree of anisotropy

$d\varepsilon_v^p$: The change rate of volumetric plastic strain

$d\varepsilon_d^p$: The change rate of shear plastic strain

η : $\eta = \frac{q}{p}$, Ratio of the shear stress and pressure

μ : Coefficient of the absolute effectiveness of the rotational hardening law

β : Coefficient of the relative effectiveness of the rotational hardening law

Here, $\langle \cdot \rangle$ and $|\cdot|$ are defined as follows.

$$\langle x \rangle = \begin{cases} x & x \geq 0 \\ 0 & x < 0 \end{cases}, \quad |x| = \begin{cases} x & x \geq 0 \\ -x & x < 0 \end{cases} \tag{4.2.163}$$

In the equation (4.2.162), it can be found that the change rate of the degree of anisotropy α is growing together as the volumetric plastic strain and shear plastic strain grow. However, as the degree of anisotropy is closer to $\alpha = (3/4)\eta$ or $\alpha = (1/3)\eta$, the contribution of the volumetric plastic strain or the shear plastic strain affecting to the change rate of the degree of anisotropy are reduced.
On the other hand, numerical problems happen in the dry side likewise other material models following the limit state theory, Macaulay bracket $\langle \cdot \rangle$ included in the equation (4.2.162) is to prevent the degree of anisotropy effusing when the yielding occurs in the dry side.
The rotational hardening law of generalized model changes as follows.

$$d\boldsymbol{\alpha}_d = \mu \left[\left(\frac{3}{4}\boldsymbol{\eta} - \boldsymbol{\alpha}_d \right) \left\langle d\varepsilon_v^p \right\rangle + \beta \left(\frac{1}{3}\boldsymbol{\eta} - \boldsymbol{\alpha}_d \right) d\varepsilon_d^p \right] \tag{4.2.164}$$

$\boldsymbol{\alpha}_d, d\boldsymbol{\alpha}_d$: Deviatoric fabric tensor and the change rate of the deviatoric fabric tensor

$\boldsymbol{\eta}$: $\boldsymbol{\eta} = \frac{\mathbf{s}}{p}$, The raio of deviatoric stress and pressure

The equation (4.2.164) is similar to the equation (4.2.162), but hardening variables are changed from the scalar values to the secondary tensor values corresponding to the respective stress components.

Destructuration law

The third hardening law, destructuration law simulates that the degree of bonding decreases gradually as the plastic strain occurs.

$$dx = a\left(\left[0-x\right]\left|d\varepsilon_v^p\right| + b\left[0-x\right]d\varepsilon_d^p\right) = -ax\left(\left|d\varepsilon_v^p\right| + bd\varepsilon_d^p\right) \quad (4.2.165)$$

x, dx : The degree of bonding and the change rate of the degree of bonding

a : Coefficient of the absolute effectiveness of the destructuraion law

b : Coefficient of the relative effectiveness of the destructuraion law

Similar to the rotational hardening law, the change rate of the degree of bonding also grows as the volumetric plastic strain and the shear plastic strain grow. However it is irrelevant to the sign of the volumetric plastic strain and only affected by its magnitude. Also, it can be found that the change rate of the degree of bonding is reduced as the degree of bonding x is closer to $x = 0$, because it simulates the weakened bonding phenomenon as the plastic strain increseas as a result.

2.21 CWFS (Cohesion Weakening and Frictional Strengthening)

By the development of the tunnel excavation technology, it is possible to construct structures in deep geological environments and bedrock, and these structures under the high confining pressure can be occurred brittle fracture like spalling or slabbing by the excavation of the cavity. These failure phenomena can not be predicted properly with perfectly elastoplastic, strain softening, brittle models applying the traditional failure criteria. CWFS model predicted the swelling effects of bedrock and the failure behavior in deep geological environments more exactly than the brittle model, therefore this model is included in FEA NX.

Shear yield function

CWFS model taking advantage of the Mohr-Coulomb yield function is that the hardening/softening behavior of table is possible. Therefore shear plastic behavior is represented as follow equation.

$$f_s = R_{mc}\sqrt{3J_2} + \frac{1}{3}I_1\tan\phi(\kappa) - c(\kappa) = 0 \quad (4.2.166)$$

ϕ : Friction angle

c : Cohesion

κ : Equivalent plastic strain

Shear flow rule

The flow rule uses the following plastic potential based on the non-associated plastic flow rule. Here, It uses the smoothing formula in order to avoid singularity occurred in the corner. For more information, refer to chapter modified UBCSAND.

$$g_s = \sqrt{\left(\varepsilon c \tan\psi_m\right)^2 + 3R_{mw}{}^2 J_2} + \frac{I_1}{3}\tan\psi$$
$$R_{mw} = \frac{4\left(1-e^2\right)\cos^2\Theta + \left(2e-1\right)^2}{2\left(1-e^2\right)\cos\Theta + \left(2e-1\right)\sqrt{4\left(1-e^2\right)\cos^2\Theta + 5e^2 - 4e}} R_{mc}\left(\frac{\pi}{3}, \phi\right) \quad (4.2.167)$$

ψ : Dilatancy angle

Shear hardening behavior

In order to define the shear hardening, the relation of the plastic multiplier λ and the hardening variable κ are defined as follows.

$$\kappa = \lambda\sqrt{\frac{1}{3}\left(1+\sin^2\psi\right)} \quad (4.2.168)$$

FEA NX can define the hardening behavior about cohesion c, friction angle ϕ and dilatancy angle ψ using the table.

2.22 Geogrid

Geogrid is generally used as the material for reinforcing soil/ground. Geogrid is made of the polymer fabric, and it is working with the weight of soil/ground. It is only resisted the tension, and mainly used as a sub-material of reinforced earth retaining wall.

Nonlinear elastic

The geogrid material in FEA NX shows the tension-only behavior. The stress-strain relationship of geogrid is shown in the following figure.

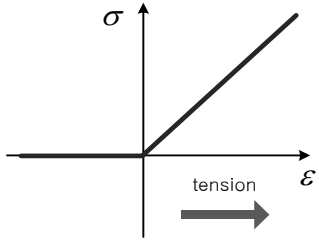

Figure 4.2.36 Tension-only behavior of geogrid

The 2D geogrid shows an independent behavior each other in the axial plane.

$$\begin{Bmatrix} \sigma_{xx} \\ \sigma_{yy} \\ \tau_{xy} \end{Bmatrix} = \begin{bmatrix} \frac{E_1}{1-\nu^2} & 0 & 0 \\ 0 & \frac{E_2}{1-\nu^2} & 0 \\ 0 & 0 & G_{12} \end{bmatrix} \begin{Bmatrix} \varepsilon_{xx} \\ \varepsilon_{yy} \\ \gamma_{xy} \end{Bmatrix} \quad (4.2.169)$$

Yield function

The yield function and plastic potential function of geogrid material are same since it follows the associated flow rule.

The plastic behavior of each direction is independently and the yield condition is as follows.

$$f(\boldsymbol{\sigma}) = \sigma - \sigma_{yield} = 0 \quad (4.2.170)$$

The yield condition of 1-axis and 2-axis can be applied differently.

2.23 Concrete smeared crack

In FEA NX, the concrete smeared crack model is used to simulate the plain concrete. The concrete-smeared crack model assumes that the monotonic load is applied to concrete under low confining pressure. The low confining pressure corresponds to the stress less than 1/5 to 1/4 of the maximum compressive strength of concrete. For reinforced concrete, the embedded elements are used. In this case, effects such as bond slip from the interface of concrete and steel are considered through tension stiffening.[25]

The concrete smeared crack model simulates the compression part of concrete using a typical isotropic elasto-plastic model, and the tensile part of concrete is simulated using a smeared crack model. The smeared crack model is a method of simulating the crack by adjusting the stress and stiffness at the integration point, without reconfiguring the mesh. In the smeared crack model, the band-width obtained based on the size of the element is reflected in the crack behavior to avoid mesh dependencies (Bazant and Oh 1983). The square root of an area for a two-dimensional element and the cubic root of a volume for a three-dimensional element are the crack width of the element. For the higher order element, the half of the square root and the cubic root are the crack width. The tensile/compression uniaxial behavior of the concrete smeared crack model is shown in the figure below.

Figure 4.2.37
Uniaxial behavior of concrete smeared crack

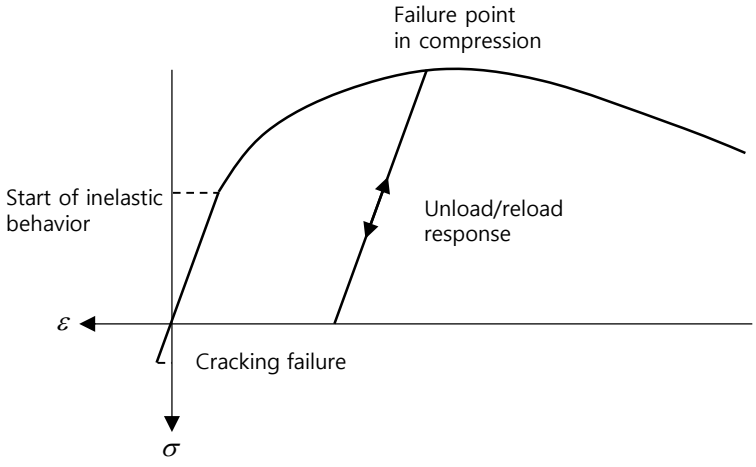

[25] H. D. Hibbit, "A simplified model for concrete at low confining pressure", Nuclear engineering and design, 104.3, 1987, 313-320

Strain Decomposion

The following strain decomposition is used in the concrete smeared crack model.

$$d\boldsymbol{\varepsilon} = d\boldsymbol{\varepsilon}^{el} + d\boldsymbol{\varepsilon}_c^{pl} + d\boldsymbol{\varepsilon}_t^{pl} \tag{4.2.170}$$

$d\boldsymbol{\varepsilon}_c^{pl}$: Incremental change of compressive plastic strain

$d\boldsymbol{\varepsilon}_t^{pl}$: Incremental change of tensile plastic strain

The above equation can be integrated as follows.

$$\boldsymbol{\varepsilon} = \boldsymbol{\varepsilon}^{el} + \boldsymbol{\varepsilon}_c^{pl} + \boldsymbol{\varepsilon}_t^{pl} \tag{4.2.171}$$

Compressive behavior

The concrete smeared crack model simulates compressive behavior using a typical elasto-plastic model.

Compression plastic flow

Associated flow ruls is used.

$$d\boldsymbol{\varepsilon}_c^{pl} = d\lambda_c \left(1 + c_0 \left(\frac{p}{\tau_c}\right)^2\right) \frac{\partial f_c}{\partial \boldsymbol{\sigma}} \tag{4.2.172}$$

c_0 is the value which makes the ratio of $\boldsymbol{\varepsilon}_{11}^{pl}$ of the monotonic biaxial test and $\boldsymbol{\varepsilon}_{11}^{pl}$ of the monotonic uniaxial test to be constant.

Compression yield surface

$$f_c = q - \sqrt{3} a_0 p - \sqrt{3} \tau_c = 0 \tag{4.2.173}$$

p : Effective stress ($-\frac{1}{3} trace(\boldsymbol{\sigma})$)

q : Mises equivalent effective stress ($\sqrt{\frac{3}{2}\mathbf{S}:\mathbf{S}}$, $\mathbf{S}$: deviatoric stress)

a_0 is the value calculated from the ratio of the compressive strength in the uniaxial stress state to the compressive strength of the biaxial stress state.

τ_c is the yield stress under the pure shear stress, calculated from the compression curve entered by the user.

$$\tau_c = \left(\frac{1}{\sqrt{3}} - \frac{a_0}{3} \right) \sigma_c \qquad (4.2.174)$$

Tensile behavior

Cracks occur when the stress is outside the crack detection surface, a type of yield function. If a crack occurs, the stress is returned using an implicit backward Euler method, and the direction of the maximum principal strain is the direction of the crack. This direction is stored to simulate the anisotropy by cracking in subsequent analyses. Since the orthogonal fixed crack model is used in the smeared crack model, the subsequent crack shall be in a direction orthogonal to the existing crack direction and up to three in the case of the three-dimensional model. If the elastic strain in the direction of the crack is tensile after the crack has occurred, it is behaved as damaged elastic and it is considered that the crack is closed when it is compressed.

Figure 4.2.38
Tensile behavior of concrete semared crack

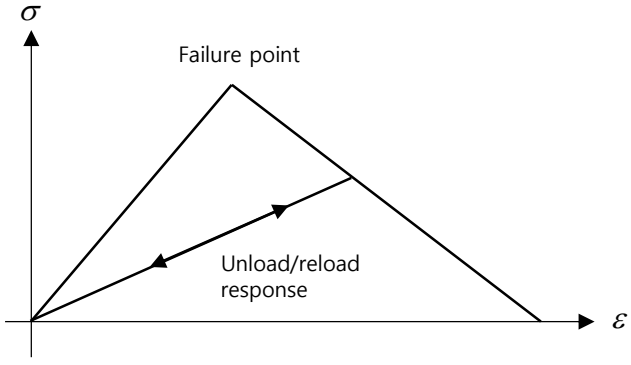

Crack detection surface

Crack detection surface is Coulomb line.

$$f_t = \hat{q} - \left(3 - b_0 \frac{\sigma_t}{\sigma_t^u} \right) \hat{p} - \left(2 - \frac{b_0}{3} \frac{\sigma_t}{\sigma_t^u} \right) \sigma_t = 0 \qquad (4.2.175)$$

σ_t^u : Failure stress in uniaxial tension

$\hat{p}$, $\hat{q}$: p and q for which open-crack related components are neglected.

b_0 is obtained by using the tensile strength value when the stress in one direction of the main stress is the compressive strength in a plane stress condition.

Tension flow rule

As with compression, associated flow ruls is used.

$$d\boldsymbol{\varepsilon}_t^{pl} = d\lambda_t \frac{\partial f_t}{\partial \boldsymbol{\sigma}} \tag{4.2.176}$$

Damaged elasticity

The relationship between stress-elastic strain of concrete-smeared crack model is as follows:

$$\boldsymbol{\sigma} = \mathbf{D} : \boldsymbol{\varepsilon}^{el} \tag{4.2.177}$$

$\mathbf{D}$: Elastic Stiffness Matrix of Concrete Model

In uncracked concrete, $\mathbf{D}$ is a linear isotropic elastic matrix. If the elastic strain in the direction of the crack is tensile after the crack occurs, the stress and stiffness are behaved as damaged elasticity by reference to the tensile curve entered by the user.

If α is the direction of the crack, the stress and elastic strain in that direction are $\sigma_{\overline{\alpha\alpha}}$ and $\varepsilon_{\overline{\alpha\alpha}}^{el}$. If $\varepsilon_{\overline{\alpha\alpha}}^{el} > 0$, the component, $\overline{\alpha\alpha}\beta\gamma$, of the concrete elastic stiffness matrix resulting from Poisson ratio is not considered.

$$\mathbf{D}_{\overline{\alpha\alpha}\beta\gamma} = 0 \text{ for } \beta \neq \alpha,\ \gamma \neq \alpha \tag{4.2.178}$$

If the maximum value of the elastic strain produced in the α direction is $\varepsilon_{\overline{\alpha\alpha}}^{open}$, and the stress at the corresponding elastic strain is $\sigma_{\overline{\alpha\alpha}}^{open}$, the damaged components of the elastic stiffness matrix are as follows.

$$\mathbf{D}_{\overline{\alpha\alpha}\alpha\alpha} = \frac{\sigma_{\overline{\alpha\alpha}}^{open}}{\varepsilon_{\overline{\alpha\alpha}}^{open}} \tag{4.2.179}$$

The shear stiffness associated with the direction of the crack is calculated by the shear function entered by the user.

2.24 Bond Slip

In reinforced concrete, the interaction between the reinforcement and the concrete is governed by secondary transverse and longitudinal cracks in the vicinity of the reinforcement. This behavior can be modeled with a bond-slip mechanism where the relative slip of the reinforcement and the concrete is described in a phenomenological sense.

In FEA NX, the relationship between the normal traction and the normal relative displacement is assumed to be linear elastic, whereas the relationship between the shear traction and the slip is assumed as a nonlinear function.

$$\begin{aligned} t_n &= k_n \Delta u_n \\ t_t &= f_t\left(\Delta u_t\right) \end{aligned} \tag{4.2.180}$$

Differentiating (4.2.180) results in expressions for the tangential stiffness coefficients.

$$\begin{bmatrix} D_{11} = k_n & D_{12} = 0 \\ D_{21} = 0 & D_{22} = \dfrac{\partial f_t}{\partial \Delta u_t} \end{bmatrix} \tag{4.2.181}$$

FEA NX offers a predefined curve, 'polynomial function', for the relationships between shear traction and slip, and a user-defined multi-linear function is also available.

Polynomial function

The polynomial function describes the relationship between shear stress and slip as shown in the figure below, and the formula is shown below.

Figure 4.2.39
Shear behavior of bond slip

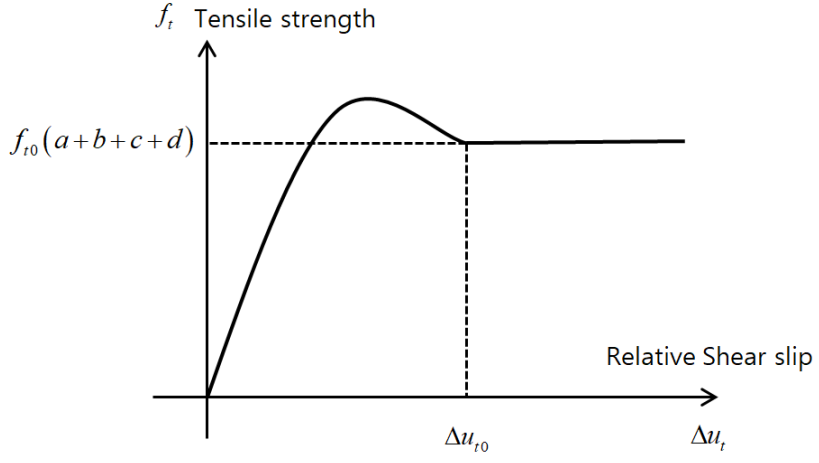

$$f_t = \begin{cases} f_{t0}\left(a + b\left(\dfrac{\Delta u_t}{\Delta u_{t0}}\right) + c\left(\dfrac{\Delta u_t}{\Delta u_{t0}}\right)^2 + d\left(\dfrac{\Delta u_t}{\Delta u_{t0}}\right)^3\right) & \text{if } 0 \le \Delta u_t \le \Delta u_{t0} \\ f_{t0}\left(a + b + c + d\right) & \text{if } \Delta u_{t0} < \Delta u_t \end{cases} \quad (4.2.182)$$

2.25 Discrete Cracking

The constitutive law for discrete cracking in FEA NX is based on a total deformation theory, which expresses the tractions as a function of the total relative displacements. The relationship between normal traction and crack width and the relationship between shear traction and slip are assumed as nonlinear functions.

$$\begin{aligned} t_n &= f_n\left(\Delta u_n\right) \\ t_t &= f_t\left(\Delta u_t\right) \end{aligned} \tag{4.2.183}$$

In the above equation, the relationship between the normal traction and shear traction is independent to each other, so the stiffness can be expressed as follows.

$$\begin{bmatrix} D_{11} = \dfrac{\partial f_n}{\partial \Delta u_n} & D_{12} = 0 \\ D_{21} = 0 & D_{22} = \dfrac{\partial f_t}{\partial \Delta u_t} \end{bmatrix} \tag{4.2.184}$$

In general, the normal traction is governed by a tension softening relation. For structural interface elements, FEA NX supports the following relations:

1. Brittle cracking model
2. Linear tension softening model
3. Nonlinear tension softening model

Brittle cracking model

Brittle cracking model is characterized by the full reduction of the strength after the strength criterion has been reached.

$$t_n = \begin{cases} f_n\left(\Delta u_n\right) & if \quad \Delta u_n \le \dfrac{f_t}{k_n} \\ 0 & if \quad \dfrac{f_t}{k_n} < \Delta u_n \end{cases} \tag{4.2.185}$$

Linear tension softening model

In case of linear tension softening, the relation of the crack stress and displacement in the normal direction is given by the figure below.

Figure 4.2.40
Linear tension softening behavior

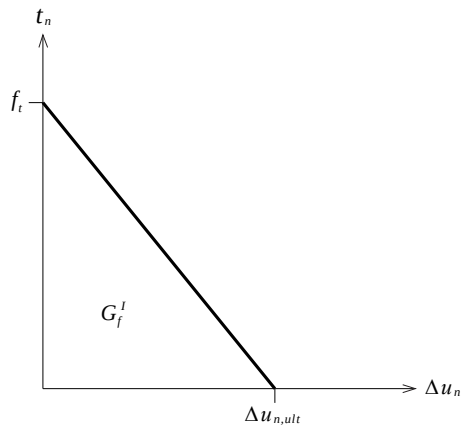

$$t_n = \begin{cases} f_t\left(1 - \dfrac{\Delta u_n}{\Delta u_{n,ult}}\right) & if \quad 0 < \Delta u_n < \Delta u_{n,ult} \\ 0 & if \quad \Delta u_{n,ult} < \Delta u_n \end{cases} \tag{4.2.186}$$

$\Delta u_{n,ult} \quad := 2 G_f^I / f_t$

G_f^I : Mode-I fracture energy

f_t : Tensile strength

Unloading and reloading can be modeled according to a secant approach or an elastic approach. In the secant approach, the relation between the traction and the relative normal displacement is linear up to the origin, after which the initial stiffness is recovered. In the elastic approach, the initial stiffness is recovered immediately after the relative normal displacement has become less than the current maximum relative normal displacement.

Nonlinear tension softening model

Hordijk , Cornelissen & Reinhardt proposed an expression for the softening behavior of concrete as shown in the figure below

Figure 4.2.41
Linear tension softening behavior

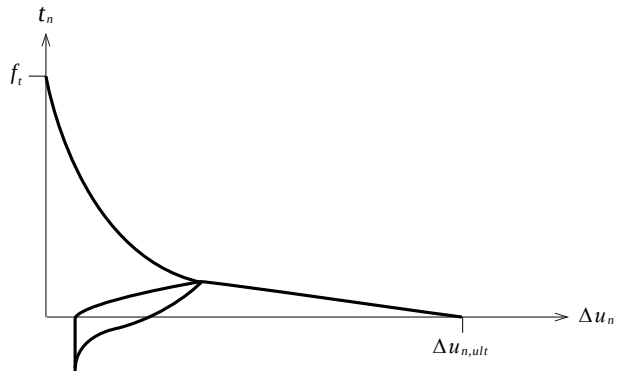

$$t_n = \begin{cases} f_t \left(\left(1 + \left(c_1 \frac{\Delta u_n}{\Delta u_{n,ult}} \right)^3 \right) \exp\left(-c_2 \frac{\Delta u_n}{\Delta u_{n,ult}} \right) - \frac{\Delta u_n}{\Delta u_{n,ult}} (1 + c_1^3) \exp(-c_2) \right) & \text{if} \quad 0 < \Delta u_n < \Delta u_{n,ult} \\ 0 & \text{if} \quad \Delta u_{n,ult} < \Delta u_n \end{cases} \tag{4.2.187}$$

$$\Delta u_{n,ult} := 5.136 G_f^I / f_t$$

$$c_1 := 3$$

$$c_2 := 6.93$$

Unloading and reloading can be modeled according to a secant approach, an elastic approach or by application of hysteresis.

Shear Retention

In general, the shear traction is reduced after cracking according to the following equation.

$$t_t = \begin{cases} k_t \Delta u_t & if \quad \Delta u_t < \Delta u_{t0} \\ \beta k_t \Delta u_t & if \quad \Delta u_n \geq \Delta u_{t0} \end{cases} \tag{4.2.188}$$

βk_t : Reduced shear stiffness

Δu_{t0} : Initial shear slip

In general, β may vary between 0.1 and 0.3. If the crack surface is assumed to be smooth after Mode-I cracking, β is defined as zero. But generally, it is assumed that the crack surface is not smooth and hence $0 < \beta \leq 1$.

2.26 Masonry

The Masonry material model is a material model that simulates the behavior of the Masonry wall under lateral load using homogenization techniques. First, homogenize the brick and the head joint, and then homogenize the homogenized material and the bed joint to obtain the physical properties of the entire homogenized material. In the masonry material, tensile cracking is considered to be the only nonlinearity. Cracks can occur on both bricks and on two joints. In the event of a crack, the elastic modulus of the crack is reduced by a predetermined proportion. Then, the newly homogenized material is obtained by reflecting the reduced elastic modulus.

The assumptions applicable to the Masonry Model are as follows.

1. Brick has linear elastic behavior and brittle failure occurs.
2. Mortar behaves linear elastically.
3. Brick and mortar are perfectly bonded.
4. Head joints are continuous.

Figure 4.2.42 shows a coordinate system of the Masonry Model for homogenizationi, where indexes b, hj, and bj represent bricks, head joints, and bed joints, respectively.

Figure 4.2.42
Coordinate system of masonry model

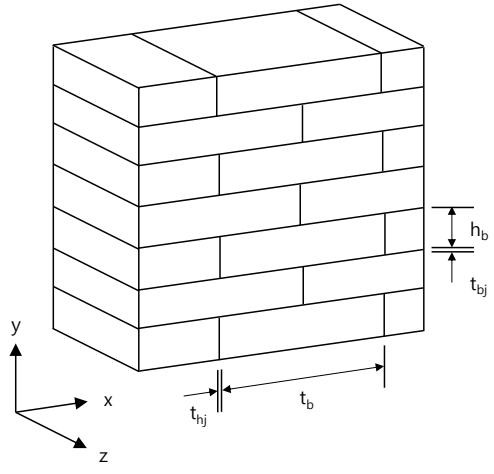

The stress/strain relationship of the homogenized masonry material is represented by

$$\bar{\boldsymbol{\varepsilon}} = \bar{\boldsymbol{C}}\bar{\boldsymbol{\sigma}} \tag{4.2.189}$$

Where $\bar{\boldsymbol{C}}$ is the compliance matrix for the homogenized Masonry model and is obtained by nine independent modulus of elasticity as shown below.

$$\bar{\boldsymbol{C}} = \begin{bmatrix} \frac{1}{\bar{E}_x} & -\frac{\bar{\nu}_{xy}}{\bar{E}_x} & -\frac{\bar{\nu}_{xz}}{\bar{E}_x} & & & \\ -\frac{\bar{\nu}_{yx}}{\bar{E}_y} & \frac{1}{\bar{E}_y} & -\frac{\bar{\nu}_{yz}}{\bar{E}_y} & & & \\ -\frac{\bar{\nu}_{zx}}{\bar{E}_z} & -\frac{\bar{\nu}_{zy}}{\bar{E}_z} & \frac{1}{\bar{E}_z} & & & \\ & & & \frac{1}{\bar{G}_{xy}} & & \\ & & & & \frac{1}{\bar{G}_{yz}} & \\ & & & & & \frac{1}{\bar{G}_{xz}} \end{bmatrix} \tag{4.2.190}$$

Structural matrix $\boldsymbol{A}$ is used to obtain the stress of each brick and joint from the average stress of the Masonry model.

$$\begin{aligned} \boldsymbol{\sigma}_{bj} &= \boldsymbol{A}_{bj}\boldsymbol{\sigma} \\ \boldsymbol{\sigma}_{hj} &= \boldsymbol{A}_{hj}\boldsymbol{\sigma} \\ \boldsymbol{\sigma}_{b} &= \boldsymbol{A}_{b}\boldsymbol{\sigma} \end{aligned} \tag{4.2.191}$$

Homogenization of brick and head joints

Calculate the ratio of the length of the brick and head joint.

$$t_b = \frac{l_b}{l_b + t_{hj}},\ \mathrm{t}_{hj} = \frac{t_{hj}}{l_b + t_{hj}} \tag{4.2.192}$$

Calculate the coefficients needed to obtain the physical properties.

$$\begin{aligned} \alpha &= \frac{t_{hj}E_{hj}\left(1-\nu_b^2\right) + t_bE_b\left(1-\nu_{hj}^2\right)}{\left(1-\nu_{hj}^2\right)\left(1-\nu_b^2\right)} \\ \zeta &= \frac{t_{hj}\nu_{hj}E_{hj}\left(1-\nu_b^2\right) + t_b\nu_bE_b\left(1-\nu_b^2\right)}{\left(1-\nu_{hj}^2\right)\left(1-\nu_b^2\right)} \\ \chi_b &= \frac{t_b\nu_b}{\left(1-\nu_b\right)},\ \chi_{hj} = \frac{t_{hj}\nu_{hj}}{\left(1-\nu_{hj}\right)},\ \chi = \chi_b + \chi_{hj} \end{aligned} \tag{4.2.193}$$

Calculate Poisson's ratio and modulus of elasticity.

$$\begin{aligned}
&\hat{v}_{yz} = \frac{\zeta}{\alpha},\ \hat{v}_{zx} = \hat{v}_{yx} = \chi\left(1-\hat{v}_{yz}\right)\\
&E_y^{'} = E_z^{'} = \alpha - \zeta v_{zy}^{'}\\
&\frac{1}{E_x^{'}} = \frac{t_{hj}}{E_{hj}} + \frac{t_b}{E_b} + 2\chi_{hj}\left(\frac{\hat{v}_{zx}}{\hat{E}_z} - \frac{v_{hj}}{E_{hj}}\right) + 2\chi_b\left(\frac{\hat{v}_{zx}}{\hat{E}_z} - \frac{v_b}{E_b}\right)\\
&\hat{v}_{xz} = \hat{v}_{zx}\frac{\hat{E}_x}{\hat{E}_z},\ \hat{v}_{zy} = \hat{v}_{yz}\frac{\hat{E}_z}{\hat{E}_y},\ \hat{v}_{xy} = \hat{v}_{yx}\frac{\hat{E}_x}{\hat{E}_y}
\end{aligned} \tag{4.2.194}$$

Calculate the shear modulus.

$$\begin{aligned}
&\frac{1}{G_{xy}^{'}} = \frac{1}{G_{xz}^{'}} = \frac{t_{hj}}{G_{hj}} + \frac{t_b}{G_b}\\
&G_{yz}^{'} = t_{hj}G_{hj} + t_bG_b
\end{aligned} \tag{4.2.195}$$

Homogenization with bed joints

Calculate the ratio of the length of the brick and bed joint.

$$\hat{t} = \frac{h_b}{h_b + t_{bj}},\ \mathrm{t}_{bj} = \frac{t_{bj}}{h_b + t_{bj}} \tag{4.2.196}$$

Calculate the coefficients needed to obtain the physical properties.

$$\begin{aligned}
&\bar{\alpha} = \frac{t_{bj}}{1-v_{bj}^2} + \frac{\hat{t}\hat{E}}{1-\hat{v}_{xz}\hat{v}_{zx}}\\
&\bar{\beta} = \frac{t_{bj}E_{bj}}{1-v_{bj}^2} + \frac{\hat{t}\hat{E}_z}{1-\hat{v}_{xz}\hat{v}_{zx}}\\
&\bar{\zeta} = \frac{t_{bj}v_{bj}E_{bj}}{1-v_{bj}^2} + \frac{\hat{t}E_z\hat{v}_{xz}}{1-\hat{v}_{xz}\hat{v}_{zx}}\\
&\bar{\chi}_{bj} = \frac{t_{bj}v_{bj}}{1-v_{bj}},\ \hat{\bar{\chi}} = \frac{\hat{t}\left(\hat{v}_{zy} + \hat{v}_{zx}\hat{v}_{xy}\right)}{1-\hat{v}_{xz}\hat{v}_{zx}},\ \chi = \chi_{bj} + \hat{\chi}\\
&\bar{\lambda}_{bj} = \bar{\chi}_{bj},\ \hat{\bar{\lambda}} = \frac{\hat{t}\left(\hat{v}_{xy} + \hat{v}_{zy}\hat{v}_{xz}\right)}{1-\hat{v}_{xz}\hat{v}_{zx}},\ \lambda = \lambda_{bj} + \hat{\lambda}
\end{aligned} \tag{4.2.197}$$

Calculate Poisson's ratio and modulus of elasticity.

$$\bar{v}_{zx} = \frac{\bar{\zeta}}{\bar{\alpha}},\ \bar{v}_{zy} = \bar{\chi} - \frac{\bar{\lambda}\bar{\zeta}}{\bar{\alpha}},\ \bar{v}_{xy} = \bar{\lambda} - \frac{\bar{\chi}\bar{\zeta}}{\bar{\beta}}$$

$$\bar{E}_z = \frac{\bar{\alpha}\bar{\beta} - \bar{\zeta}^2}{\bar{\alpha}},\ \bar{E}_x = \frac{\bar{\alpha}\bar{\beta} - \bar{\zeta}^2}{\bar{\beta}}$$

$$\frac{1}{\bar{E}_y} = \frac{t_{bj}}{E_{bj}} + \frac{\hat{t}}{\hat{E}_y} + \bar{\chi}_{bj}\left(\frac{\bar{v}_{xy}}{\bar{E}_z} - \frac{v_{bj}}{E_{bj}}\right) + \hat{\bar{\chi}}\left(\frac{\bar{v}_{zy}}{\bar{E}_z} - \frac{\hat{v}_{zy}}{\hat{E}_z}\right) + \lambda_m\left(\frac{v_x y}{E_x} - \frac{v_m}{E_m}\right) + \hat{\lambda}\left(\frac{\bar{v}_{xy}}{\bar{E}_x} - \frac{\hat{v}_{xy}}{\hat{E}_x}\right) \tag{4.2.198}$$

$$\bar{v}_{yx} = \bar{v}_{xy}\frac{\bar{E}_y}{\bar{E}_x},\ \bar{v}_{xz} = \bar{v}_{zx}\frac{\bar{E}_x}{\bar{E}_z},\ \bar{v}_{yz} = \bar{v}_{zy}\frac{\bar{E}_y}{\bar{E}_z}$$

Calculate the shear modulus.

$$\frac{1}{\bar{G}_{xy}} = \frac{t_{bj}}{G_{bj}} + \frac{\hat{t}}{\hat{G}_{xy}}$$

$$\bar{G}_{xz} = t_{bj} + \hat{t}\hat{G}_{xz} \tag{4.2.199}$$

$$\frac{1}{\bar{G}_{yz}} = \frac{t_{bj}}{G_{bj}} + \frac{\hat{t}}{\hat{G}_{yz}}$$

Stress of bead joint, head joint, and brick

Structural matrix $\boldsymbol{A}$, which provides stress of individual components from the average stress of the masonry, is as follows.

$$\boldsymbol{A} = \begin{bmatrix} a_{11} & a_{12} & a_{13} & & & \\ a_{21} & a_{22} & a_{23} & & & \\ a_{31} & a_{32} & a_{33} & & & \\ & & & a_{44} & & \\ & & & & a_{55} & \\ & & & & & a_{66} \end{bmatrix} \tag{4.2.200}$$

The coefficients of the structure matrix $\boldsymbol{A}^{bj}$ for the bed joints are as follows:

$$
\begin{aligned}
a_{11}^{bj} &= 1 + C_{bj}E_{bj}\left(\frac{1}{\bar{E}_x} - \frac{1}{E_{bj}}\right) - C_{bj}E_{bj}\nu_{bj}\left(\frac{\bar{\nu}_{zx}}{\bar{E}_z} - \frac{\nu_{bj}}{E_{bj}}\right) \\
a_{12}^{bj} &= -C_{bj}E_{bj}\left(\frac{\bar{\nu}_{xy}}{\bar{E}_x} - \frac{\nu_{bj}}{E_{bj}}\right) - C_{bj}E_{bj}\nu_{bj}\left(\frac{\bar{\nu}_{zy}}{\bar{E}_z} - \frac{\nu_{bj}}{E_{bj}}\right) \\
a_{13}^{bj} &= -C_{bj}E_{bj}\left(\frac{\bar{\nu}_{xz}}{\bar{E}_x} - \frac{\nu_{bj}}{E_{bj}}\right) + C_{bj}E_{bj}\nu_{bj}\left(\frac{1}{\bar{E}_z} - \frac{1}{E_{bj}}\right) \\
a_{22}^{bj} &= 1.0 \\
a_{31}^{bj} &= C_{bj}E_{bj}\nu_{bj}\left(\frac{1}{\bar{E}_x} - \frac{1}{E_{bj}}\right) - C_{bj}E_{bj}\left(\frac{\bar{\nu}_{zx}}{\bar{E}_z} - \frac{\nu_{bj}}{E_{bj}}\right) \\
a_{32}^{bj} &= -C_{bj}E_{bj}\nu_{bj}\left(\frac{\bar{\nu}_{xy}}{\bar{E}_x} - \frac{\nu_{bj}}{E_{bj}}\right) - C_{bj}E_{bj}\left(\frac{\bar{\nu}_{zy}}{\bar{E}_z} - \frac{\nu_{bj}}{E_{bj}}\right) \\
a_{33}^{bj} &= 1 - C_{bj}E_{bj}\nu_{bj}\left(\frac{\bar{\nu}_{xz}}{\bar{E}_x} - \frac{\nu_{bj}}{E_{bj}}\right) + C_{bj}E_{bj}\left(\frac{1}{\bar{E}_z} - \frac{\nu_{bj}}{E_{bj}}\right) \\
a_{44}^{bj} &= 1.0,\ a_{55}^{bj} = 1.0,\ a_{66}^{bj} = \frac{G_{bj}}{\bar{G}_{xz}}
\end{aligned}
\tag{4.2.201}
$$

C_{bj} : $\dfrac{1}{1-\nu_{bj}^2}$

The head joints and bricks are obtained by multiplying the common structural matrix $\hat{\boldsymbol{A}}$ by the partial structural matrix $\boldsymbol{P}_b, \boldsymbol{P}_{hj}$.

$$
\begin{aligned}
\boldsymbol{A}_{hj} &= \boldsymbol{P}_{hj}\boldsymbol{A} \\
\boldsymbol{A}_b &= \boldsymbol{P}_b\boldsymbol{A}
\end{aligned}
\tag{4.2.202}
$$

The coefficients for the common structural matrix are as follows:

$$
\begin{aligned}
\hat{a}_{11} &= 1+\hat{C}\hat{E}_x\left(\frac{1}{\bar{E}_x}+\frac{1}{\hat{E}_x}\right)-\hat{C}\hat{E}_z\hat{v}_{xz}\left(\frac{\bar{v}_{zx}}{\bar{E}_z}-\frac{\hat{v}_{zx}}{\hat{E}_z}\right)\\
\hat{a}_{12} &= -\hat{C}\hat{E}_x\left(\frac{\bar{v}_{xy}}{\bar{E}_x}-\frac{\hat{v}_{zy}}{\hat{E}_x}\right)-\hat{C}\hat{E}_z\hat{v}_{xz}\left(\frac{\bar{v}_{zy}}{\bar{E}_z}-\frac{\hat{v}_{zy}}{\hat{E}_z}\right)\\
\hat{a}_{13} &= -\hat{C}\hat{E}_x\left(\frac{\bar{v}_{xz}}{\bar{E}_x}-\frac{\hat{v}_{xz}}{\hat{E}_x}\right)+\hat{C}\hat{E}_z\hat{v}_{xz}\left(\frac{1}{\bar{E}_z}-\frac{1}{\hat{E}_z}\right)\\
\hat{a}_{22} &= 1.0\\
\hat{a}_{31} &= \hat{C}\hat{E}_x\hat{v}_{zx}\left(\frac{1}{\bar{E}_x}-\frac{1}{\hat{E}_x}\right)-\hat{C}\hat{E}_z\left(\frac{\bar{v}_{zx}}{\bar{E}_z}-\frac{\hat{v}_{zx}}{\hat{E}_z}\right)\\
\hat{a}_{32} &= -\hat{C}\hat{E}_x\hat{v}_{zx}\left(\frac{\bar{v}_{xy}}{\bar{E}_x}-\frac{\hat{v}_{xy}}{\hat{E}_x}\right)-\hat{C}\hat{E}_z\left(\frac{\bar{v}_{zy}}{\bar{E}_z}-\frac{\hat{v}_{zy}}{\hat{E}_z}\right)\\
\hat{a}_{33} &= 1-\hat{C}\hat{E}_x\hat{v}_{zx}\left(\frac{\bar{v}_{xz}}{\bar{E}_x}-\frac{v_{xz}}{E_x}\right)+\hat{C}\hat{E}_z\left(\frac{1}{\bar{E}_z}-\frac{1}{\hat{E}_z}\right)\\
\hat{a}_{44} &= 1.0,\ \hat{a}_{55}=1.0,\ \hat{a}_{66}=\frac{\hat{G}_{xz}}{\bar{G}_{xz}}
\end{aligned}
\qquad (4.2.203)
$$

$$
\hat{C} \quad : \frac{1}{1-\hat{v}_{xz}\hat{v}_{zx}}
$$

The coefficients for the partial structural matrix are as follows:

$$
\begin{aligned}
p_{11} &= 1.0 \\
p_{21} &= C_i E_i \nu_i \left(\frac{\hat{\nu}_{zx}}{\hat{E}_z} - \frac{\nu_i}{E_i} \right) - C_i E_i \left(\frac{\hat{\nu}_{yx}}{\hat{E}_y} - \frac{\nu_i}{E_i} \right) \\
p_{22} &= 1 - C_i E_i \nu_i \left(\frac{\hat{\nu}_{zy}}{\hat{E}_z} - \frac{\nu_i}{E_i} \right) + C_i E_i \left(\frac{1}{\hat{E}_y} - \frac{1}{E_i} \right) \\
p_{23} &= C_i E_i \nu_i \left(\frac{1}{\hat{E}_z} - \frac{1}{E_i} \right) - C_i E_i \nu_i \left(\frac{\hat{\nu}_{yx}}{\hat{E}_y} - \frac{\nu_i}{E_i} \right) \\
p_{31} &= -C_i E_i \left(\frac{\hat{\nu}_{zx}}{\hat{E}_z} - \frac{\nu_i}{E_i} \right) - C_i E_i \nu_i \left(\frac{\hat{\nu}_{yx}}{\hat{E}_y} - \frac{\nu_i}{E_i} \right) \\
p_{32} &= -C_i E_i \left(\frac{\hat{\nu}_{zy}}{\hat{E}_z} - \frac{\nu_i}{E_i} \right) + C_i E_i \nu_i \left(\frac{1}{\hat{E}_y} - \frac{1}{E_i} \right) \\
p_{33} &= 1 + C_i E_i \left(\frac{1}{\hat{E}_z} - \frac{1}{E_i} \right) - C_i E_i \nu_i \left(\frac{\hat{\nu}_{yz}}{\hat{E}_y} - \frac{\nu_i}{E_i} \right) \\
p_{44} &= 1.0,\ p_{55} = \frac{G_i}{\hat{G}_{yz}},\ p_{66} = 1.0
\end{aligned}
\tag{4.2.204}
$$

C_i : $\frac{1}{1-\nu_i^2}$

In the above expression, index i is a head joint (hj) or brick (b).

2.27 Combined Cracking-Shearing-Crushing

Combined-Cracking-Shear-Crushing (CCSC) model in FEA NX is based on the formula presented by Lourenco[26] and enhanced by Van Zijl[27]. It is based on multi-surface plasticity, comprising a Coulomb friction model combined with a tension cut-off and an elliptical compression cap. Softening acts in all three modes and is preceded by hardening in the case of the cap mode.

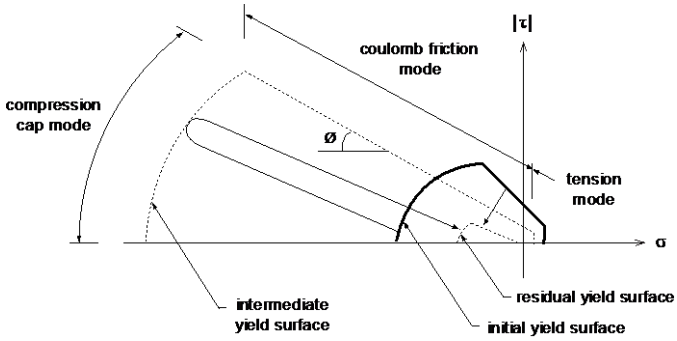

Figure 4.2.43
Three yield surfaces in two dimension

The interface model is derived in terms of the generalized stress and strain vectors.

$$\boldsymbol{\sigma} = \begin{pmatrix} \sigma \\ \mathbf{t}_t \end{pmatrix} \quad , \boldsymbol{\varepsilon} = \begin{pmatrix} u_n \\ \mathbf{u}_t \end{pmatrix} \tag{4.2.205}$$

$$\mathbf{D} = diag\begin{bmatrix} k_n & k_s & k_t \end{bmatrix} \tag{4.2.206}$$

σ, u_n : Stress and relative displacement in the normal direction

$\mathbf{t}_t, \mathbf{u}_t$: Stress and relative displacement in the tangential directioin

k_n : Stiffness in the normal direction

k_s, k_t : Stiffness in the tangential direction

Shear slip failure

A Coulomb friction model describes the shear-slipping in the CCSC model and adhesion and internal friction angle assume softening behavior.

[26] P. B. Lourenço, "Compulational strategies for masonry structures", Delft University Press, 1996

[27] G.P.A.G. van Zijl, "Compulational modelling of masonry creep and shrinkage", The Netherlands by Meinema BV, Delft, 1999

$$f = \|\boldsymbol{t}_t\| + \sigma\Phi - c$$
$$c = c_0 e^{-\frac{c_0}{G_f^{II}}\kappa} \qquad (4.2.207)$$
$$\Phi = \Phi_0 + \left(\Phi_r - \Phi_0\right)\frac{c_0 - c}{c_0}$$

Φ : Internal friction angle

Φ_0, Φ_r : Initial friction ($\tan\phi$) and residual friction

c_0 : Initial adhesion

κ : Plastic relative displacement

G_f^{II} : Mode-II fracture energy

From the observations of experiments[27], shear failure energy and normal stress assume the following linear relationships.

$$G_f^{II} = \begin{cases} a\sigma + b & if \ \ \sigma < 0 \\ b & if \ \ \sigma \geq 0 \end{cases} \qquad (4.2.208)$$

a, b : Material constants

Tension cut-off

Tensile failure and softening behavior are defined as follows, and plastic flow functions are defined using the associated plastic flow rule.

$$f_t = \sigma - \sigma_t$$
$$\sigma_t = f_t e^{-\frac{f_t}{G_f^I}\kappa_t} \qquad (4.2.209)$$

κ_t : Tensile plastic strain

f_t : Tension force

G_f^I : Mode-I fracture energy

Compression cap

The yield function of the compression cap is defined as follows, and the function of compressive plastic flow is defined using the associative plastic flow rule.

$$f_c = \sigma^2 + C_s \left\| \boldsymbol{t}_t \right\|^2 - \sigma_c^2$$
$$\kappa_c = \sqrt{\boldsymbol{\varepsilon}_p^T \boldsymbol{\varepsilon}_p} \qquad (4.2.210)$$
$$\sigma_c = \sigma_c \left(f_c, \kappa_p \right)$$

κ_c : Compressive plastic strain

σ_c : Compression force

C_s : Shear stress contribution parameter

f_c : Compression failure energy

κ_p : Plastic strain at peak

Compression force is expressed by the initial hardening behavior and softening behavior defined by compression failure energy.

Figure 4.2.44
Hardening and softening behavior for compression

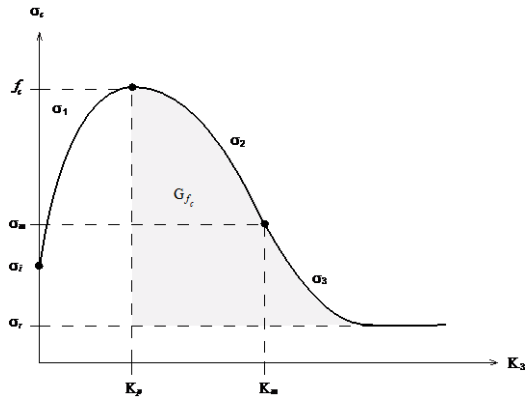

Therefore, the compression force is defined in three areas as follows:

$$\sigma_c^1(\kappa_c) = \bar{\sigma}_i + (f_c - \bar{\sigma}_i)\sqrt{\frac{2\kappa_c}{\kappa_p} - \frac{\kappa_c^2}{\kappa_p^2}} \qquad ,\bar{\sigma}_i = \tfrac{1}{3} f_c$$

$$\sigma_c^2(\kappa_c) = f_c + (\bar{\sigma}_m - f_c)\left(\frac{\kappa_c - \kappa_p}{\kappa_m - \kappa_p}\right)^2 \qquad ,\bar{\sigma}_m = \tfrac{1}{2} f_c \qquad (4.2.211)$$

$$\sigma_c^3(\kappa_c) = \bar{\sigma}_r + (\bar{\sigma}_m - \bar{\sigma}_r)\exp\left(2\left(\frac{\bar{\sigma}_m - f_c}{\kappa_m - \kappa_p}\right)\left(\frac{\kappa_c - \kappa_m}{\bar{\sigma}_m - \bar{\sigma}_r}\right)\right) \qquad ,\bar{\sigma}_r = \tfrac{1}{7} f_c$$

Section 3 Drained/Undrained Materials

3.1 Isotropic Materials

The pore pressure in stress analysis can be divided into the steady state pore pressure, which does not change with time, and the unsteady pore pressure, which changes with time or changes in load/boundary states, for convenience.

$$p = p_{steady} + p_{unsteady} \tag{4.3.1}$$

Here, the state where the unsteady pore pressure is close to '0' is called the drained condition and the analysis under this condition is called drained analysis. Generally, it is appropriate to perform drained analysis for the following states.

- When the change in steady state pore pressure is insignificant, due to external boundary conditions or use of sand like materials which have large coefficients of permeability
- When simulating the process after consolidation, where the excessive pore pressure has been dissipated

Pore water can display instantaneous undrained behavior, due to the use of clay like materials with small coefficients of permeability or external conditions such as the existence of impermeable layers. In this case, un-negligible unsteady pore pressure occurs for the change in external load state. This unsteady state pore pressure is called the excessive pore pressure. When the pore pressure is assumed not to change with the seepage condition time, it is determined by the permeability coefficient and the volume change of the porous ground due to the compressibility of the pore water. FEA NX uses this process of dissipating excessive pore pressure, caused by load state change, with time to simulate consolidation analysis.

The state where excessive pore pressure occurs due to the compressibility of the pore water is called the undrained condition, and the analysis under this condition is called undrained analysis. The general undrained conditions are as follows.

- When the permeability coefficient is small, or the load change is very large
- When instantaneous behavior and safety due to load change is of interest

3.2 Undrained Constitutive Equation

Drained conditions do not have stiffness for change in load condition. Hence, drained materials follow the behavior of the ground skeleton material.
On the other hand, undrained material models consider the stiffness for the compressibility of the pore water in addition to the ground skeleton material behavior. Pore water does not have shear stiffness and has volume change stiffness. The relationship between the excessive pore pressure change and volume change of the ground is as follows.

$$dp_{unsteady} = dp_{excess} = -\frac{K_w}{n}\mathbf{m}^T d\boldsymbol{\varepsilon}^{mech} \tag{4.3.2}$$

K_w : Bulk modulus of water

n : Porosity

$\mathbf{m}$: Normal unit vector (in 3D, $\mathbf{m} = [1,1,1,0,0,0]^T$)

$d\boldsymbol{\varepsilon}^{mech}$: Amount of mechanical strain change

Assuming saturated linear elastic istropic materials for convenience, the modified strain-stress relationship can be obtained.

$$d\boldsymbol{\sigma} = d\boldsymbol{\sigma}' - \mathbf{m}dp_{excess} = \mathbf{C}^{el,u} d\boldsymbol{\varepsilon}^{mech} \tag{4.3.3}$$

$\mathbf{C}^{el,u} = \mathbf{C}^{el} + \frac{K_w}{n}\mathbf{m}\mathbf{m}^T$: Undrained elasticity matrix

$\mathbf{C}^{el}$: Effective elasticity matrix

The bulk modulus of water (K_w) is generally a very large value and so, the undrained Poisson's ratio ν_u is close to 0.5 and the porous material displays nearly incompressible behavior. When partial low order elements are used in this case, volumetric locking occurs and the accuracy of the solution falls greatly. Hence, modeling using high order elements is recommended for undrained analysis.

To account for undrained effects and guarantee the solution accuracy, FEA NX does not use the bulk modulus of water directly and uses the user input undrained Poisson's ratio or Skempton factor (B) as a base to back-calculate the bulk modulus of water directly. The undrained Poisson's ratio has a default value of '0.495'.

Using equation (4.3.3), the equation for calculating the bulk modulus of pore water is as follows, when the undrained Poisson's ratio or Skempton factor is given.

$$K_f = \frac{K_w}{n} = \frac{E'(\nu_u - \nu')}{(1-2\nu')(1+\nu')(1-2\nu_u)} \tag{4.3.4}$$

K_f : Bulk modulus of pore water

E', ν' : Effective modulus of elasticity and effective Poisson's ratio

The Skempton factor (B) is defined as the ratio between the undrained bulk modulus and bulk modulus of pore water. In other words,

$$K_f = BK_u \tag{4.3.5}$$

K_u : Undrained bulk modulus

Using equations (4.3.2) and (4.3.4), the relationship between the undrained Poisson's ratio and Skempton factor can be expressed as follows.

$$\nu_u = \frac{3\nu' + B(1-2\nu')}{3 - B(1-2\nu')} \tag{4.3.6}$$

Using this, the bulk modulus of pore water can be calculated. From equation (4.3.6), it can be seen that the undrained Poisson's ratio approaches '0.5' as the Skempton factor approaches '1'.

3.3 Undrained Material Type

Effective stiffness/effective strength

This is the most general case where the input stiffness parameters and strength parameters are the parameters of the ground skeleton. Like drained analysis, FEA NX uses the input stiffness/strength parameters for undrained analysis. The disadvantage is that the effective strength parameters in the undrained state are hard to obtain through experimentation.

► Available material model

: Linear elastic material, Mohr-Coulomb, Drucker-Prager, Duncan-Chang, Hoek-Brown, Strain Softening, Modified Cam-clay, Jardine, D-min, Modified Mohr-Coulomb, User-supplied, Modified UBCSAND, Sekiguchi-Ohta

Effective stiffness/undrained strength

The undrained load path of simple material models like the Mohr-Coulomb model is known to be difficult to express accurately. Hence, the undrained shear stiffness, which is determined by the friction angle and cohesion, can be overestimated. If the empirical undrained shear stiffness (s_u) is known, the undrined strength can be directly input using the cohesion when the friction angle is 0. By using the actual undrained strength, results that satisfy the shear stiffness can be obtained. However, this case has the same disadvantage that the undrained load path is difficult to estimate accurately.

► Available material model

: Mohr-Coulomb, Drucker-Prager, Modified Mohr-Coulomb

Undrained stiffness/undrained strength

This method directly inputs the undrained stiffness, which considers the compressibility of the pore water. Hence, FEA NX does not calculate the excessive pore pressure and its effects are included in the calculated stress. In other words, the calculated stress is the total stress that includes the pore pressure. The undrained stiffness and undrained strength parameters can be directly input when known by lab testing.

- Available material model: Linear elastic material, Mohr-Coulomb, Drucker-Prager, Modified Mohr-Coulomb

Section 4 Seepage Material Properties

4.1 Constitutive Equation

Darcy's Law is used to display the seepage phenomena within the ground.

$$\mathbf{q} = \mathbf{k}\nabla h = -\mathbf{k}\mathbf{n}_g + \frac{1}{\gamma_w}\mathbf{k}\nabla p_w \tag{4.4.1}$$

- $\mathbf{q}$: Seepage velocity
- $\mathbf{k}$: Permeability coefficient matrix
- h : Total head
- $\mathbf{n}_g$: Gravitational direction unit vector

Darcy's Law expresses the proportionality between the ground seepage velocity and the total head gradient. Darcy's Law was originally derived for saturated soils, but various researches have shown that it can be applied to unsaturated flow. Also, Darcy's Law is effective for slow viscous flow and can be applied to most groundwater flow.

For seepage materials, FEA NX uses the permeability coefficient matrix that considers only the diagonal component of each direction. Here, the direction is the MCS direction.

$$\mathbf{k} = \begin{bmatrix} k_x & 0 & 0 \\ 0 & k_y & 0 \\ 0 & 0 & k_z \end{bmatrix} \tag{4.4.2}$$

The seepage velocity $\mathbf{q}$ has velocity units, and the actual flow velocity in the soil has a value of the seepage velocity $\mathbf{q}$ divided by the porosity of the soil.

$$\mathbf{v} = \frac{\mathbf{q}}{n} \tag{4.4.3}$$

4.2 Permeability Coefficient

The permeability coefficient is a criterion for how much the groundwater within the soil moves in unit time and it is dependent on the water content and void ratio change Δe of the ground. The permeability coefficient has the largest value at the saturated state because the path size increases with larger water content. Also, because water content is dependent on pore pressure, the permeability coefficient also changes with pore pressure. The void ratio change is considered in consolidation analysis and fully coupled stress-seepage analysis. The void ratio change is calculated from the initial condition of the void ratio.

To express the change in permeability coefficient with pore pressure and void ratio change, FEA NX uses the saturated permeability coefficient $\mathbf{k}_{sat}$, permeability ratio function $k_r = k_r(p)$ depending on pore pressure change. The c_k that defines the permeability ratio depending on the void ratio change Δe. The unsaturated permeability coefficient can be found using the following equation.

$$\mathbf{k} = 10^{\frac{\Delta e}{c_k}} \; k_r(p)\, \mathbf{k}_{sat} \tag{4.4.4}$$

Figure 4.4.1 Permeability ratio for negative pore pressure

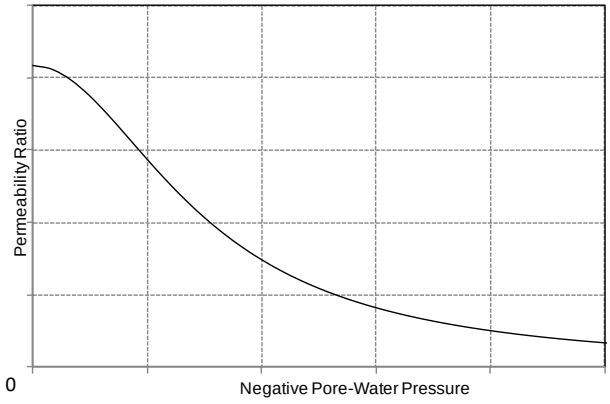

The permeability coefficient with the pore pressure is directly input as a table in FEA NX, but widely known permeability coefficient formulas can be used. The supported formulas in FEA NX are as follows and the h represents the negative pore pressure head.

Gardner function

$$k_r = \frac{1}{1 + a(h)^n} \tag{4.4.5}$$

a, n : Curve fitting parameters

Frontal function

$$\begin{aligned} h \le 0 \qquad & k_r = 1 \\ 0 < h < H_0 \qquad & k_r = \frac{h(r-1)}{H_0} + 1 \\ h \le H_0 \qquad & k_r = r \end{aligned} \tag{4.4.6}$$

r : Minimum permeability ratio

H_0 : Limit negative pore pressure head

Van Genuchten function

$$k_r = \frac{\left[1-\left((ah)^{n-1}\right)\left(\left(1+(ah)^n\right)^{-m}\right)\right]^2}{\left[1+(ah)^n\right]^{m/2}} \tag{4.4.7}$$

a, n, m : Curve fitting parameters

4.3 Volumetric Water Content

When water flows within the ground, a certain amount is retained and this amount is determined by the ground properties and capillary suction. This is called the water content. Seepage analysis generally uses the volumetric water content, the ratio between the total volume and water volume.

$$\theta = \frac{V_w}{V} = nS \tag{4.4.8}$$

θ : Volumetric water content

V_w : Water volume

V : Total volume

n : Porosity

S : Degree of saturation

The change in volumetric water content for pore pressure is used for element calculation for seepage and consolidation analysis, as explained in chapter 3. Differentiating equation (4.4.8) for pore pressure can express it using the porosity and degree of saturation.

$$\frac{\partial \theta}{\partial p} = S\frac{\partial n}{\partial p} + n\frac{\partial S}{\partial p} \tag{4.4.9}$$

The first term of the right hand side represents the slope of the volumetric water content for the saturated condition. This term is represented using the specific storage S_s, which represents the volumetric ratio of the water inflow or outflow in the ground due to the pore pressure head change.

$$S\frac{\partial n}{\partial p} = \frac{\partial V_v}{\partial h}\frac{\partial h}{\partial p} = \frac{S_s}{\gamma} \tag{4.4.10}$$

V_v : Void volume

The second term of the right hand side represents the slope of the volumetric water content for the unsaturated condition. This value uses the slope of the user input soil-water characteristic curve. The soil-water characteristic curve represents the relationship between the volumetric water content and pore pressure for unsaturated conditions. The general curve is shown in Figure 4.4.2.

Figure 4.4.2 Soil-water characteristic curve

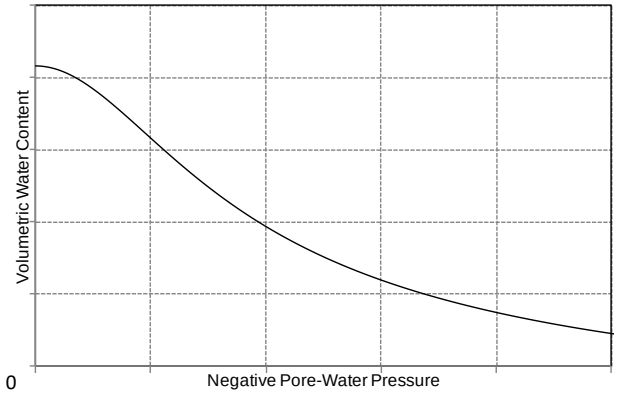

Like the permeability coefficient, the volumetric water content is directly input as a table. Widely known formulas can also be used. The supported formulas in are as follows. $\overline{p}$ represents the negative pore pressure head.

Van Genuchten fuction

$$\theta = \theta_r + \frac{\theta_s - \theta_r}{\left(1 + (a\overline{p})^n\right)^m} \tag{4.4.11}$$

θ_r : Minimum volumetric water content

θ_s : Maximum volumetric water content

a , n , m : Curve fitting parameters

4.4 Ductile Function

The permeability coefficient and volumetric water content above were defined individually for pore pressure or pore pressure head. However, nonlinear characteristics (permeability coefficient and volumetric water content) of actual soils are affected by the pressure head change simultaneously in a coupled form.

FEA NX reflects these characteristics and uses ductile function forms (pressure head-water content, water content-permeability ratio function or pressure head-degree of saturation, degree of saturation-permeability ratio function) to define the characteristics of unsaturated materials. When the pressure head-degree of

saturation and degree of saturation-permeability ratio ductile function are defined, the volumetric water content is calculated using the porosity.

Section 5

Viscous Material Properties

The typical behavior of visco-elastic and visco-plastic material is appeared to creep (increasing strain at constant stress) and stress relaxation (decreasing stress at constant strain) phenomenon. Also, viscous can be changed depending on the material temperature and strain rate. The visco-elastic property means that having both viscosity and elasticity. Similarly, the visco-plastic property means that having both viscosity and plasticity. FEA NX includes age independent and age dependent model for visco-elastic material, and Soft Soil Creep, Sekiguchi-Ohta(viscid) model for visco-plastic material.

Table 4.5.1 Available viscous materials for each element type

Material type	Element type								
	Truss	Beam	Interface	Geogrid	Plane Stress	Shell	Plane strain	Axisymmetric Solid	Solid
Age independent	V				V	V	V	V	V
Age dependent	V	V			V	V	V	V	V
Soft Soil Creep							V	V	V
Sekiguchi-Ohta (Viscid)							V	V	V

5.1 Age Independent Visco-elastic Material

At the macroscopic level, the creep phenomenon is best observed in the uniaxial creep test under constant load and the relaxation test under constant strain at constant temperature. A specimen subjected to a constant uniaxial tension exhibits three distinct phases in the time frame: primary creep stage, secondary creep stage and the tertiary creep stage to rupture as shown in Figure 4.5.1. In the first stage of so-called primary creep, we observe a decreasing strain rate. In the second stage of so-called secondary creep, the creep strain rate is approximately constant. In the third stage of tertiary creep, the creep strain tare increases. The tertiary creep, similar to necking in plasticity, is considered as a localized instability phenomenon, which is beyond the scope of this creep analysis. The primary and secondary creep behavior can be used for isotropic material in FEA NX.

Figure 4.5.1 Uniaxial creep test under constant load at constant temperature

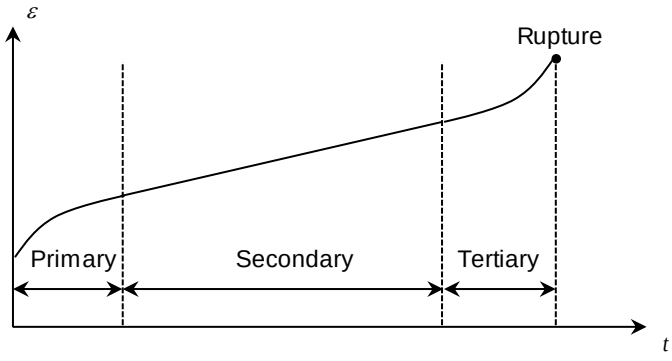

If the specimen is unloaded after some creep deformation, the elastic strain is immediately recovered and a portion of the creep strain is gradually recovered as shown in Figure 4.5.2. The recoverable portion of the creep deformation is called primary creep and the non-recoverable portion is called secondary creep.

Figure 4.5.2 Creep strain relaxation upon load removal

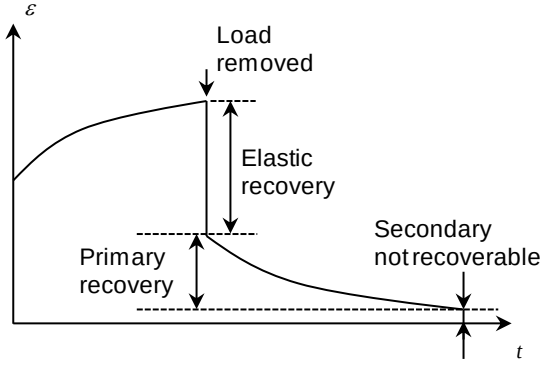

The Kelvin-Maxwell model is employed in the formulation of the creep capability as a generalization of the age independent visco-elastic material behavior. This model consists of one elastic spring and two viscous dampers. The Kelvin-Voigt model, which is a spring and a damper connected in parallel, represents the primary creep and a damper connected in series to the Kelvin-Voigt model represents the secondary creep.

Figure 4.5.3 Kelvin-Maxwell creep model

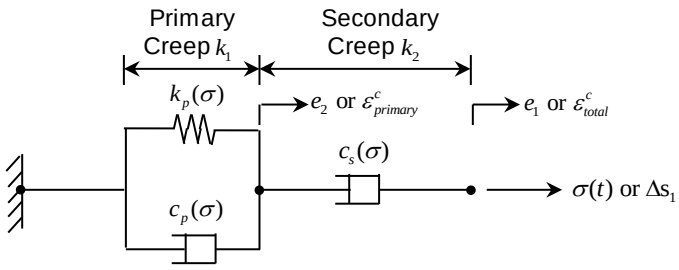

The creep strain and time-dependent increase in creep strain under constant stress is given as

$$\varepsilon^c_{total} = \frac{\sigma}{c_s}t + \varepsilon^c_{primary}$$
$$\varepsilon^c_{primary} = \frac{\sigma}{k_p}\left[1 - e^{-(k_p/c_p)t}\right] \qquad (4.5.1)$$

The creep strain can be calculated with two empirical laws as follows:

$$\text{Empirical law 1}: \ \varepsilon^c_{total} = A(\sigma)\left[1 - \exp\left(-R(\sigma)t\right)\right] + K(\sigma)t$$
$$A(\sigma) = a\sigma^b \quad \text{or} \quad a\exp(b\sigma)$$
$$R(\sigma) = c\exp(d\sigma) \quad \text{or} \quad c\sigma^d \qquad (4.5.2)$$
$$K(\sigma) = e\left[\sinh(f\sigma)\right]^g \quad \text{or} \quad e\exp(f\sigma)$$
$$\text{Empirical law 2}: \ \varepsilon^c_{total} = a\sigma^b t^d + \mathrm{e}\sigma^f t$$

a, b, c, d, e, f : Material constants

t : Time

In empirical law1, $k_p = \frac{\sigma}{A(\sigma)}$, $c_p = \frac{\sigma}{A(\sigma)R(\sigma)}$, $c_s = \frac{\sigma}{K(\sigma)}$ and k_p, c_p, c_s are calculated by the primary and secondary differential equations for ε^c_{total} in empirical law2.

The equilibrium equation of Kelvin-Maxwell creep model in the uniaxial condition is as follows:

$$\mathbf{C}\Delta\dot{\mathbf{e}} + \mathbf{k}\Delta\mathbf{e} = \Delta\mathbf{s}$$
$$\mathbf{C} = \begin{bmatrix} c_s & -c_s \\ -c_s & (c_p + c_s) \end{bmatrix}, \ \mathbf{k} = \begin{bmatrix} 0 & 0 \\ 0 & k_p \end{bmatrix}, \ \Delta\mathbf{s}^T = \begin{Bmatrix} \Delta s_1 & 0 \end{Bmatrix} \qquad (4.5.3)$$

Substitution of the increase in creep strain using central difference method into equation (4.5.3) gives the following equation:

$$\left[\frac{2}{\Delta t}\mathbf{C}+\mathbf{k}\right]\Delta\mathbf{e}=2\mathbf{C}\dot{\mathbf{e}}+\Delta\mathbf{s} \tag{4.5.4}$$

The stiffness of the primary, secondary creep elements and equivalent creep stiffness in Kelvin-Maxwell creep model can be determined by

$$k_1=k_p+\frac{2c_p}{\Delta t},\ k_2=\frac{2c_s}{\Delta t},\ k_c=\frac{k_1k_2}{k_1+k_2} \tag{4.5.5}$$

Using equation (4.5.4) and (4.5.5), the pseudo incremental strain ($\Delta\varepsilon'$) which represent the stress relaxation is as follows:

$$\Delta\varepsilon'=\frac{\Delta s'}{k_c}=2\left[\frac{c_s}{k_2}\left(\dot{\varepsilon}^c_{total}-\dot{\varepsilon}^c_{primary}\right)+\frac{c_p}{k_1}\dot{\varepsilon}^c_{primary}\right] \tag{4.5.6}$$

In multi-axial creep deformation, a unique set of rheological parameters ($\bar{k}_p$, $\bar{c}_p$, $\bar{c}_s$) based on the effective stress is used and the pseudo incremental strain may be expressed with the following equation:

$$\begin{aligned} k_1&=\frac{2}{3}\left(\bar{k}_p+\frac{2\bar{c}_p}{\Delta t}\right),\ k_2=\frac{2}{3}\left(\frac{2\bar{c}_s}{\Delta t}\right)\\ \Delta\boldsymbol{\varepsilon}'&=\frac{4}{3}\left[\frac{\bar{c}_s}{k_2}\left(\dot{\boldsymbol{\varepsilon}}^c_{total}-\dot{\boldsymbol{\varepsilon}}^c_{primary}\right)+\frac{\bar{c}_p}{k_1}\dot{\boldsymbol{\varepsilon}}^c_{primary}\right] \end{aligned} \tag{4.5.7}$$

With the total strain increment which is the summation of elastic and creep strain increment, the stress-strain relationship gives the following equation:

$$\Delta\boldsymbol{\sigma}=\left[\mathbf{D}^e+\mathbf{D}^c\right]\left[\Delta\boldsymbol{\varepsilon}^e+\Delta\boldsymbol{\varepsilon}^c\right] \tag{4.5.8}$$

$\mathbf{D}^e$: Material matrices for elasticity

$\mathbf{D}^c$: Material tangent matrices for creep

Since the summation of elastic and creep strain increment should be equal to the exception of the pseudo incremental strain from the total strain increment, the stress-strain relationship is as follows:

$$\Delta\boldsymbol{\sigma} = \mathbf{D}^{e}\left[\Delta\boldsymbol{\varepsilon} - \Delta\boldsymbol{\varepsilon}'\right] \tag{4.5.9}$$

For isotropic material, the elastic-creep tangent matrix $\mathbf{D}^{ec}$ may be conveniently obtained by

$$\mathbf{D}^{ec} = \begin{bmatrix} K+\frac{2}{3}k_{ec} & K-\frac{1}{3}k_{ec} & K-\frac{1}{3}k_{ec} & 0 & 0 & 0 \\ & K+\frac{2}{3}k_{ec} & K-\frac{1}{3}k_{ec} & 0 & 0 & 0 \\ & & K+\frac{2}{3}k_{ec} & 0 & 0 & 0 \\ & & & \frac{1}{2}k_{ec} & 0 & 0 \\ & \textit{symmetric} & & & \frac{1}{2}k_{ec} & 0 \\ & & & & & \frac{1}{2}k_{ec} \end{bmatrix} \tag{4.5.10}$$

$$\frac{1}{k_{ec}} = \frac{1}{2G} + \frac{1}{k_c}$$

K : Bulk modulus

G : Shear modulus

5.2 Age Dependent Visco-elastic Material

The properties of material such as concrete are changed with time and non-mechanical deformation of creep and shrinkage occurs. Also, the deformation with time varies depending on the time of the stress occurred in creep deformation.

When a uniaxial stress exerts on a concrete specimen at the age τ, creep deformation with time can be expressed as creep compliance (total strain at the age t), specific creep (creep function excluding elastic deformation) and creep coefficient (ratio of creep strain to elastic strain). Various creep functions can be used depending on the time of the specific stress applied. If the stress changes with time, the increased/decreased stress at each time requires an independent creep function. Creep strain at a particular time is calculated through superposition of individually calculated strains due to the stresses increased/decreased from the time that stress starts changing. In order to use the superposition method, the histories of all the element stresses are saved, and the creep strains are calculated from the initial steps to the present for all the stresses at every step. Extensive data storage and calculations are thus required to use the superposition method. However, FEA NX does not save the entire histories of stresses, rather uses the following integration method to increase the calculation efficiency.

The total creep deformation from a particular time to a final time can be expressed as a superposition integration of creeps due to the stresses resulting from each stage.

$$\varepsilon_c(t) = \int_0^t C(t,\tau)\frac{\partial\sigma(\tau)}{\partial\tau}d\tau \tag{4.5.11}$$

$\varepsilon_c(t)$: Creep strain at time t

$C(t,\tau)$: Specific creep

τ : Time at which the load is applied

If we assume from the above expression that the stress at each stage is constant, the total creep strain can be expressed as a sum of the strains at each stage.

$$\varepsilon_c^n = \sum_{j=1}^{n-1}\Delta\sigma_j C(t_n,\tau_j) \tag{4.5.12}$$

Using the equation (4.5.12), the incremental creep strain between the times $t_n - t_{n-1}$ can be expressed as follows:

$$\Delta\varepsilon_c^n = \varepsilon_c^n - \varepsilon_c^{n-1} = \sum_{j=1}^{n-1}\Delta\sigma_j C(t_n,\tau_j) - \sum_{j=1}^{n-2}\Delta\sigma_j C(t_{n-1},\tau_j) \tag{4.5.13}$$

If the specific creep is expressed by the degenerate kernel(Dirichlet functional summation), the incremental creep strain can be calculated without having to save the entire stress history.

$$C(t,\tau) = \sum_{i=1}^{m} a_i(t)\left[1 - e^{-(t-\tau)/\Gamma_i}\right] \tag{4.5.14}$$

$a(t)$: Coefficients related to the initial shapes of specific creep curves at the time of loading τ

Γ : Values related to the shapes of specific creep curves over a period of time

In FEA NX, you can use the Aging-Kelvin creep model using the five Γ and the Aging-Viscous creep model which excludes spring from the Aging-Kelvin creep model.

Figure 4.5.4 Aging-Kelvin creep model

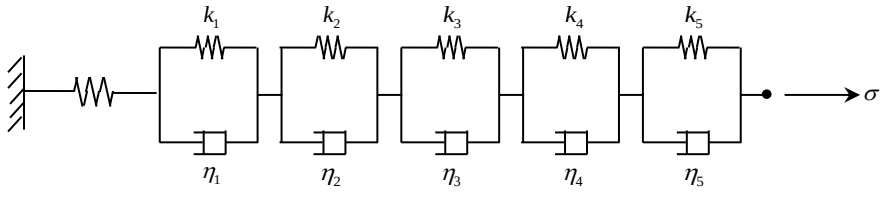

By introducing the specific creep formula, the incremental strain can be expressed as follows:

$$\Delta\varepsilon = \Delta\sigma\left(\frac{1}{E} + \sum_{i=1}^{5} a_i(t)\left(1-\lambda_i\right)\right) + \sum_{i=1}^{5}\left(1-\beta_i\right)\varepsilon_c^{n-1}$$
$$\lambda_i = (1-\beta_i)\Gamma_i/\Delta t \qquad (4.5.15)$$
$$\beta_i = e^{-\Delta t/\Gamma_i}$$

ε_c^{n-1} : Creep strain of previous stage

E : Elastic modulus

From the above expression, it can be rearranged using $\frac{1}{\overline{E}} = \frac{1}{E} + \sum_{i=1}^{5} a_i(t)\left(1-\lambda_i\right)$ and $\Delta\varepsilon^{"} = \sum_{i=1}^{5}\left(1-\beta_i\right)\varepsilon_c^{n-1}$ to give the following equation:

$$\Delta\sigma = \overline{E}(\Delta\varepsilon - \Delta\varepsilon^{"}) \qquad (4.5.16)$$

Finally, including the shrinkage strain, it can be expressed as follows:

$$\Delta\sigma = \overline{E}(\Delta\varepsilon - \Delta\varepsilon^{"} - \Delta\varepsilon_{sh}) \qquad (4.5.17)$$

5.3 Soft Soil Creep

The Soft Soil Creep model simulates the creep behavior expanded to three-dimensional based on one-dimensional creep theory[28,29,30].

Unlike the primary consolidation by the dissipation of excessive pore pressure, the secondary consolidation is a phenomenon caused by changes in the clay structure skeleton. It has the time dependency behavior what the compression is occurring continuously over time. Therefore, the Soft Soil Creep model is suitable for representing the creep behavior with time dependency

[28] Buisman, K., Results from long duration settlement tests., Proc. 1st International Conference on Soil Mechanics and Foundation Engineering, Cambridge, 1936, Vol. 1, p. 103-107.
[29] Bjerrum, L., Engineering geology of Norwegian normallyconsolidated marine clays as related to settlements of buildings (Seventh Rankine Lecture) Geotechnique, 1967, Vol. 17, p. 83-118.
[30] Garlanger, J.E., The consolidation of soils exhibiting creep under constant effective stress. Geotechnique, 1972, Vol. 22, p. 71-78.

Figure 4.5.5 Primary and secondary consolidation curve with time

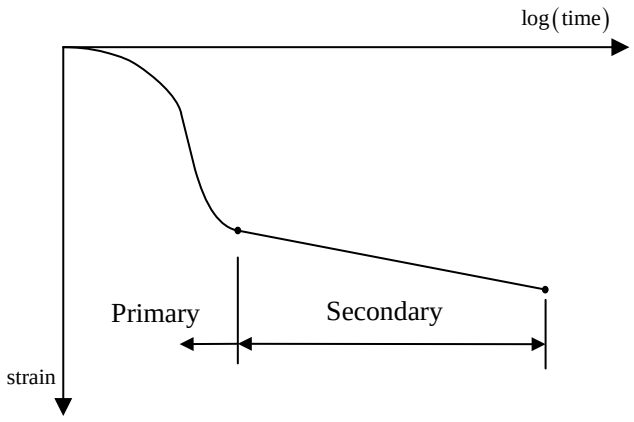

Characteristics

The Soft Soil Creep model is to simulate the time-dependent secondary consolidation (creep behavior), the stress-dependent stiffness and the failure behavior according to the Mohr-Coulomb criterion.

1D creep model and 3D extended model

The 1D creep strain is expressed as the following equation what the total strain rate is the sum of an elastic strain $\dot{\varepsilon}^e$ and a time-dependent creep strain $\dot{\varepsilon}^c$. The creep strain can be considered to a time-dependent creep strain, i.e., a visco-plastic strain.

$$\dot{\varepsilon} = \dot{\varepsilon}^e + \dot{\varepsilon}^c = \frac{\kappa}{1+e_0}\frac{\dot{\sigma}}{\sigma} + \frac{\mu}{1+e_0}\frac{1}{\tau}\left(\frac{\sigma}{\sigma_p}\right)^{\frac{\lambda-\kappa}{\mu}}$$
$$\sigma_p = \sigma_{p0}\exp\left[-\left(\frac{1+e_0}{\lambda-\kappa}\right)\varepsilon^c\right] \qquad (4.5.18)$$

$\dot{\varepsilon}^e$: Elastic strain rate

$\dot{\varepsilon}^c$: Creep strain rate

κ : Swelling index

λ : Compression index

e_0 : Initial void ratio

μ : Creep index

τ : Reference time, precisely one day[31]

[31] Vermeer, P. A., & Neher, H. P., A soft soil model that accounts for creep, Proceedings of the international symposium 'Beyond 2000 in Computational Geotechnics', 1999, Amsterdam, p.249–261.

σ_p : Pre-consolidation stress

From the above equation of 1D creep behavior, the total strain rate of 3D extended Soft Soil Creep model can be expressed as follows:

$$\dot{\boldsymbol{\varepsilon}} = \dot{\boldsymbol{\varepsilon}}^e + \dot{\boldsymbol{\varepsilon}}^c = \mathbf{D}^{-1}\dot{\boldsymbol{\sigma}} + \frac{\mu}{1+e_0}\frac{1}{p_{,p}^{eq}\tau}\left(\frac{p^{eq}}{p_p}\right)^{\frac{\lambda-\kappa}{\mu}}\frac{\partial p^{eq}}{\partial \boldsymbol{\sigma}}$$
$$p_p = p_{p0}\exp\left[-\frac{1+e_0}{\lambda-\kappa}\varepsilon_v^c\right] \tag{4.5.19}$$

$\mathbf{D}$: Elasticity matrix

p^{eq} : Equivalent pressure

p_p : Pre-consolidation pressure

From the above equation (4.5.19), the volumetric creep strain ε_v^c can be expressed with the following equation:

$$\dot{\varepsilon}_v^c = \frac{1}{(1+e_0)}\frac{\mu}{\tau}\left(\frac{p^{eq}}{p_p}\right)^{\frac{\lambda-\kappa}{\mu}} \tag{4.5.20}$$

If the equation (4.5.20) is integrated over time Δt for constant p^{eq}, the volumetric creep strain increment is given as

$$\Delta\varepsilon_v^c = \frac{\mu}{(1+e_0)}\cdot\ln\left[1+\frac{\Delta t}{\tau}\left(\frac{p^{eq}}{p_{p0}}\right)^{\frac{\lambda-\kappa}{\mu}}\right] \tag{4.5.21}$$

Equivalent pressure and yield function

Using the well-known stress invariants for isotropic stress p and deviatoric stress q, the equivalent pressure p^{eq} in Soft Soil Creep model can be defined as follows:

$$p^{eq} = \sqrt{(p+\Delta p)^2 + \alpha q^2} \tag{4.5.22}$$

α : Cap parameter in Modified Mohr-Coulomb model

α is constant which defined by input parameter or ground material.

The Soft Soil Creep model has the Modified Mohr-Coulomb model criterion without strain hardening to prevent excessive deviatoric stress. Therefore, the total strain rate (4.5.19) additionally includes the plastic strain rate by shear failure as follows:

$$\dot{\varepsilon} = \dot{\varepsilon}^e + \dot{\varepsilon}^p + \dot{\varepsilon}^c \tag{4.5.23}$$

$$\dot{\varepsilon}^p = \dot{\lambda}\frac{\partial g}{\partial \sigma}$$
$$g = q - \frac{6\sin\psi}{3-\sin\psi}(p+\Delta p) \tag{4.5.24}$$

g : Plastic potential function

ψ : Dilatancy angle

The plastic strain rate follows the flow rule of Modified Mohr-Coulomb model and for fine grained, cohesive soils, the dilatancy angle tends to be small, it may often be assumed that dilatancy angle is equal to zero.

Figure 4.5.6 Equivalent pressure shape and yield function

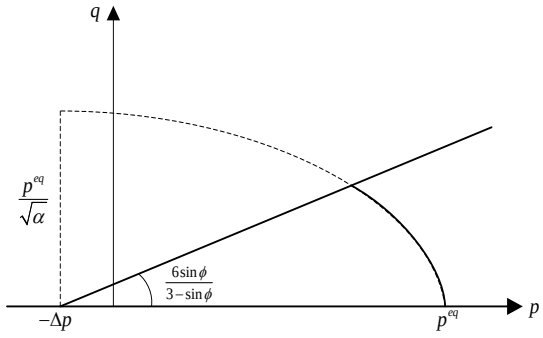

5.4 Sekiguchi-Ohta (Viscid)

The Viscid type of Sekiguchi-Ohta model follows the nonstationary flow surface theory[32] among various visco-plastic theories for simulating creep behavior of ground. The nonstationary flow surface theory model is basically based on the plastic model, but there is a difference that it contains the time dependent function.

The Viscid type follows the assumption[33] that the creep is in progress with a constant stress state in initial state ground before loading.

Like Inviscid type, it resolves a numerical problem using the specificity algorithms of Inviscid type since it contains a stress state that the plastic flow is only undetermined in the yield function. However, except the specificity problem, convergence problem occurs when the stress state locates dry side due to the model characteristics. In FEA NX, it resolves convergence problem by correcting the softening behavior in the stress state of dry side.

[32] Liingaard, M., Augustesen, A., Lade, P. V., "Characterization of models for time-dependent behavior of soils", International Journal of Geomechanics, 2004, 4.3: 157-177.

[33] Sekiguchi, H. and Ohta H., "Induced anisotropy and time dependency in clays", 9th ICSMFE, Tokyo, Constitutive equations of Soils, 1977, 229-238

Yield function

The flow function of Viscid type is defined as follows:

$$F = \alpha \ln\left[1 + \frac{\dot{\nu}_0 t}{\alpha} \exp\left(\frac{\bar{f}(\sigma)}{\alpha}\right)\right] - \varepsilon_v^{vp} = 0 \tag{4.5.25}$$

α : Coefficient of secondary compression

$\dot{\nu}_0$: Change speed of initial volumetric strain rate

ε_v^{vp} : Visco-plastic volumetric strain

The $\bar{f}(\sigma)$ of equation (4.5.25) is defined as follows:

$$\bar{f}(\sigma) = MD \ln\left(\frac{p}{p_0}\right) + D\bar{\eta} \tag{4.5.26}$$

The detailed explanation of equation (4.5.26) can be found in '2.16. Sekiguchi-Ohta (Inviscid)'.
However, in case of directly using the flow function of equation (4.5.25) for yield function, the problem[34] that elastic range cannot be defined occurs since the left term always has a positive value. In this case, the associated plastic flow rule cannot be used due to the violation of Hill's principle of maximum plastic work. In order to resolve this problem, Iizuka and Ohta[35] transformed the equation (4.5.25) as follows:

$$f(\sigma, h) = \bar{f}(\sigma) - h\left(\varepsilon_v^{vp}, t\right) = 0 \tag{4.5.27}$$

Here, the hardening function (h) is defined as follows:

$$h\left(\varepsilon_v^{vp}, t\right) = \alpha \ln\left[\frac{\alpha}{\dot{\nu}_0 t}\left\{\exp\left(\frac{\varepsilon_v^{vp}}{\alpha}\right) - 1\right\}\right] \tag{4.5.28}$$

However, there is a problem that the hardening function (h) is not defined when the initial visco-plastic volumetric strain rate is zero ($\varepsilon_{v0}^{vp} = 0$). Therefore, the numerical problem is resolved by setting the initial value

[34] Takeyama, T., Pipatpongsa, T., Iizuka, A., Mizuta, T., Ohno, S., Ohta, H., "Soil/water coupled FE Simulation of field performance of 5 embankments placed on homogeneous clay." Proceedings of the Sri Lankan Geotechnical Society's First International Conference on Soil & Rock Engineering, 2007

[35] Iizuka, A., Ohta, H., "An interpretation of Sekiguchi and Ohta's model based on viscoplasticity theory.", Proceedings of the 34th Japanese National Conference on Geotechnical Engineering, 1999, 595-596

of the visco-plastic volumetric strain rate (ε_v^{vp}) which makes $h\left(\varepsilon_v^{vp}, t_1\right) = 0$ at t_1 when the stress state is judged to the visco-plastic state violating the initial yield function with load change or overtime.

$$\varepsilon_{v0}^{vp} = \alpha \ln\left[\frac{\dot{v}_0 t_1}{\alpha} + 1\right] \tag{4.5.29}$$

Figure (4.5.7) shows the yield function at triaxial stress state. Like the Cam-Clay material model, it is called that the right is wet side and the left is dry side based on the critical state line. Generally, the material model which follows critical state theory shows the hardening behavior at wet side and the softening behavior at dry side. However, in the viscid type of Sekiguchi-Ohta model, it is known that the over-consolidation ratio is high and the convergence problem[36] occurs when the stress state locates dry side due to the nature of yield function. In FEA NX, the convergence problem is resolved by preventing the softening behavior at dry side.

Figure 4.5.7 Simplified yield function and critical state line in triaxial stress state

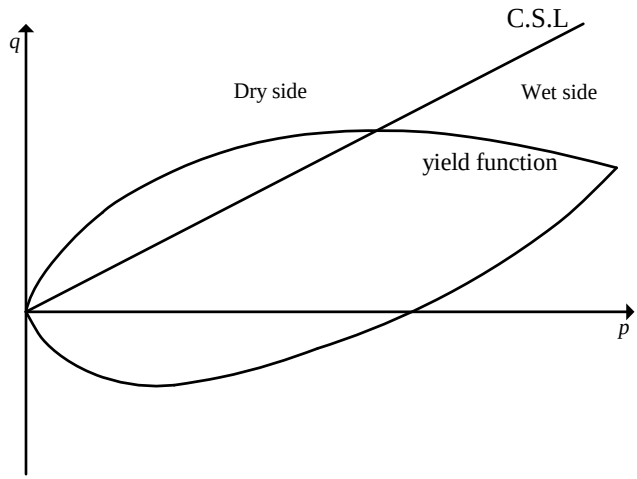

[36] Takeyama, T., Ohno, S., Pipatpongsa, T., Iizuka, A., Ohta, H., "The stress update using implicit integration for the viscid version of sekiguchi-ohta model", Technical report, 2005

Section 6

Hysteresis Material Properties

When the crack and yield occurs by irregular cyclic load, the displacement history to the current affects the later relationship between restoring force and displacement. The relationship between force and deformation for uniaxial load is called the Skeleton curve. When the cyclic load is applied based on the Skeleton curve, the rule of the relationship between force and deformation for unloading and reloading is called hysteresis model. The properties of each hysteresis model are explained in this chapter. Table 4.6.1 lists the available hysteresis models for each element.

Table 4.6.1 Available hysteresis models for each element type

Hysteresis model	Element type									
	Truss	Elastic Link	Beam	Interface	Geogrid	Plane Stress	Shell	Plane strain	Axisymmetric Solid	Solid
Multilinear	V	V	V							
Normal Bilinear	V	V	V							
Kinematic	V	V	V							
Origin-Oriented	V	V	V							
Peak-Oriented	V	V	V							
Clough	V	V	V							
Degrading	V	V	V							
Takeda	V	V	V							
Modified Takeda	V	V	V							
Modified Ramberg Osgood	V	V	V			V	V	V	V	V
Modified Hardin-Drnevich	V	V	V			V	V	V	V	V

6.1

Normal Bilinear model

Figure 4.6.1 Normal Bilinear model

Response points at initial loading move about on a bilinear skeleton curve.

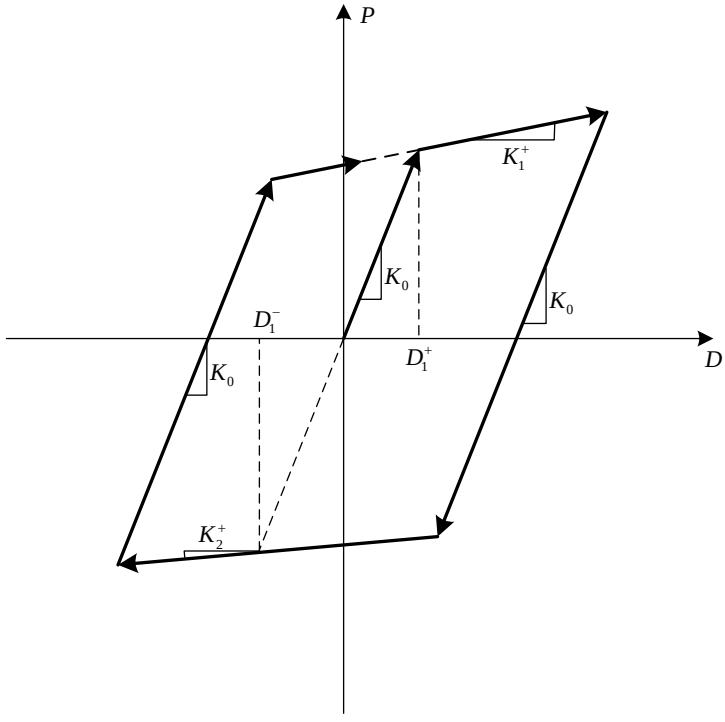

Hysteresis rule

- In case of $|D_{max}| < D_1$, it is a linear elastic and moves on a elastic gradient straight line crossing the origin.
- In case of the deformation D first overpass $D_1^{\pm}$, or the maximum deformation point to the current, it moves on a second gradient straight line.
- In case of unloading in the condition of $D_1^+ > D$, $D_1^- < D$, it moves on a second gradient straight line by unloading a elastic gradient according to the Masing rule.

6.2 Kinematic model

Response points at initial loading move about on a trilinear skeleton curve. The unloading stiffness is identical to the elastic stiffness, and stiffness reduction after yielding is possible only for positive (+) and negative (-) symmetry. In case of kinematic model, the interaction of axial force and biaxial bending component can be considered by the plastic theory.

Figure 4.6.2 Kinematic model

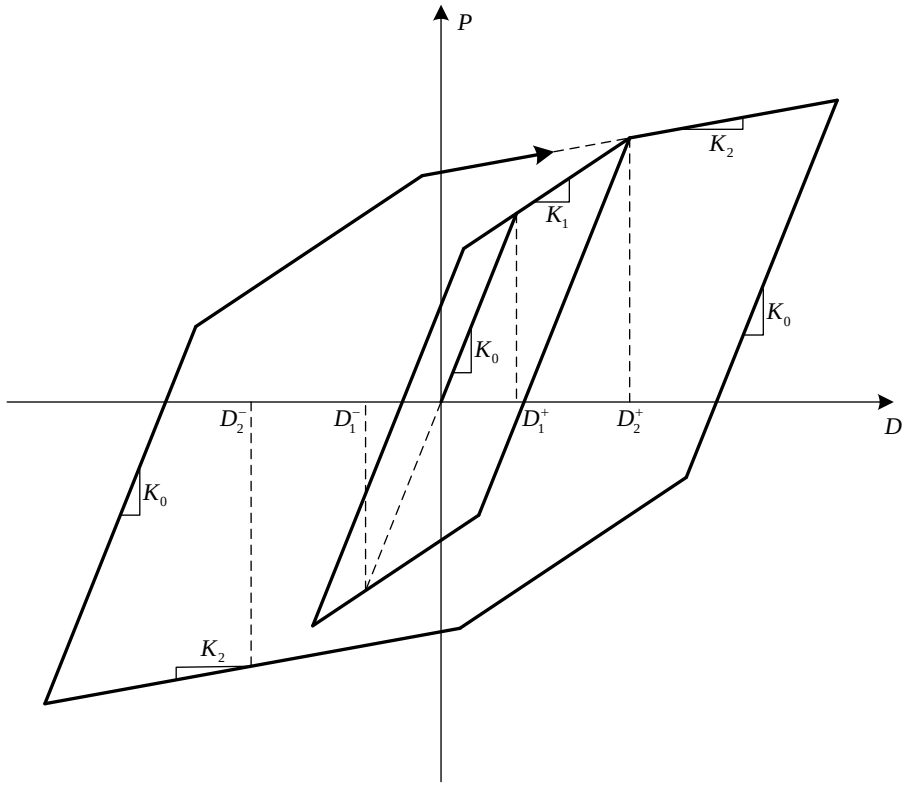

Uniaxial hysteresis rule

- In case of $|D_{max}| < D_2$, it behaves like a bilinear.
- In case of $|D_{max}| > D_2$, it moves on a third gradient straight line.
- In case of unloading, it moves on a elastic gradient according to the Masing rule.

Multi-axial hysteresis rule

It considers the interaction between axial force and biaxial bending component by the kinematic hardening rule based on the plastic theory. The yield domain is the following equation.

$$f(P,M_y,M_z)=\left\{\left(\frac{M_y}{M_{y,\max}}\right)^{\gamma}+g_y\left(M_y,M_z\right)^{\frac{\gamma}{\alpha}}\left(\frac{P-P_{bal,y}}{P_{\max}-P_{bal,y}}\right)^{\beta_y}\right\}^{\frac{\alpha}{\gamma}}$$
$$+\left\{\left(\frac{M_z}{M_{z,\max}}\right)^{\gamma}+g_z\left(M_y,M_z\right)^{\frac{\gamma}{\alpha}}\left(\frac{P-P_{bal,z}}{P_{\max}-P_{bal,z}}\right)^{\beta_z}\right\}^{\frac{\alpha}{\gamma}}-1\le 0$$

$$g_y\left(M_y,M_z\right)=\frac{\left(\frac{M_y}{M_{y,\max}}\right)^{\alpha}}{\left(\frac{M_y}{M_{y,\max}}\right)^{\alpha}+\left(\frac{M_z}{M_{z,\max}}\right)^{\alpha}} \qquad (4.6.1)$$

$$g_y\left(M_y,M_z\right)=\frac{\left(\frac{M_z}{M_{z,\max}}\right)^{\alpha}}{\left(\frac{M_y}{M_{y,\max}}\right)^{\alpha}+\left(\frac{M_z}{M_{z,\max}}\right)^{\alpha}}$$

$M_{\max}$: Maximum bending yield strength

P_{bal} : Axial force at the balanced failure

$P_{\max}$: Axial yield strength

α, β, γ : An exponent related to interaction curve

Figure 4.6.3 Movement of yield surface and stiffness change

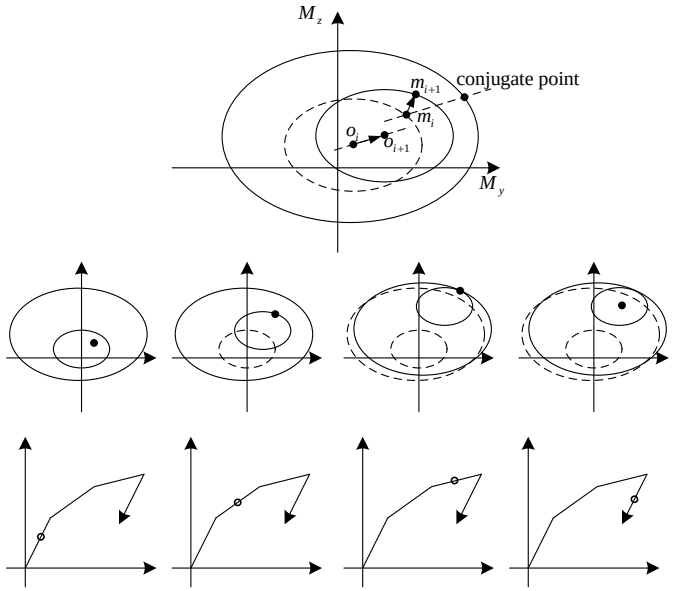

There are two yield surfaces corresponding to a trilinear skeleton curve and these two yield surfaces follow the hardening rule of modified Mroz.

6.3 Origin-Oriented model

Response points at initial loading move about on a trilinear skeleton curve. The response point moves towards the origin at the time of unloading. When it reaches the skeleton curve on the opposite side, it moves along the skeleton curve again.

Figure 4.6.4 Origin-Oriented model

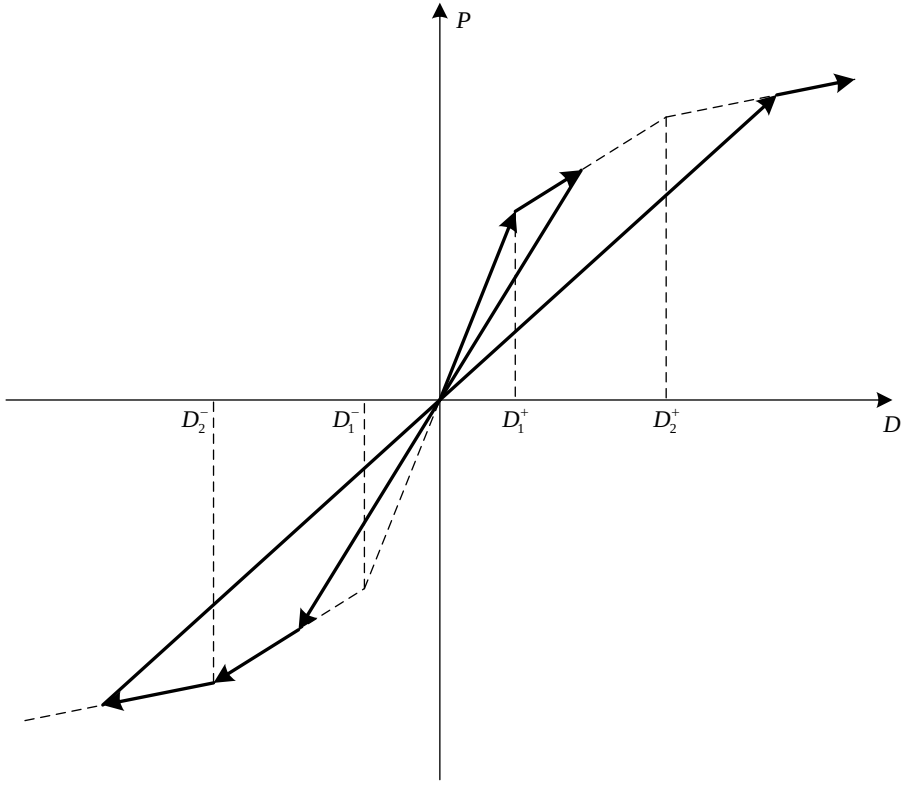

6.4 Peak-Oriented model

Response points at initial loading move about on a trilinear skeleton curve. The response point moves towards the maximum displacement point on the opposite side at the time of unloading. If the first yielding has not occurred on the opposite side, it moves towards the first yielding point on the skeleton curve.

Figure 4.6.5 Peak-Oriented model

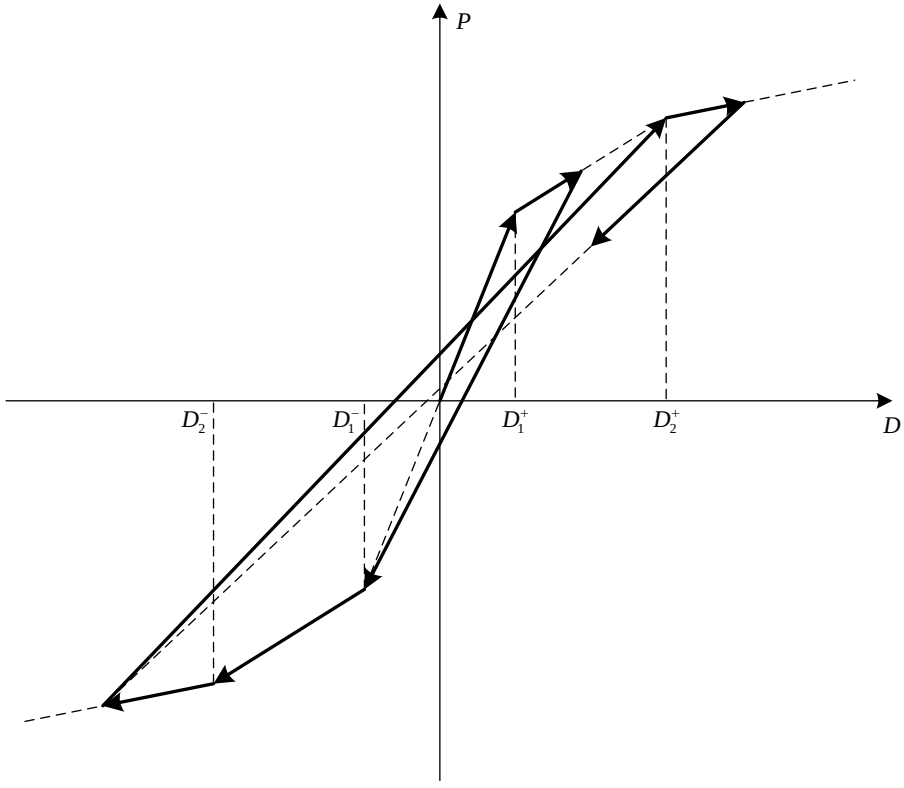

6.5 Clough model

Response points at initial loading move about on a bilinear skeleton curve. As the deformation progresses, the unloading stiffness gradually becomes reduced. When the loading sign changes at the time of unloading, the response point moves towards the maximum displacement point in the region of the progressing direction. If yielding has not occurred in the region, it moves towards the yielding point on the skeleton curve. Where unloading reverts to loading without the change of loading signs, the response point moves along the unloading path. And loading takes place on the skeleton curve as the loading increases.

Figure 4.6.6 Clough model

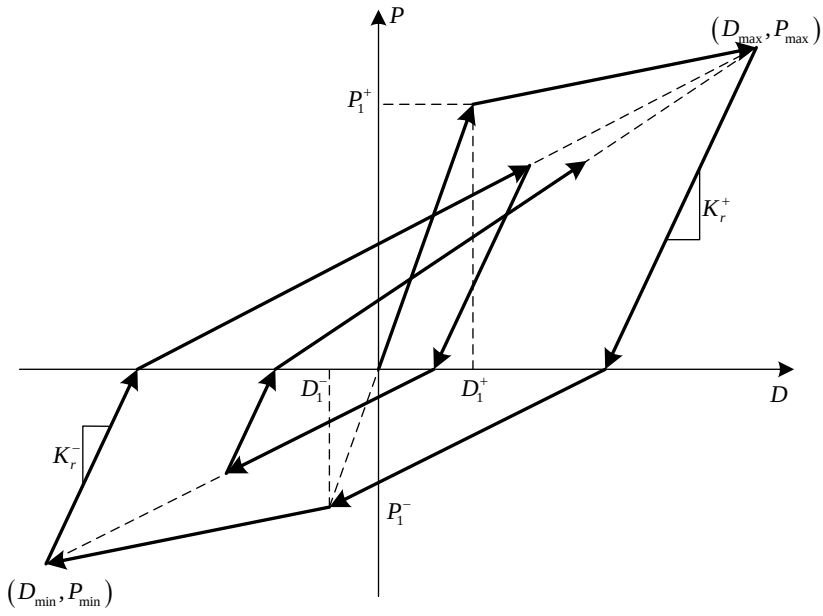

Hysteresis rule

- In case of unloading in the condition of $|D_1| < D$, it moves on the gradient of unloading stiffness, $K_r^{\pm}$.

$$K_r^+ = K_o \left(\left| \frac{D_1^+}{D_{max}} \right| \right)^{\beta} \le K_o$$
$$K_r^- = K_o \left(\left| \frac{D_1^-}{D_{min}} \right| \right)^{\beta} \le K_o \qquad (4.6.2)$$

K_o : Initial elastic stiffness

$D_1^{\pm}$: Yield displacement in the region of the first unloading

D_{max} : Maximum displacement in the region of tension

D_{min} : Maximum displacement in the region of compression

β : Constant for determining unloading stiffness

► If the sign of the load changes in the unloading process, it moves toward the maximum deformation point of the opposite side. If the opposite side is not yield, $D_1^{\pm}$ is the maximum deformation point.

6.6 Degrading model

Response points at initial loading move about on a trilinear skeleton curve. At unloading, the coordinates of the load-deformation move to a path along which the maximum deformation on the opposite side can be reached due to the change of unloading stiffness once. If yielding has not occurred on the opposite side, the first yielding point is assumed to be the point of maximum deformation. As the maximum deformation increases, the unloading stiffness gradually decreases.

Figure 4.6.7 Degrading model

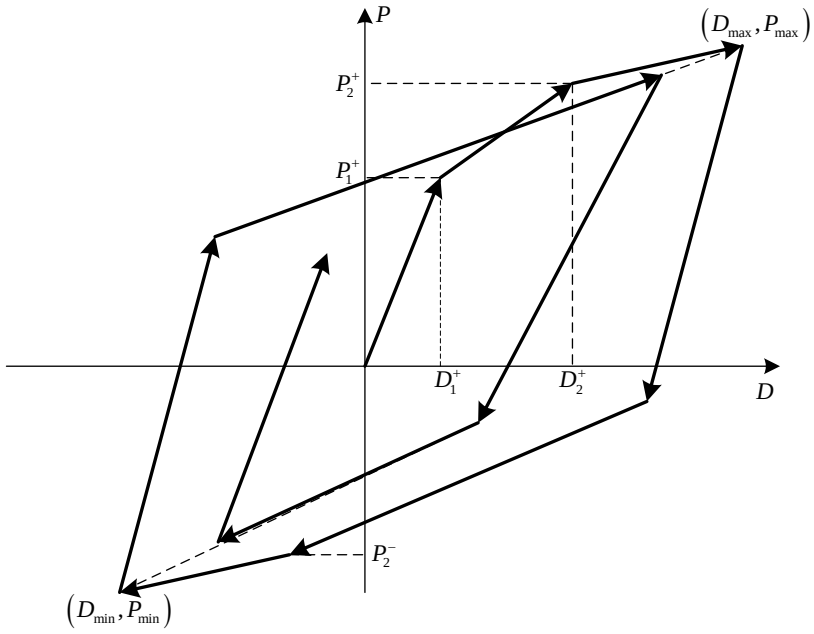

Hysteresis rule

► In case of unloading in the condition of $|D_2| > D$, it behaves like a bilinear.

► In case of unloading in the condition of $|D_2| < D$, it moves on the gradient of unloading stiffness, $K_r^{\pm}$.

$$K_r^{\pm} = K_o\left(\frac{P_{\max} - P_{\min}}{D_{\max} - D_{\min}}\frac{1}{K_{r1}}\right)$$
$$K_{r1} = \frac{P_2^+ - P_2^-}{D_2^+ - D_2^-} \qquad (4.6.3)$$

K_o : Initial elastic stiffness

$D_{\max}$: Maximum displacement in the region of tension

$D_{\min}$: Maximum displacement in the region of compression

$P_{\max}$: Maximum force in the region of tension

$P_{\min}$: Maximum force in the region of compresion

$P_2^{\pm}$: Yield stiffness in the region of the second unloading

$D_2^{\pm}$: Yield displacement in the region of the second unloading

6.7 Takeda model

Response points at initial loading move about on a trilinear skeleton curve. The unloading stiffness is determined by the location of the unloading point on the skeleton curve and whether or not the first yielding has occurred in the opposite region.

Figure 4.6.8 Takeda model

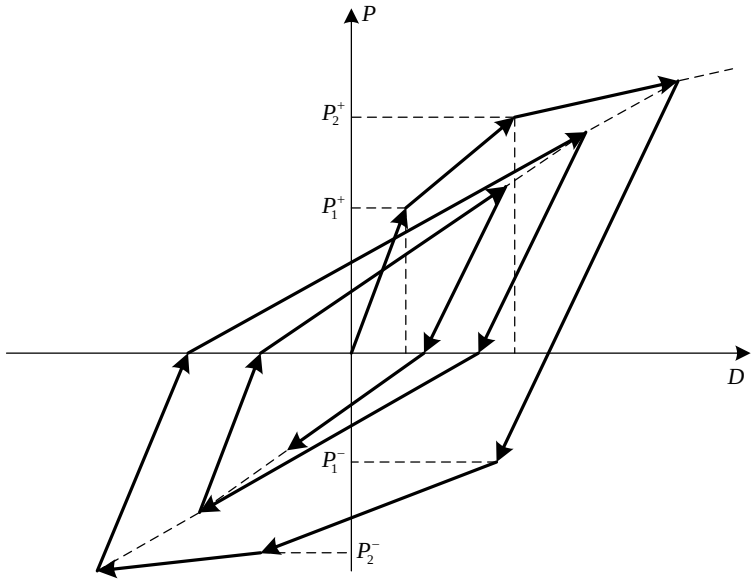

Hysteresis rule

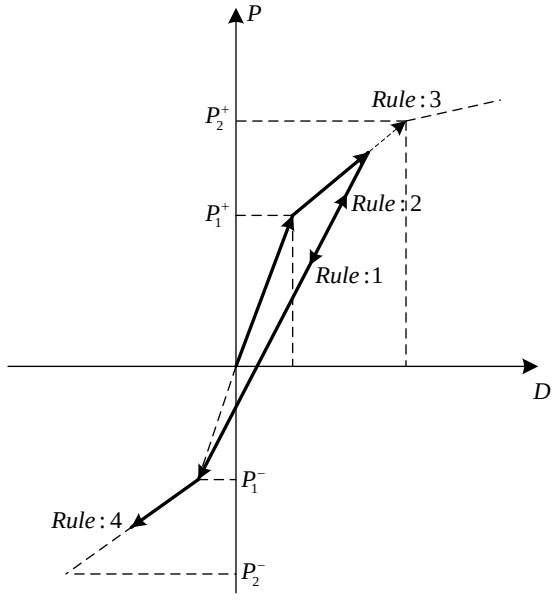

Figure 4.6.9 Hysteresis rule of the Takeda model after the first yielding

- In case of the deformation D first overpass D_1^+, the opposite first yielding is the maximum displacement point on the opposite side.
- In case of unloading on the skeleton curve, the coordinates of the load-deformation moves toward the maximum deformation point of the opposite side. (Rule 1)
- In case of reloading before it reaches to the maximum deformation point of the opposite side, the point progresses along the same unloading curve. (Rule 2)
- In case of reaching to the skeleton curve, it moves along the skeleton curve. (Rule 3)

Figure 4.6.10 Hysteresis rule of the Takeda model after the second yielding

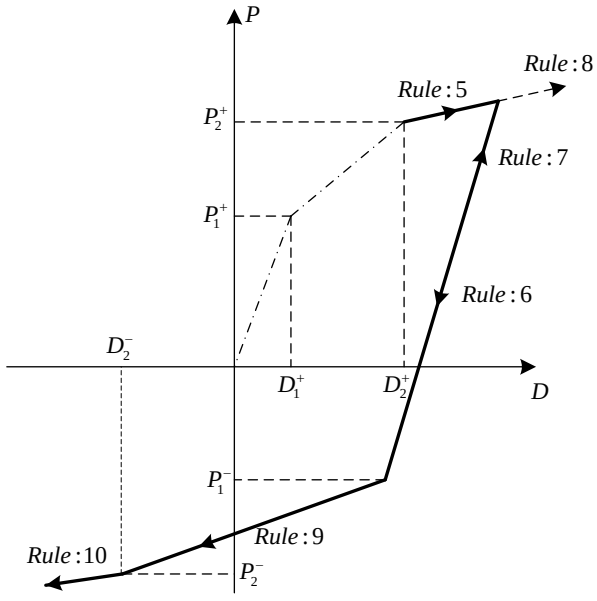

- In case of the deformation D first overpass $D_2^{\pm}$, it moves along the skeleton curve. (Rule 5)
- In case of unloading on this curve, it moves on the gradient of unloading stiffness, $K_r^{\pm}$. If the opposite side is before experiencing the first yielding, the range of $K_r^{\pm}$ is the $P_1^{\mp}$. (Rule 6)

$$K_r^+ = K_b^+ \left| \frac{D_{\max}}{D_2^+} \right|^{-0.4}$$
$$K_r^- = K_b^- \left| \frac{D_{\min}}{D_2^-} \right|^{-0.4} \qquad (4.6.4)$$
$$K_b^+ = \frac{P_2^+ - P_1^-}{D_2^+ - D_1^-}$$
$$K_b^- = \frac{P_2^- - P_1^+}{D_2^- - D_1^+}$$

- If the point exceeds the $P_1^{\mp}$, it moves toward the second yielding point. (Rule 9)

Figure 4.6.11 Hysteresis rule of the inner loop Takeda model

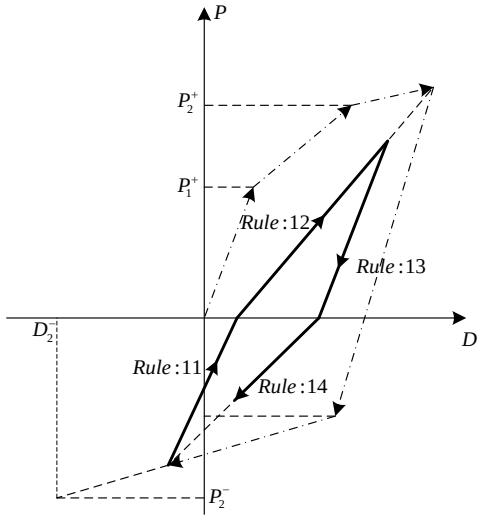

► In case of unloading on the straight line toward the maximum deformation point of the opposite side, it enters to the inner loop. (Rule 11)

► In case of the sign of restoring force changes in the process of unloading in the inner loop, it returns to the previous unloading point of the opposite side. (Rule 12)

6.8
Modified Takeda model

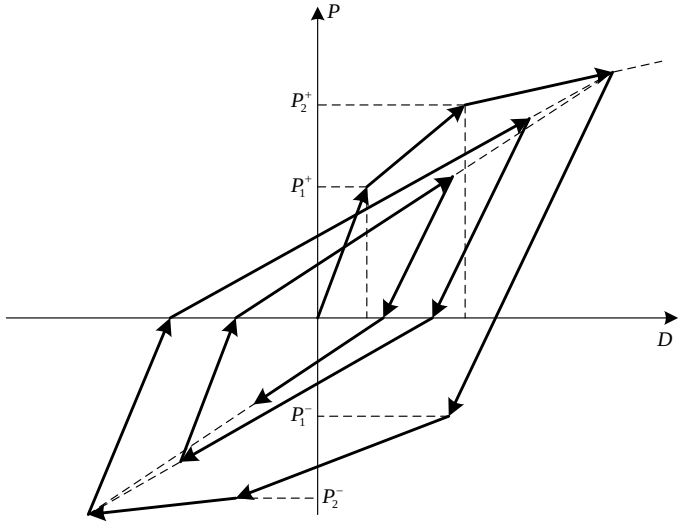

Figure 4.6.12 Modified Takeda model

Hysteresis rule

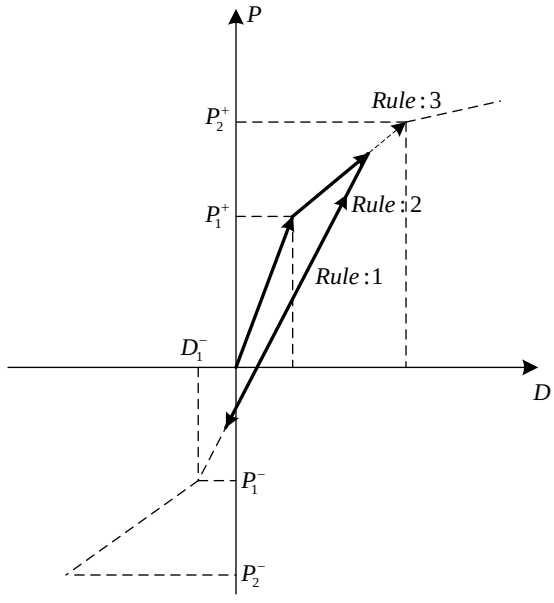

Figure 4.6.13 Hysteresis rule of the modified Takeda model after the first yielding

► In case of the deformation D first overpass $D_1^{\pm}$, the opposite first yielding is the maximum deformation point of the opposite side.

► In case of unloading on the skeleton curve, the coordinates of the load-deformation moves toward the maximum deformation point of the opposite side. (Rule 1)

► In case of reloading before it reaches to the maximum deformation point of the opposite side, the point progresses along the same unloading curve. (Rule 2)

► In case of reaching to the skeleton curve, it moves along the skeleton curve. (Rule 3)

Figure 4.6.14 Hysteresis rule of the modified Takeda model after the second yielding

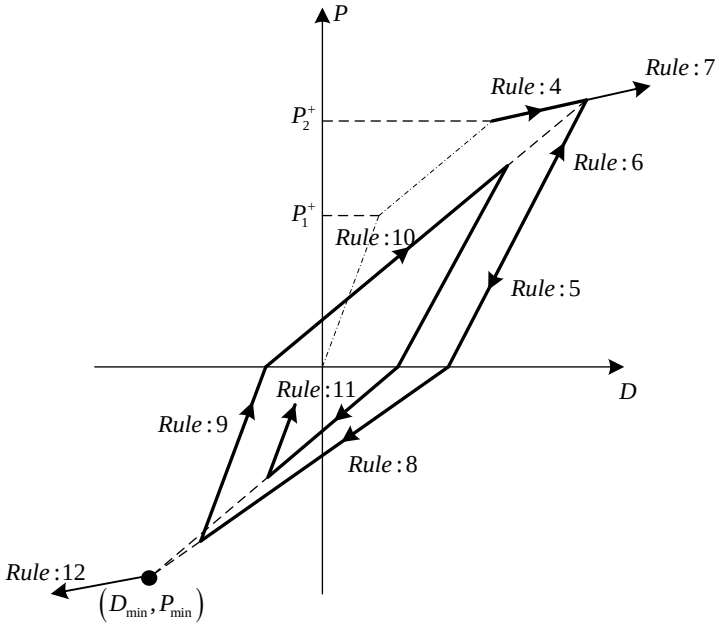

► In case of the deformation D first overpass $D_2^{\pm}$, it moves along the skeleton curve. (Rule 4)

► In case of unloading on this curve, it moves on the gradient of unloading stiffness, $K_r^{\pm}$. If the opposite side is before experiencing the second yielding, the opposite second yielding is the maximum deformation point of the opposite side. (Rule 5)

$$K_r^+ = \max\left(K_b, \left|\frac{D_{\max}}{D_1^+}\right|^{-0.4}\right), K_r^- = \max\left(K_b, \left|\frac{D_{\min}}{D_1^-}\right|^{-0.4}\right) \quad (4.6.5)$$

$$K_b = \frac{P_{\max} - P_{\min}}{D_{\max} - D_{\min}}$$

- At the time when the sign changes, , the coordinates of the load-deformation moves toward the maximum deformation point of the opposite side. (Rule 8)
- In case of unloading on the straight line toward the maximum deformation point of the opposite side, it enters to the inner loop. (Rule 9)
- At the time when the sign changes, the coordinates of the load-deformation moves toward the maximum deformation point of the opposite side. (Rule 10)

6.9 Modified Ramberg-Osgood model

The Ramberg-Osgood model is originally proposed for the dynamic model of metal material, but modified by Tatsuoka.

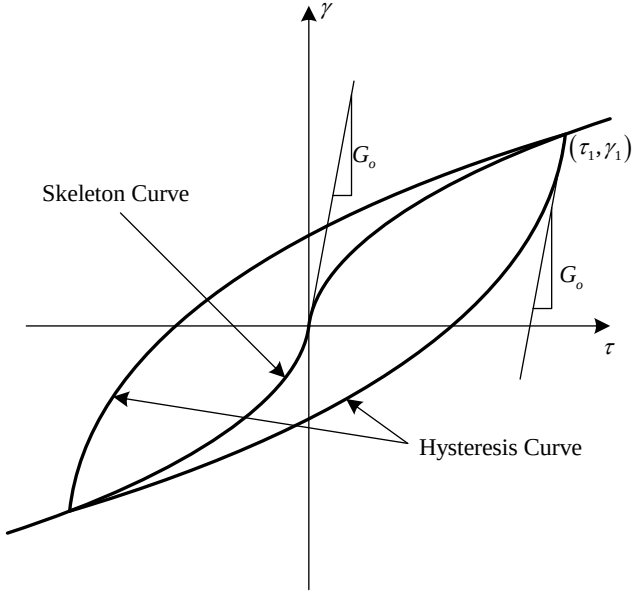

Figure 4.6.15 Modified Ramberg-Osgood model

Hysteresis rule

- In the initial loading, it moves along the following skeleton curve.

$$G_o\gamma = \tau + \alpha|\tau|^{\beta}\tau$$
$$\beta = \frac{2\pi h_{\max}}{2-\pi h_{\max}}, \alpha = \left(\frac{2}{\gamma_r G_o}\right)^{\beta} \quad (4.6.6)$$

G_o : Initial stiffness (Shear modulus)

γ_r : Reference shear strain

$h_{\max}$: Maximum damping constant

- The hysteresis curve is as follows:

$$G_o\left(\frac{\gamma \pm \gamma_1}{2}\right) = \left(\frac{\tau \pm \tau_1}{2}\right)\left(1+\alpha\left(\left|\frac{\tau \pm \tau_1}{2}\right|\right)^{\beta}\right) \quad (4.6.7)$$

If only shear stress is considered, the initial confinement pressure may be considered with the following equation.

$$G_o = G_{oi}\left(\sigma'_{mo}\right)^{n_1}$$
$$\gamma_r = \gamma_{ri}\left(\sigma'_{mo}\right)^{n_2} \quad (4.6.8)$$

G_{oi} , γ_{ri} : Normalized value at confinement pressure 1.0tf/m^2

σ'_{mo} : Initial confinement pressure

n_1 , n_2 : Influence coefficients of confinement pressure

Formulation is performed according to the additive decomposition, which divides elastic and plastic components, as shown in the following formula.

$$\gamma = \frac{\tau}{G_o} + \alpha|\tau|^{\beta}\frac{\tau}{G_o}$$
$$= \gamma_{el} + \gamma_{pl} \quad (4.6.9)$$

In a multi-axial state, the stresses are divided into hydrostatic stress and deviatoric stress, and then it is organized into deviatoric stress and deviatoric strain, and expressed in the following formula.

$$2G_o\boldsymbol{\varepsilon}_{dev} = \boldsymbol{\sigma}_{dev} + 2G_o \left\| \boldsymbol{\varepsilon}_{dev}^{pl} \right\| \frac{\boldsymbol{\sigma}_{dev}}{\left\| \boldsymbol{\sigma}_{dev} \right\|} \tag{4.6.10}$$

$\boldsymbol{\sigma}_{dev}$: Deviatoric stress tensor

$\boldsymbol{\varepsilon}_{dev}$: Deviatoric strain tensor

$\boldsymbol{\varepsilon}_{dev}^{pl}$: Plastic strain tensor

Considering the multi-axial conditions of the plastic strain in equation (4.6.9), the equivalent deviatoric strain $\varepsilon_{eq} = \sqrt{2\boldsymbol{\varepsilon}_{dev} : \boldsymbol{\varepsilon}_{dev}}$ and equivalent deviatoric stress $\sigma_{eq} = \sqrt{0.5\boldsymbol{\sigma}_{dev} : \boldsymbol{\sigma}_{dev}}$ are used to indicate the plastic strain.

$$\alpha {\sigma_{eq}}^{\beta} = 2G_o \frac{\left\| \boldsymbol{\varepsilon}_{dev}^{pl} \right\|}{\left\| \boldsymbol{\sigma}_{dev} \right\|} = G_o \frac{\varepsilon_{eq}^{pl}}{\sigma_{eq}} \tag{4.6.11}$$

Using equation (4.6.10) and equation (4.6.11), the relationship between stress and strain in a multi-axial state is defined as follows:

$$\begin{aligned} 2G_o\boldsymbol{\varepsilon}_{dev} &= \boldsymbol{\sigma}_{dev} + G_o \frac{\varepsilon_{eq}^{pl}}{\sigma_{eq}} \boldsymbol{\sigma}_{dev} \\ &= \boldsymbol{\sigma}_{dev} + \alpha {\sigma_{eq}}^{\beta} \boldsymbol{\sigma}_{dev} \end{aligned} \tag{4.6.12}$$

The deviatoric strain and the deviatoric stress tensor of the left and right sides of equation (4.6.12) are replaced with the equivalent deviatoric strain and equivalent deviatoric stress, and the scalar equation is established as follows.

$$G_o\varepsilon_{eq} = \sigma_{eq} + \alpha {\sigma_{eq}}^{\beta} \sigma_{eq} \tag{4.6.13}$$

Equation (4.6.12) and (4.6.13) are used to indicate the relationship between equivalent deviatoric stress and equivalent deviatoric strain.

$$\boldsymbol{\sigma}_{dev} = 2\frac{\sigma_{eq}}{\varepsilon_{eq}} \boldsymbol{\varepsilon}_{dev} \tag{4.6.14}$$

The differential equation for the relationship of the equivalent deviatoric strain and the equivalent deviatoric stress is as follows.

$$\partial\sigma_{eq} = \frac{G_o}{1 + \alpha(\beta + 1){\sigma_{eq}}^{\beta}} \partial\varepsilon_{eq} = G_o\psi\partial\varepsilon_{eq} \tag{4.6.15}$$

The following formula is used to define the relationship between stress and strain.

$$\begin{aligned}
\partial\varepsilon_{eq} &= 2\frac{\boldsymbol{\varepsilon}_{dev}}{J_{2\boldsymbol{\varepsilon}}}\partial\boldsymbol{\varepsilon}_{dev} \\
\partial\boldsymbol{\varepsilon}_{dev} &= \left(\mathbf{I}-\frac{1}{3}\boldsymbol{\delta}\boldsymbol{\delta}\right)\partial\boldsymbol{\varepsilon} \\
\partial\boldsymbol{\sigma}_{dev} &= 2\frac{\sigma_{eq}}{\varepsilon_{eq}}\left[\partial\boldsymbol{\varepsilon}_{dev}+\left(\frac{\partial\sigma_{eq}}{\sigma_{eq}}-\frac{\partial\varepsilon_{eq}}{\varepsilon_{eq}}\right)\boldsymbol{\varepsilon}_{dev}\right] \\
\partial p &= -K\boldsymbol{\delta}\partial\boldsymbol{\varepsilon} \\
\partial\boldsymbol{\sigma} &= \partial\boldsymbol{\sigma}_{dev}-\partial p\boldsymbol{\delta}
\end{aligned} \tag{4.6.16}$$

Using equation (4.6.15) and (4.6.16), the material stiffness matrix is calculated as follows:

$$\partial\boldsymbol{\sigma}=\left[2\frac{\sigma_{eq}}{\varepsilon_{eq}}\mathbf{I}+\frac{1}{3}\left(3K-2\frac{\sigma_{eq}}{\varepsilon_{eq}}\right)\boldsymbol{\delta}\boldsymbol{\delta}\right]\partial\boldsymbol{\varepsilon}+\left[2\frac{\sigma_{eq}}{\varepsilon_{eq}}\frac{2}{\varepsilon_{eq}}\left(\frac{G_o\psi}{\sigma_{eq}}-\frac{1}{\sigma_{eq}}\right)\boldsymbol{\varepsilon}_{dev}\boldsymbol{\varepsilon}_{dev}\right]\partial\boldsymbol{\varepsilon} \tag{4.6.17}$$

6.10 Modified Hardin-Drnevich model

This model defines the hysteresis curve by applying the Masing rule to the Hardin-Drnevich model which suggested only the skeleton curve.

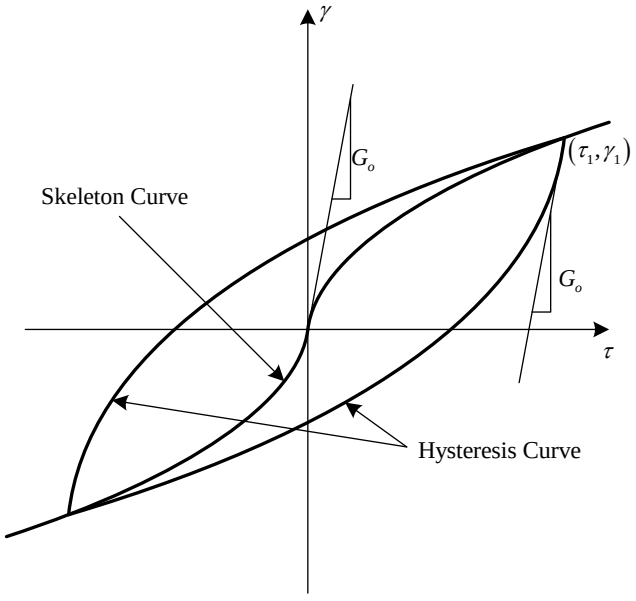

Figure 4.6.16 Modified Hardin-Drnevich model

Hysteresis rule

- In the initial loading, it moves along the following skeleton curve.

$$\tau = \frac{G_o \gamma}{1 + \left| \frac{\gamma}{\gamma_r} \right|} \tag{4.6.18}$$

G_o : Initial stiffness (Shear modulus)

γ_r : Reference shear strain

- The hysteresis curve is as follows:

$$\tau - \tau_1 = \frac{G_o (\gamma - \gamma_1)}{1 + \left| \frac{\gamma - \gamma_1}{2\gamma_r} \right|} \tag{4.6.19}$$

If only shear stress is considered, the initial confinement pressure may be considered with the following equation.

$$\begin{aligned} G_o &= G_{oi} \left(\sigma'_{mo} \right)^{n_1} \\ \gamma_r &= \gamma_{ri} \left(\sigma'_{mo} \right)^{n_2} \end{aligned} \tag{4.6.20}$$

G_{oi} , γ_{ri} : Normalized value at confinement pressure 1.0tf/m^2

σ'_{mo} : Initial confinement pressure

n_1 , n_2 : Influence coefficients of confinement pressure

Formulation is performed according to the additive decomposition, which divides elastic and plastic components, as shown in the following formula.

$$\begin{aligned} \gamma &= \frac{\tau}{G_o} + \left| \frac{\gamma}{\gamma_r} \right| \frac{\tau}{G_o} \\ &= \gamma_{el} + \gamma_{pl} \end{aligned} \tag{4.6.21}$$

Considering the multi-axial conditions of the plastic strain in equation (4.6.20), the equivalent deviatoric strain $\varepsilon_{eq} = \sqrt{2\boldsymbol{\varepsilon}_{dev} : \boldsymbol{\varepsilon}_{dev}}$ and equivalent deviatoric stress $\sigma_{eq} = \sqrt{0.5\boldsymbol{\sigma}_{dev} : \boldsymbol{\sigma}_{dev}}$ are used to indicate the plastic strain.

$$\frac{\varepsilon_{eq}^{pl}}{\gamma_r} = 2G_o \frac{\left\| \boldsymbol{\varepsilon}_{dev}^{pl} \right\|}{\left\| \boldsymbol{\sigma}_{dev} \right\|} = G_o \frac{\varepsilon_{eq}^{pl}}{\sigma_{eq}} \tag{4.6.22}$$

Subsequent relationships are the same as the Modified Ramberg-Osgood model described earlier, and the differential equation of equivalent deviatoric strain and equivalent deviatoric stress is as follows.

$$\partial\sigma_{eq} = G_o \frac{\gamma_r^2}{\left(\varepsilon_{eq} + \gamma_r\right)^2} \partial\varepsilon_{eq} = G_o \psi \partial\varepsilon_{eq} \tag{4.6.23}$$

The material stiffness matrix is calculated as follows:

$$\partial\boldsymbol{\sigma} = \left[2\frac{\sigma_{eq}}{\varepsilon_{eq}}\mathbf{I} + \frac{1}{3}\left(3K - 2\frac{\sigma_{eq}}{\varepsilon_{eq}} \right)\boldsymbol{\delta}\boldsymbol{\delta} \right]\partial\boldsymbol{\varepsilon} + \left[2\frac{\sigma_{eq}}{\varepsilon_{eq}}\frac{2}{\varepsilon_{eq}}\left(\frac{G_o\psi}{\sigma_{eq}} - \frac{1}{\sigma_{eq}} \right)\boldsymbol{\varepsilon}_{dev}\boldsymbol{\varepsilon}_{dev} \right]\partial\boldsymbol{\varepsilon} \tag{4.6.24}$$

Section 7 Thermal Material Properties

7.1 Constitutive equation

The material used for the conduction element in FEA NX is isotropic.
The heat flux-temperature gradient relationship of the isotropic thermally conductive material is as follows.

$$\begin{Bmatrix} f_x \\ f_y \\ f_z \end{Bmatrix} = -\begin{bmatrix} k & 0 & 0 \\ 0 & k & 0 \\ 0 & 0 & k \end{bmatrix} \begin{Bmatrix} g_x \\ g_y \\ g_z \end{Bmatrix} \quad (4.7.1)$$

7.2 Porous material

In the case of a porous material such as a ground, it is composed not only of the soil particles but also water and gas in the pores between the soil particles. Therefore, unlike a general isotropic material, the thermal conductivity coefficient k considering water and gas is as follows.

$$k = (1-n)k_s + nSk_w + n(1-S)k_v \quad (4.7.2)$$

k_s , k_w , k_v : Heat conductivity of soil, water and gas
n : Porosity
S : Saturation

The heat capacity (ρC) in the porous medium can also be expressed as follows.

$$\rho C = (1-n)\rho_s C_s + nS\rho_w C_w + n(1-S)\rho_v C_v \quad (4.7.3)$$

ρ_s , ρ_w , ρ_v : Mass Density of soil, water and gas
C_s , C_w , C_v : Heat capacity of soil, water and gas

7.3 Freezing of Porous Material

Below zero degrees, water changes phase to ice. In the case of the ground, the phase change of the groundwater in the air gap between the soil particles occurs, not the phase change of the soil particles themselves. At this time, additional energy must be supplied, which is called latent heat. Mentioned energy depend as well on the change of the unfrozen water content with respect to temperature. Unfrozen water content function depicts the rate at which water does not change into ice even at temperatures, generally below zero degrees.

Therefore, considering the unfrozen water content function (f_u) and the latent heat of water (H_L), the thermal conductivity and thermal capacity of the ground can be expressed by the following equation.

$$k = (1-n)k_s + nS\left(f_u k_w + (1- f_u)k_i \right) + n(1-S)k_v \tag{4.7.4}$$

$$\rho C = (1-n)\rho_s C_s + nS\rho_w \left(C_w + H_L \frac{df_u}{dT} \right) + n(1-S)\rho_v C_v \tag{4.7.5}$$

k_i : Thermal Conductivity of Ice